AD_____

Award Number: DAMD17-02-1-0124

TITLE: Optimized Hyperthermia Treatment of Prostate Cancer Using a Novel Intracavitary Ultrasound Array

PRINCIPAL INVESTIGATOR: Nadine Smith, Ph.D.
Lewis E. Harpster, M.D.
Robert M. Keolian, Ph.D.
Victor Sparrow, Ph.D.
Andrew Webb, Ph.D.

CONTRACTING ORGANIZATION: The Pennsylvania State University
University Park, Pennsylvania 16802-7000

REPORT DATE: January 2003

TYPE OF REPORT: Annual

PREPARED FOR: U.S. Army Medical Research and Materiel Command
Fort Detrick, Maryland 21702-5012

REPORT DOCUMENTATION PAGE

Form Approved
OMB No. 074-0188

1. AGENCY USE ONLY (Leave blank)	2. REPORT DATE	3. REPORT TYPE AND DATES COVERED
	January 2003	Annual (14 Dec 01 - 13 Dec 02)

4. TITLE AND SUBTITLE
Optimized Hyperthermia Treatment of Prostate Cancer Using a Novel Intracavitary Ultrasound Array

5. FUNDING NUMBERS
DAMD17-02-1-0124

6. AUTHOR(S) :
Nadine Smith, Ph.D., Lewis E. Harpster, M.D., Robert M. Keolian, Ph.D., Victor Sparrow, Ph.D., Andrew Webb, Ph.D.

7. PERFORMING ORGANIZATION NAME(S) AND ADDRESS(ES)
The Pennsylvania State University
University Park, Pennsylvania 16802-7000

E-Mail: nbs@engr.psu.edu

8. PERFORMING ORGANIZATION REPORT NUMBER

9. SPONSORING / MONITORING AGENCY NAME(S) AND ADDRESS(ES)
U.S. Army Medical Research and Materiel Command
Fort Detrick, Maryland 21702-5012

10. SPONSORING / MONITORING AGENCY REPORT NUMBER

11. SUPPLEMENTARY NOTES
Original contains color plates: All DTIC reproductions will be in black and white.

12a. DISTRIBUTION / AVAILABILITY STATEMENT
Approved for Public Release; Distribution Unlimited

12b. DISTRIBUTION CODE

13. Abstract ***(Maximum 200 Words)*** *(abstract should contain no proprietary or confidential information)*

The eventual goal this research is to produce an ultrasound hyperthermia array which will uniformally heat the prostate to clinical temperatures for the treatment of prostate disease. This goal can be achieved by accounting for the physical differences between the prostate gland and surrounding tissue structures. It is therefore possible to design transducer to cause uniform heating within the prostate while causing minimal damage to surrounding tissue. The first year of this three year research project was focused on the initial design of the array based on computer simulations of the ultrasound energy interactions with the prostate and surrounding tissue. Three major areas were examined during this term were: (a) tissue modeling (b) beam design and optimization, and (c) hyperthermia array design and fabrication. Specifically, the simulations using the k-space propagation has been implement along with temperature rise determination using the bioheat transfer equation. Construction issue regarding the transducer dicing, matching layers and assemble have been dealt along with design of the final applicator body. To summarize, there are no deviations from the original research plan and this research is progressing on schedule.

14. SUBJECT TERMS:
ultrasound, hyperthermia, array, noninvasive, minimally invasive, magnetic resonanace imaging

15. NUMBER OF PAGES
93

16. PRICE CODE

17. SECURITY CLASSIFICATION OF REPORT	18. SECURITY CLASSIFICATION OF THIS PAGE	19. SECURITY CLASSIFICATION OF ABSTRACT	20. LIMITATION OF ABSTRACT
Unclassified	Unclassified	Unclassified	Unlimited

Table of Contents

I. INTRODUCTION:

Recent studies have shown that localized hyperthermia as a useful adjuvant to chemotherapy and radiotherapy in treatment of prostate cancer. Intracavitary ultrasound offers an attractive means of noninvasive localized hyperthermia treatment for prostate cancer with reduced side effects compared to competing modalities. For effective hyperthermia treatment, our goal is to uniformly heat the prostate to 43°C for 30-60 minutes. The proposal can be accomplished if the applied ultrasonic wavefields are optimized to specifically target prostate tissue. Recent advances in tissue modeling, numerical methods for ultrasound simulation, and MR thermometry can now be synthesized to achieve this optimization of ultrasound hyperthermia treatment. The proposed study is based on the hypothesis that ultrasonic wavefields can be optimized to specifically target prostate tissue, resulting in uniform hyperthermia treatment within the prostate and minimal effects to surrounding tissue. The goals of the proposed research are to determine optimal wavefield characteristics for specific thermal treatment of the prostate, to design and implement a transducer optimized for prostate hyperthermia, and to confirm the new transducer's performance through *in vitro* and *in vivo* experiments using magnetic resonance imaging (MRI). This year 1 annual report will describe the current progress and results.

II. BODY:

Ultrasonic hyperthermia is a promising technique for treatment of prostate cancer. When performed in conjunction with chemotherapy or radiotherapy, hyperthermia increases the damage to cancer cells caused by radiation, and prevents subsequent repair of cancerous tumors. Intracavitary ultrasound arrays are an ideal tool for performance of hyperthermia treatments, because deep localized heating can be achieved with precise power control and without any ionizing radiation. Clinical studies of hyperthermia using intracavitary ultrasound arrays have shown promising results for the clinical treatment of prostate cancer [1;2]. By accounting for the physical differences between the prostate gland and surrounding tissue structures, it is possible to design a transducer to cause uniform heating within the prostate (the ideal for prostate hyperthermia therapy), while causing minimal damage to surrounding tissue. The proposed study is based on the hypothesis that ultrasonic wavefields can be optimized in this way. The goal of prostate-specific ultrasonic hyperthermia treatment will be achieved by simulation studies of prostate hyperthermia, beam and transducer design based on simulation results, and laboratory experiments. Summarizing from the original grant application, the overall specific aims from this project are:

Specific Aims (briefly):

1. Realistic modeling of ultrasound prostate hyperthermia: An anatomically and physically accurate model will be implemented to simulate high-amplitude ultrasonic propagation in the prostate and surrounding tissues.
2. Beam design and optimization: Using the new model for ultrasound-prostate interaction, optimal sonications for therapeutic hyperthermia will be determined.
3. Hyperthermia array design and fabrication: A two-dimensional array transducer will be designed for practical realization of the optimal sonication methods. Based on the optimal design, array prototypes will be constructed and tested. Exposimetry of the ultrasound pressure field will be used to compare theoretical and experimental results.
4. *In vitro* and *in vivo* hyperthermia monitored with MR thermometry: Evaluation of the two-dimensional array will be conducted using MR thermometry.
5. *In vivo* prostate hyperthermia and evaluation: Using the two-dimensional ultrasound array, *in vivo* prostate hyperthermia will be administered to dogs.

Within the first year, plus or minus a few months, the timeline for progress of this research was broken into three major areas: (a) tissue model (b) beam design and optimization, and (c) hyperthermia array design and fabrication.
Year 1Timeline:

- Create reference three-dimensional tissue map for the prostate region by segmentation of the NIH Visible Human data set. (Months 1-6)
- Implement relaxation absorption, acoustic nonlinearity, and heat transfer effects into k-space method. (Months 1-6)
- Create additional models of the prostate region, using modified geometries based on clinical image data. (Months 6-12)

- Simulate hyperthermia treatments in the tissue models and compute FOM as a function of wave and beam parameters. (Months 6-18)
- Optimize wavefield and beam parameters for prostate hyperthermia treatments. (Months 9-18)
- Design transducer for realization of ultrasonic beams corresponding to optimal temperature distributions. (Months 8-18)
- Transducer construction and crystal dicing. Machining of transducer body. Cabling and crystal matching to resonance frequency. (Months 10-15)

The results herein will describe the progress and results achieved on this project over this past year in three sections.

IIa. Tissue modeling:

A k-space propagation code has recently been made to work on an older, small PC running under the Red Hat Linux operating system. The addressable memory space of this computer is inadequate, however, for modeling sound propagation to the prostate. A larger PC workstation with the Red Hat Linux operating system has been procured. The k-space propagation code still needs to be exercised with Visible Human Project [3] data.

Data from the Visible Human Project (VHP) has been downloaded and it can be seen that some of the geometry and pixels need to be modified to make a realistic model. For example, as can be seen in Fig. 1, the rectal wall in the cadaver has an irregular shape. In a clinical setting the ultrasonic probe will be surrounded by a latex condom filled with chilled, slightly pressurized water. The condom is then expected to push against the rectal wall, smooth out the wrinkles and change the overall shape of the rectum to conform to the transducer. The VHP data will need to be modified to take this into account. It still remains to convert the VHP images into sound speed and attenuation maps.

The broad framework of the optimization problem has become clearer. These ideas are tentative and need to be checked with the numerical model. As stated earlier, the goal is to achieve a uniform heating of the prostate to 43° C for 30-60 minutes. The total treatment time needs to be reasonably short, however, because of cost and patient discomfort. Therefore, the ultrasound cannot be focused on a series of spots each for 30-60 minutes. The whole prostate needs to be heated at once to keep the overall treatment time on the order of an hour. If focusing is going to be used, therefore, the focus must be moved very rapidly throughout the prostate, using the heat capacity of the prostate to average out fast temperature fluctuations, so as to achieve a uniform temperature rise.

Regardless of the focusing strategy, if the treatment time is going to be held to about an hour, it appears that the active area of the transducer needs to be quite large, as described by the following argument. For simplicity, assume a uniform linear (in amplitude) acoustic attenuation of 1 dB/cm, a typical value for various tissue types at 1.2 MHz. For linear attenuation of traveling waves, the heat deposited by sound in a volume is proportional to the acoustic power flowing through that volume, both being proportional to the acoustic pressure amplitude squared. In other words, the local heating is proportional to the local acoustic intensity. For 1 dB/cm attenuation the beam looses half its power (3 dB) in 3 cm. As it turns out, the distance between the transducer and the

middle of the prostate is about 3 cm. Let us approximate the cross sectional size of the prostate as 3 cm x 3 cm in a plane normal to the acoustic direction. Suppose that a strategy is found for focusing the sound to uniformly heat the prostate over this cross sectional area (i.e. the spot size is large, at 3 cm x 3 cm). Since the beam will lose half its energy on its way to the prostate, it will then be necessary to let the transducer have twice the prostate's area, with a size of 3 cm x 6 cm say, so that the acoustic intensity (power per area) and therefore the heating per volume is about the same at the rectal wall as it is at the prostate. Under these conditions the temperature rise everywhere between the transducer and the prostate will be about the same as at the prostate itself, unless active cooling is applied. For a smaller transducer active area, the wall heating will be worse.

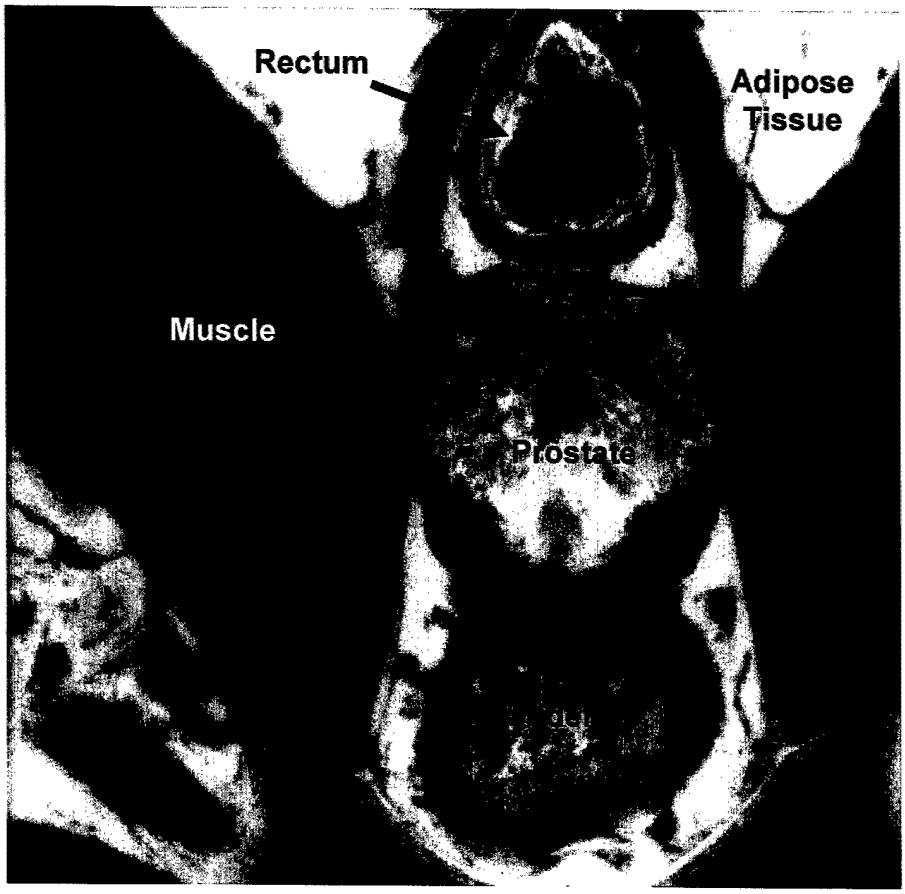

Figure 1. Axial or transverse view from the Visible Human Project through the rectum, the middle of the prostate and the bottom of the bladder used for determining the characterization of the tissue surrounding the prostate and distances.

One strategy under simulation is focusing the beam to a smaller spot and moving the spot. For the same transducer power (the same heating at the rectal wall), let there be N foci in a cross sectional plane through the middle of the prostate. Then the intensity at the foci will be N times greater than it was in the case above. However, to achieve the same overall treatment time (about an hour), the fraction of time the sound can dwell on

any one focus, the duty cycle, must be *1/N*. So the average power deposited in this plane is the same as in the case above, assuming linear acoustics. Therefore, focusing the sound to a tighter spot does not relieve the need for a large transducer. Also, the planes in front of or behind the focal plane get about the same amount of heating as the focal plane since about the same average acoustic power is passing through them as well, even though they are out of focus. There is less peak intensity, but the overlap of the acoustic beams, and so the higher duty cycle at any one spot, compensates for this.

Considering this argument and what would break it down, it seems that there are four effects that may be used to heat the prostate more than the tissue between the prostate and the rectum: (1) The transducer area could be even larger than about twice the cross sectional area of the prostate. (2) The rectal wall could be actively cooled with chilled water. Simulations have shown [4] that this cooling works close to the rectum, but does not extend very far toward the prostate. There is a very sharp temperature gradient near the rectal wall. (3) There may be enhanced attenuation and energy deposition due to acoustic nonlinearities at a tight focus. In this case a small spot size moved rapidly around the prostate would be an advantageous strategy. (4) The treatment time could be greatly extended so that *N* sections of the prostate could be heated, each for 30-60 minutes, in sequence. Blood perfusion would keep the out of focus regions cool but the treatment time would shoot up to *N* times 30 to 60 minutes. Note that the push toward a large transducer is driven by heating considerations, not by a diffraction limit due to the finite transducer aperture.

The apparent need for a large transducer has caused the consideration of an alternate transducer geometry than the prototype planar phased array transducer described in Sections IIb and IIc below. A large transducer implies a large angle between the normal to the transducer plane (the "axial" direction) and the direction of propagation between a peripheral element and a desired spot on the prostate. For example, for a 6 cm long transducer, a 3 cm diameter prostate centered 3 cm from the transducer face, an individual element at the end of the transducer needs to be non-directional enough that appreciable acoustic energy can propagate at an angle of 65° from the axial direction. A central element needs illuminate within a plus or minus 30° range to cover the prostate. The elements therefore need to be fairly small. At 1.2 MHz the wavelength is about 1.25 mm. The fraction of a wavelength λ for half power at these angles implies that the element size needs to be 0.49λ (0.61 mm) for the peripheral element and 0.89λ (1.11 mm) at the center. Therefore, a 3 cm x 6 cm 2-D planer phased array with a typical element size of 0.86 mm x 0.86 mm should have 2400 elements if fully covered

However, an idea that may be worth pursuing is to aim each element toward the center of the prostate. A clay model of this phased planer "Fresnel" transducer is shown in Fig. 2. Unfortunately, the acoustic beams from each element still need an average half angle beam width of about 26° to cover the prostate, which leads to elements that are about 1.01 λ (1.26 mm) on a side. A fully populated 3 cm x 6 cm (or 2 cm x 9 cm) transducer would still need 1100 elements—still quite a few. The grating side lobe situation should be much better, however, since each element's beam pattern tends to have a zero in the direction that the planar array has a grating side lobe. All this needs to be checked with simulation.

It may be possible to make a more practical Fresnel transducer with 64 elements by sparsely populating the array. The same 1.26 mm elements could be spaced every 5.3

mm to be distributed over a 3 cm x 6 cm active area. For this to work, active and perfusion cooling would have to be sufficient near the transducer face until the individual beams substantially overlapped and tissue heating is uniform. This sparse an array may have an excessive grating side lobe problem, however. The somewhat unconstructive results of this Section need to be reconciled with current practice since prostate hyperthermia seems to work fine without thousands of elements.

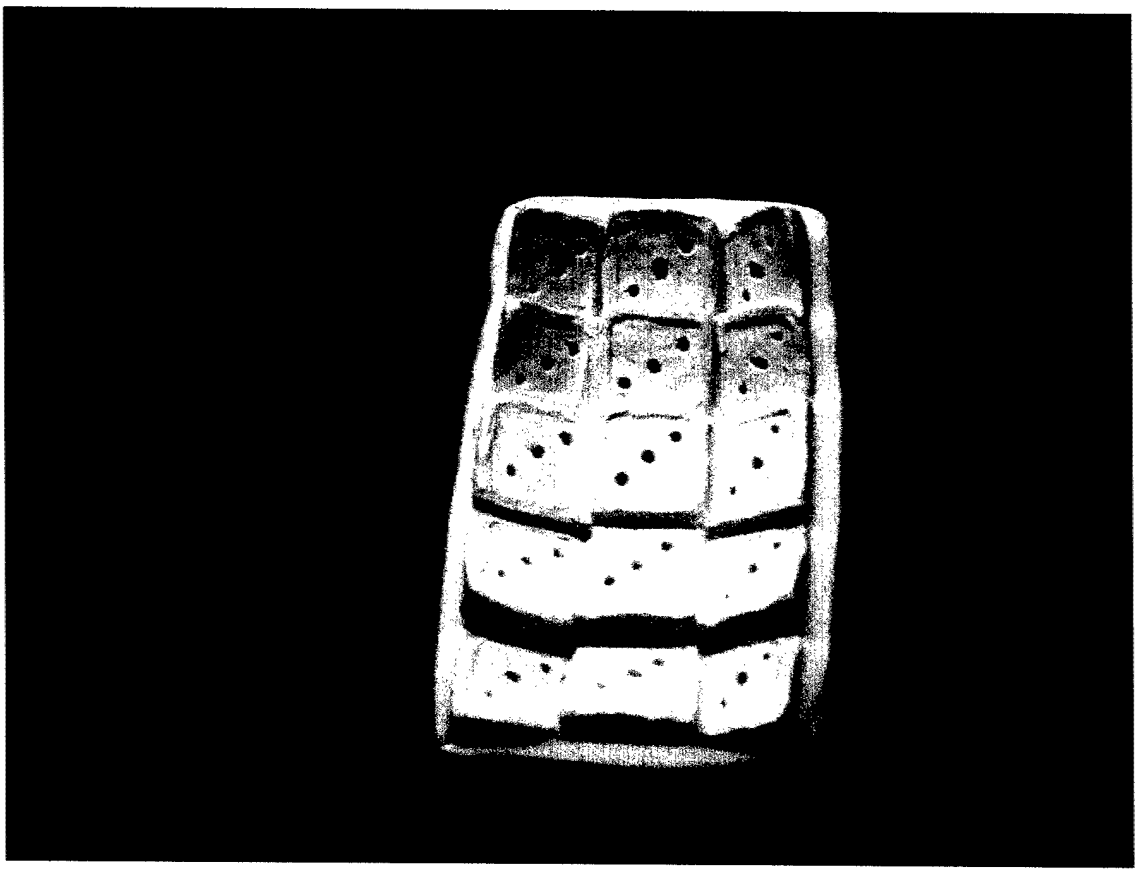

Figure 2. Clay model of a substrate for a planer phased "Fresnel" array transducer, here with only 3 x 5 (=15) elements. The elements all point toward the center of the prostate. Individual PZT elements would be glued to the ridges at the edge of each facet. A gap between the substrate and the element due to the ridge causes the elements to be air backed. The central hole in each facet would hold a pin or wire to make contact to the electrically "hot" side of the element. The other two holes vent the back space for cooling and in a prototype would detect a water leak. In the actual transducer the substrate would be made of plastic, perhaps acrylic. An electrically grounded matching layer that is water tight would be applied over all the elements.

IIb. Beam Design and Optimization for Temperature Simulations

For the simulations, separate programs have been written for applications prior to particular prostate tissue characterization results. Specifically, programs which model for the temperature rise from a pressure field determined from the results of Section IIa have been written and implemented based on our initial aperiodic design. Although the simulations are incomplete, based on an initial prototype piezoceramic design, a great deal of the final transducer engineering has been implemented in anticipation of the final simulation results.

The current feasible prototype design under construction which will be used for the *in vitro* experiments will be an eight-by-eight element 2-D ultrasound tapered phased array (1.2 MHz). The individual element widths and lengths used were:

widths = [2.00 2.33 2.66 3.00 3.00 2.66 2.33 2.00] mm
lengths = [2.00 2.33 2.66 3.00 3.00 2.66 2.33 2.00] mm

Both dimensions of the array were chosen to be identical in order to have same steering angle in both directions, and thus having the same focusing and steering capabilities in both X (transverse) and Y (radial) directions with respect to the transducer face. The maximum possible steering angle was $tan^{-1}(1.0/4.0) = 14^{o}$, which means that this array was capable of focusing anywhere between the angles -14^{o} *and* -14^{o} in both X (transverse) and Y (radial) directions. Both the element widths and lengths were designed to be tapered (end elements were thinner than center elements in both directions) in order to reduce side lobes and increase the maximum allowable width and length. Figure 3a shows the normalized pressure focused off-axis at 8, 8, 40 mm (transverse, radial and axial, respectively).

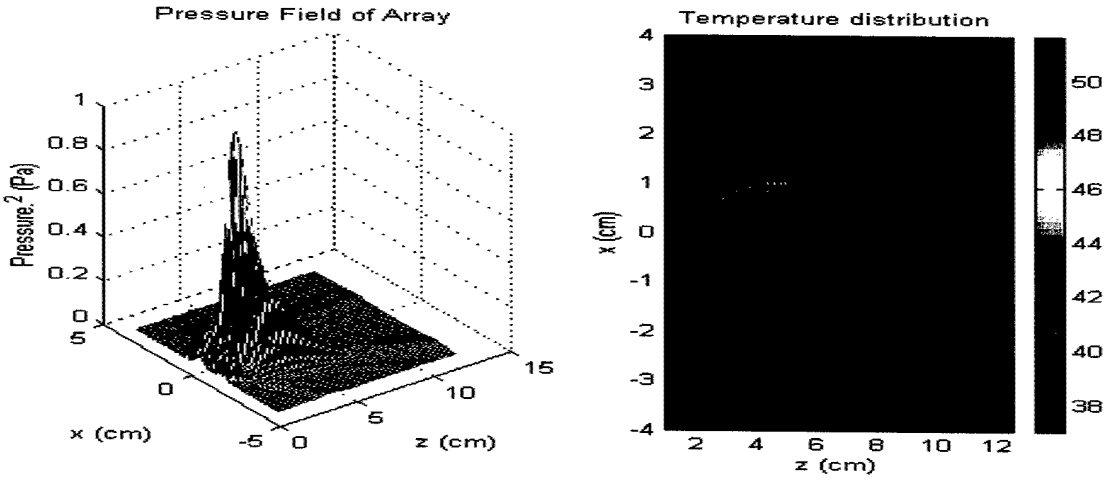

Fig. 3 For the eight-by-eight element 2-D ultrasound tapered phased array (1.2 MHz) was the (a) pressure and (b) temperature field for this array was theoretically determined and is currently under test.

From a simulated pressure field, the bioheat transfer equation (BHTE) has been used to determine the temperature distributions in the tissue using,

$$\rho C_t \frac{\partial T}{\partial t} = K\left(\frac{\partial^2 T}{\partial x^2} + \frac{\partial^2 T}{\partial y^2} + \frac{\partial^2 T}{\partial z^2}\right) - wC_b(T - T_a) + q(x, y, z)$$

where c_t is the specific heat of the tissue, K is the thermal conductivity, T is the tissue temperature, T_a is the arterial blood temperature (37°C), w is the tissue perfusion (in kg/m^{3}s), c_b is the specific heat of blood (3770 J/kg°C), and q is the power deposited locally in the tissue, given by [5]. This power was calculated from the pressure field of the array design and the BHTE was solved using a numerical finite difference method with the boundary conditions set 37°C. The temperature rise based on the simulated transducer is shown in Fig. 3b.

Any variation in size or frequency of a simulated design can be used with the bioheat transfer equation. As another example of an application, calculation of the acoustic field of the phased array and the simulation of the temperature using the BHTE to reproduce the tissue response for a single element spherical transducer (F number = 0.8, 10 cm diameter and 1.5 MHz) have been implemented. If a spherical shape is optimized over the flat ceramic design, the temperature rise within the tissue can also be determined. Figure 4 - left shows a three dimensional (axial, radial) result from a spherical design while the. Temperature distributions sliced through Fig. 4-left at the temperature maximum in the axial (Fig 4, bottom right) and the radial (Fig 4, top right) direction are shown.

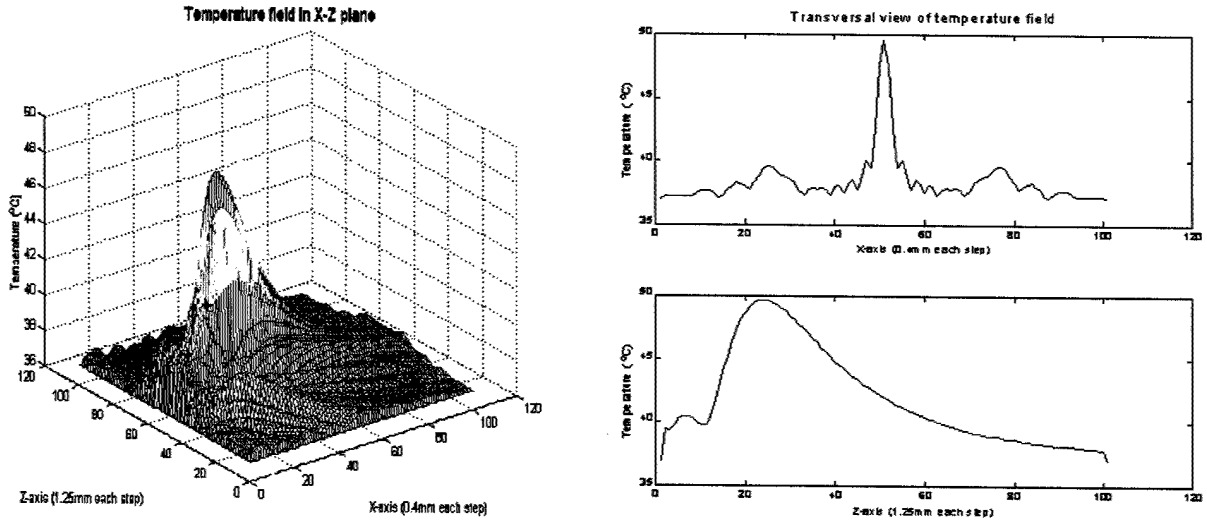

Fig. 4 For a single element spherical transducer (0.8 F# number, 10 cm diameter and 1.5 MHz) the temperature distribution in the Z (axial) and X=Y (radial) plane (left). The temperature distribution taken directly at the temperature maximum in the axial (bottom right) and the radial (top right) direction plotted.

As indicated in the clay model of a substrate (Fig. 2), the final tranducer design will probably be a multi-element spherical design. Once the design is finalized, the results from this section indicate that the temperature rise in the tissue can be easily incorporated into the software for final implementation.

IIc. Hyperthermia Array Design and Fabrication

Although the pattern of the dicing of the ceramic has not been finalized, issues regarding the piezoceramic have been worked out in advance. This section presents results from a prototype 64 element array exploring the issues of transducer matching layers, cabling and dicing. The construction of the prototype transducer required three major steps. First, a matching layer was put on the face of the transducer, second, appropriate cabling was used to deliver the electrical power to the transducer, and third, electrical matching circuits were built and put in between the amplifier and the individual 64 elements of the transducer. After the transducer construction was completed, it was necessary to verify the simulated results from exposimetry of the acoustic field using a calibrated hydrophone. Programs regarding the automated exposimetry have been written for the final hyperthermia array design.

For the transducer to be able to deliver maximum possible acoustic power from the piezoelectric material to the prostate, a matching layer is necessary. Applying the continuity of normal specific acoustic impedance at the boundaries with some algebraic manipulation yields that the maximum power transmission coefficient occurs when the thickness of the matching layer is an odd integer multiple of a quarter wavelength and the characteristic impedance of the matching layer material equals the geometric mean of the characteristic impedances of the piezoelectric material and the prostate. To construct the matching layer, the transducer was surrounded with a rubber dam and the silver conducting matching layer was poured onto the transducer surface. The matching layer was a 2:1, epoxy to silver mixture and 2-3 micron silver epoxy.

Permittivity is an important factor in determining the electrical performance of lead zirconate titanate (PZT) ceramics. The effect of permittivity becomes more evident when the surface area of the individual elements of the array are small, which is exactly the case in this design. For a PZT-8 material element with dimensions of 2 mm x 2 mm and resonance frequency of 1.5 MHz, the element capacitance was found to be 20.63 pF, which means an element impedance of 5.14 kΩ magnitude. Since the load impedance (element impedance) was high, the cable has to be a low capacitance cable which effectively means high cable impedance, so a cable with high characteristic impedance is necessary for our requirement.

The cuts through the piezoelectric material were made using a dicing saw (Model 780, K & S-Kulick and Soffa Industries, Willow Grove, PA) at the former NIH Medical Ultrasonic Transducer Technology Resource Center here at Penn State. The electrical connection to the amplifier side was attached using loose crimp contacts while the connection to the PZT (Fig. 5a) used Indalloy # 1E, which is a low temperature soldering material that was used to insure that the temperature during soldering did not exceed the Curie temperature for PZT-8 material. As an early phase prototype and not a clinical device, a water tight magnet compatible assembly for the 64 element phased array is shown in Fig. 5b. The array is shown connected to a 2.3 m long DL cable connector

cable. The DL connector can easily be attached to a specially built amplifier driving system (Advanced Surgical Systems, Inc, Tucson, AZ). With this design, each element of the transducer was matched to the 50 ohm impedance of the amplifier.

Fig. 5. The wiring of the prototype array (a) after finishing soldering the coaxial cable to the array (b) the final prototype array that includes a 2.3 m coaxial cable and a water proof housing.

Initial exposimetry data was taken and compared to theory. Figure 6 shows the normalized intensity for a focus at 3 cm away from the face of the transducer, it shows a good agreement between theory (blue) and experiment (red). To summarize, during the last year, the prototype transducer construction was completed. Exposimetry data was taken, it showed good agreement with theoretical results. Simulated temperature profiles were also performed, which will be compared to *in vivo* temperature profiles that will be performed soon.

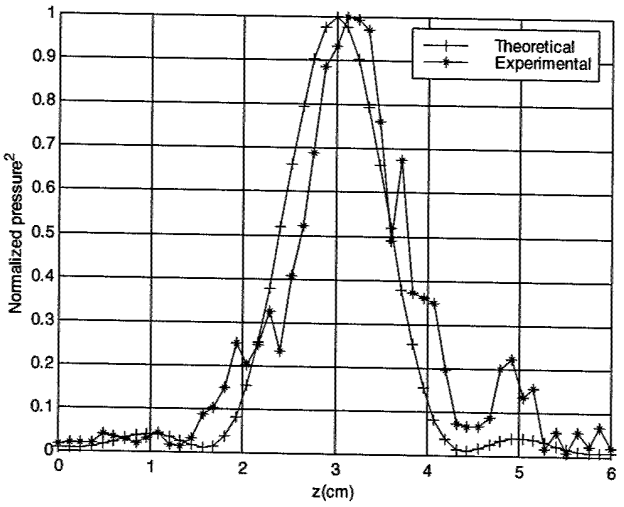

Fig. 6. Normalized intensity at 3 cm away from the face of the transducer, theoretical (blue) and experimental (red).

As proposed in the grant, the array will be designed so that it is capable of heating the entire prostate volume from the limited confines of the rectum. This dictates the shape and size of both the overall applicator body and the ultrasound array. To prevent

patient discomfort, the size of the applicator diameter was limited to 21 mm or less. The shaft of the applicator, which would extend through the anus for the duration of the treatment and was thus considered important to minimize, was limited to 15 mm. While these dimensions are somewhat larger than those seen in typical transrectal ultrasound imaging systems, no treatments were limited due to excessive patient discomfort associated with the applicator size in previous clinical studies. Given these constraints, the applicator body is shown in Fig. 7a with an interchangeable bed (Fig. 7b) to hold the diced ceramic. The interchangeable bed will allow for ease of switching array designs with the necessity to construct multiple array bodies. Figure 7 has been forwarded to one of the expert machinist here on the Penn State campus for construction in the coming year.

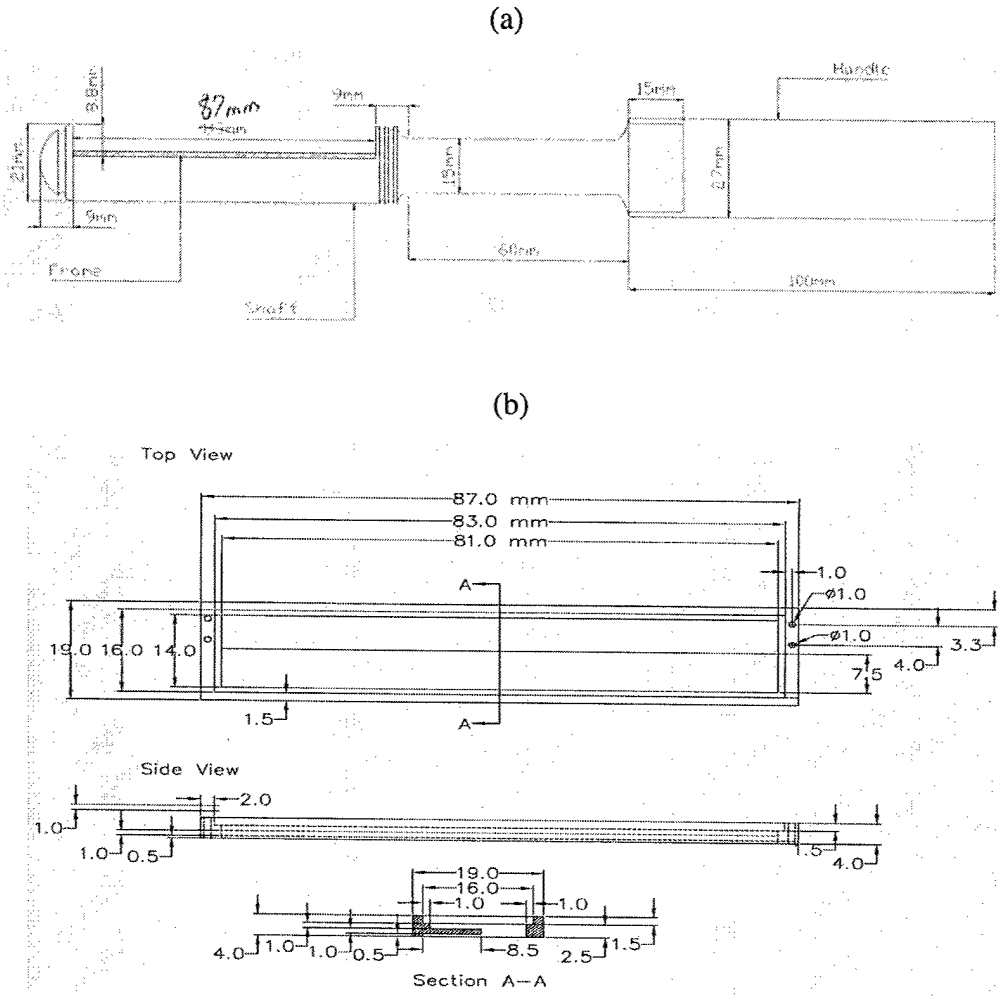

Fig 7. (a) Based on the limited confines within the rectum, the applicator to hold the multi-element array as been design. (b) A frame has been designed to easily interchangeable several multielement ceramic designs.

Consideration of the raw materials for the applicator have been assessed since even non-ferrous metals will disturb the magnetic resonance image—as little metal as possible will be used in the construction of the applicator. Therefore the polycarbonate

applicator body will be machined from Delrin® (DuPont Films, Circleville, OH). Water lines and coaxial cables will be passed through the lumen of the applicator body to the array. Brass tubes will be used for water flow since they are non-magnetic and will be necessary to minimize the volume of the tube. Water and air input and output flow tubes will be located along separate conduits within the applicator body. Details regarding the water flow system for cooling the rectal wall through an o-ring secured bolus will be finalized in year 2.

To summarize regarding the schedule, there are no deviations from the original research plan and this research is progressing on schedule.

III. KEY RESEARCH ACCOMPLISHMENTS:

- k-space propagation code operational
- Visible Human Project data accessed
- Progress on optimization strategy
- Novel "Fresnel" transducer under consideration
- Implementation of the bioheat transfer equation used for determining temperature rise in tissue based on pressure field simulation
- Exposimetry system constructed for determining pressure and intensity fields from arrays
- Matching layer design for maximum power transfer from transducer to tissue
- Evaluation of piezoceramics and cables for the high powered array
- Clinical applicator body design multielement array

IV. REPORTABLE OUTCOMES:

Funding from this award has been used to produce a manuscript and conference proceeding. As indicated in the grant, a graduate research student, Mr. Al-Bataineh, has benefited from this award and has produced a Thesis Proposal for the PhD Degree in Bioengineering which will focus on this research. In all publications and invited talks using the data resulting from this grant, the Department of Defense Congressionally Directed Medical Prostate Cancer Research Program has been gratefully acknowledged. Copies of the manuscripts, proceeding and presentations are included in the appendix.

Manuscripts:

Saleh, K. and Smith, N.B., Two Dimensional Array Design for Tissue Ablation for Treatment of Benign Prosthetic Hyperplasia, International Journal of Hyperthermia, 2002, *submitted.*

Presentations:

Smith, N.B. "Therapeutic Applications of Ultrasound: Treatment of Prostate Disease and Noninvasive Drug Delivery", Invited seminar to Case Western Reserve University- Department of Biomedical Engineering, 14 March 2002.

Saleh, K. and Smith, N.B., Two Dimensional Array Design for Tissue Ablation for Treatment of Benign Prosthetic Hyperplasia, International Society of Magnetic Resonance in Medicine (ISMRM) Workshop on MRI-Guided Focused Ultrasound Surgery, 19-21 June 2002, Cambridge, MA. pp 63-66 (paper and oral presentation)

Al-Bataineh, O. "Optimized Ultrasound Phased Array for Thermal Treatment of Prostate Diseases", Thesis Proposal for the PhD Degree in Bioengineering. January 2003 *(manuscript).*

V. CONCLUSIONS:

For this research in the treatment of prostate disease, the overall goal is produce an ultrasound device to treat the cancerous tissue using hyperthermia. Intracavitary ultrasound offers an attractive means of noninvasive localized hyperthermia treatment for prostate cancer with reduced side effects compared to competing modalities. For effective hyperthermia treatment, the goal is to uniformly heat the prostate to 43°C for 30-60 minutes. To achieve this goal, the clinical ultrasound device under construction is designed such that ultrasonic wavefields are optimized to specifically target prostate tissue, resulting in uniform hyperthermia treatment within the prostate and minimal effects to surrounding tissue.

This first year of this research project focused on the initial design of the array based on computer simulations of the ultrasound energy interactions with the prostate and surrounding tissue. In accordance with the specific aims and timetable within our original proposal, the three areas examined during this year were: (a) elucidation of the ultrasound interaction with the prostate tissue (tissue modeling) (b) beam design and optimization, and (c) hyperthermia array design and fabrication. Previously, much research in this area has treated the prostate and surrounding tissue as homogeneous media. For our design, the simulations take into account the inhomogeneity of the prostate to produce a uniform heating pattern using k-space propagation and application of the non-linear bioheat transfer equation to determine the optimal thermal treatment. In conjunction with the continuing simulations, construction of the clinical applicator can progress along with tackling with construction issues regarding the transducer dicing, matching layers and assembly. In contrast to clinical imaging transducers, much novel research is required for tranducer construction in applications of high powered ultrasound hyperthermia given of constraints as an intracavitary device. To date, there are no deviations from the original research plan and this research is progressing on schedule.

So what is the impact of this research? Previous and recent clinical studies of hyperthermia using intracavitary ultrasound arrays have shown promising results for the clinical treatment of prostate cancer [1,2]. With the increasing aging population within the US, there are increasing incidents of prostate cancer. With an estimated 37,000 deaths per year, prostate cancer is the second leading cause of cancer death in men. Although age is perhaps the most important risk factor, the incidence and mortality rate is twice as high for African-American men as for Caucasian men [6-8]. Moreover, the knowledge gained from this research can further me applied to noninvasive treatment of other cancers such as breast cancer or cancers of the liver or kidney.

VI. REFERENCES:

Reference List

1. H. Fosmire et al., *Int.J.Radiation Oncology Biol.Phys.* 26, 253-259 (1993).

2. Hurwitz, M. D., Kaplan, I., Svensson, G. K, Hansen, J., and Hynynen, K. H. Feasibility and patient tolerance of a novel transrectal ultrasound hyperthermia system for treatment of prostate cancer. International Journal of Hyperthermia 17(1), 31-37. 2001.

3. National Library of Medicine (US) Board of Regents. Electronic Imaging:Report of the Board of Regents. NIH Publication , 90-2197. 1990.

4. C. J. Diederich and K. H. Hynynen, *IEEE Trans.Biomed.Eng.* 36, 432-438 (1989).

5. W. L. Nyborg, *J Acoust Soc Amer* 70, 310-312 (1981).

6. L. A. G. Reis, C. L. Kosary, B. F. Hankey, B. A. Miller, "Cancer Statistics Review, 1973-1994: Tables and Graphs" *Report No. NIH Publication No. 97-2789* (National Cancer Institute, Bethesda, MD, 1997).

7. P. A. Wingo, L. A. Ries, S. L. Parker, C. W. Heath, *Cancer Epidemiol.Biomarkers Prev.* 7, 271-282 (1998).

8. R. T. Greenlee, T. Murray, S. Bolden, P. A. Wingo, *CA Cancer J.Clin.* 50, 7-33 (2000).

VII. APPENDICES:

List of items in appendix (4 total):

Manuscripts:

Saleh, K. and Smith, N.B., Two Dimensional Array Design for Tissue Ablation for Treatment of Benign Prosthetic Hyperplasia, International Journal of Hyperthermia, 2002, *submitted.*

Presentations:

Saleh, K. and Smith, N.B., Two Dimensional Array Design for Tissue Ablation for Treatment of Benign Prosthetic Hyperplasia, International Society of Magnetic Resonance in Medicine (ISMRM) Workshop on MRI-Guided Focused Ultrasound Surgery, 19-21 June 2002, Cambridge, MA. pp 63-66 (paper and oral presentation)

Al-Bataineh, O. "Optimized Ultrasound Phased Array for Thermal Treatment of Prostate Diseases", Thesis Proposal for the PhD Degree in Bioengineering. January 2003 *(manuscript).*

Smith, N.B. "Therapeutic Applications of Ultrasound: Treatment of Prostate Disease and Noninvasive Drug Delivery", Invited seminar to Case Western Reserve University- Department of Biomedical Engineering, 14 March 2002.

Two Dimensional Ultrasound Phased Array Design for Tissue Ablation for Treatment of Benign Prosthetic Hyperplasia

Khaldon Y. Saleh[1] and Nadine Barrie Smith [1,2]

Department of Bioengineering[1]
Graduate Program in Acoustics[2]
College of Engineering
The Pennsylvania State University
206 Hallowell Building
University Park, PA 16802

Please send correspondence to:
Khaldon Y. Saleh, M.Sc.
Department of Bioengineering
College of Engineering
The Pennsylvania State University
206 Hallowell Building
University Park, PA 16802
Fax: (814)863-0490
Phone: (814)865-8451
kysbio@engr.psu.edu

Abstract

This paper describes the design, construction and evaluation of a two dimensional ultrasound phased array to be used in the treatment of benign prosthetic hyperplasia. With two dimensional phased arrays, the focal point position can be controlled by changing the electrical power and phase to the individual elements for focusing and electronically steering in a three dimensional volume. The array was designed with a steering angle of ±14° in both transverse and longitudinal directions. A piezoelectric ceramic (PZT-8) was used as the material of the transducer since it can handle the high power needed for tissue ablation and a matching layer was used for maximum acoustic power transmission to tissue. Analysis of the transducer ceramic and cable impedance has been designed for high power transfer with minimal capacitance and diameter. For this initial prototype, the final construction used magnet compatible housing and cabling for future application in a clinical magnetic resonance imaging system for temperature mapping of the focused ultrasound. To verify the capability of the transducer for focusing and steering, exposimetry was performed and the results correlated well with the calculated field. *Ex vivo* experiments were performed and indicated the capability of the transducer to ablate tissue using short sonications. For sonications with exposure time of 10, 15 and 20 seconds, the lesion size was roughly 1.8, 3.0 and 4.3 mm in diameter, respectively, which indicates the feasibility of this device.

Key words: ultrasound transducer, two dimensional array, focusing, matching layer, necrosis.

1. Introduction

Focused ultrasound surgery (FUS), or high intensity focused ultrasound (HIFU), is a clinical method for treating benign prosthetic hyperplasia (BPH), a benign growth of prosthetic cells that is not life threatening but can cause blockage to the urine flow as a result of the prostate pushing against the urethra and the bladder (Stephens 2000). With FUS, tissue is noninvasively necrosed by elevating the temperature at the focal point above 60°C using short sonications (10-30 seconds) and deep FUS has been reported to successfully ablate prostate tissue without inducing damage to the rectal wall (Tan *et al.* 2000, Seip and Sanghvi 2001, Ebbini *et al.* 2001, Yao *et al.* 2001).

Existing techniques for treating BPH include hyperthermia, focused ultrasound, transurethral resection, prostatectomy, and surgery. Although preferable, surgical techniques have numerous complications that appear in about one in four cases which include impotence, incontinence, urinary tract infections and often requires a lengthy hospitalization (Barrett 2000). With FUS, the ultrasound beam is focused at a specific location in the target volume to be necrosed. Since the tissue volume to be necrosed is larger than the geometric focus of the array, the transducer needs to be physically moved repeatedly to destroy the desired volume and unnecessarily extend the treatment time. Phased arrays overcome this problem by electrically steering the focal point from one location to another by changing the phase and power to the individual elements of the array.

Previous effective prostate ultrasound devices include both mechanically and electrically steered designs. One example of a commercial design is a focused, single element transducer which was mechanically maneuvered to ablate tissue (Sonablate^{TM}

500, Focus Surgery Inc., Indianapolis, IN, USA). Electrically steered include an experimental design which used a one dimensional 57 x 1 aperiodic, linear array (87 x 15 mm^2) which reduced grating lobes and could steer the focus in the radial and longitudinal but not the transverse direction (Hutchinson and Hynynen 1996). Another experimental design was a 60 x 1, linear array (75 x 15 mm^2) with a mechanical translation which could electrically steer the focus in the radial and longitudinal but not the transverse direction (Sokka and Hynynen 2000). The drawbacks behind these designs are that they can only steer the focus in the radial and longitudinal directions or require complex mechanisms to move the focus. The advantage with a two dimensional (2D) phased array is that it can electrically focus and steer in the radial, longitudinal and transverse directions, which means that it has the capability of focusing and steering in a three dimensional (3D) volume without the need to physically move the array.

Issues regarding the construction of an array used for FUS of the prostate initially deal with the frequency and size of the ceramic to be diced into an array. The resonance frequency should be greater than 500 kHz (Buchanan and Hynynen 1994) while the size of the transducer needs to be large enough to be able to deliver high power but small enough to be an intracavitary device. Before construction, computer simulations can be performed to determine the acoustic field. Pressure wave and temperature simulations indicated that a tapered array design reduced grating lobes significantly compared to equal element size arrays. Based on the computer model, a tapered array that satisfied grating lobes, frequency, and size limitations was designed. Lead zirconate titanate (PZT) was chosen as the ceramic material of the array since it has the capability of handling the high electrical powers used in focused ultrasound. To maximize the

acoustical power transmission from the elements and improve the structural integrity of the array face, a conductive matching layer was designed and fabricated. Issues regarding the cabling and electrical matching of the elements were also considered. Exposimetry of the acoustic field from the array was performed to compare experimental and calculated theoretical results. *Ex vivo* experiments using porcine kidney were also performed to demonstrate the feasibility of the array to necrose tissue. This research describes the design, construction and evaluation of a two dimensional ultrasound phased array that is capable of focusing and steering in a three dimensional volume to be used in the treatment of BPH.

2. Materials and Methods

2.1 Simulations

Computer simulation programs were written to determine the number and the size of the phased array elements in addition to determining the pressure and temperature field from the device. The array was modeled (figure 1) as a 2D square array in order to have focusing and steering capabilities in both x and y directions (x = transverse, y = longitudinal and z = radial). The phase of each element was determined such that signals from individual elements were coherent at the shifting focal point. Measuring the difference in path length between each element to the focus in comparison to the path from the centre of the array to the focus determined the element phase calculation. The phase, ϕ_i, (degrees) of element i was given by:

$$\phi_i = \frac{360^\circ}{\lambda}(d_i - d_o) - 360^\circ n \qquad (1)$$

where λ is the wavelength (m), d_i is the distance (m) from the centre of element i to the focal point, d_o is the distance (m) from the centre of the array to the focus and n is an integer to keep $0 \leq \phi_i \leq 360°$. Huygen's principle was used to model the pressure field as a summation of simple sources (Zemanek 1971). Thus, the total acoustic pressure at any point in the field can be calculated using:

$$p(\mathrm{x},\mathrm{y},\mathrm{z}) = \sum_{i=1}^{n} \sqrt{\frac{2P\rho}{cA}} \left(\frac{fS}{d_i}\right) \exp\left[j\left(\phi_i - \frac{2\pi d_i}{\lambda}\right) - d_i\alpha \right] \qquad (2)$$

where p is the total acoustic pressure in Pascals (Pa), P is the total acoustic power emitted by the array in watts (W), ρ is the density of the medium (998 $\mathrm{kg \cdot m^{-3}}$), c is the speed of sound in the water (1500 $\mathrm{m \cdot s^{-1}}$), A is the total surface area of the array ($\mathrm{m^2}$), f is the resonance frequency (1.2 MHz), S is the area of the corresponding element ($\mathrm{m^2}$) and α is the attenuation in soft tissue (10 $\mathrm{Np \cdot m^{-1} \cdot MHz^{-1}}$).

[Insert figure 1 about here]

From the pressure field of the simulated array, the temperature distribution in the tissue was modeled using the Pennes' bioheat transfer equation (BHTE) (Pennes 1948):

$$\rho C_t \frac{\partial T}{\partial t} = K\left(\frac{\partial^2 T}{\partial \mathrm{x}^2} + \frac{\partial^2 T}{\partial \mathrm{y}^2} + \frac{\partial^2 T}{\partial \mathrm{z}^2}\right) - wC_b(T - T_a) + q(\mathrm{x},\mathrm{y},\mathrm{z}) \qquad (3)$$

where C_t is the specific heat of the tissue (3770 $\mathrm{J \cdot kg^{-1} \cdot °C^{-1}}$), K is the thermal conductivity (0.5 $\mathrm{W \cdot m^{-1} \cdot °C^{-1}}$), T is the temperature at time t at the point x, y, z in °C, T_a is the arterial blood temperature (37°C), w is the perfusion in the tissue in $\mathrm{kg \cdot m^{-3} \cdot s^{-1}}$, C_b is the specific heat of the blood (3770 $\mathrm{J \cdot kg^{-1} \cdot °C^{-1}}$) and q(x, y, z) is the power deposited at the point x, y,

z. The power was calculated from the pressure field of the array design while the BHTE was determined using a numerical finite difference method with the boundary conditions set at 37°C. The total intensity at point (x, y, z) was also calculated from the pressure field of the simulated array and is given by (Nyborg 1981):

$$I(x,y,z) = \frac{p^2(x,y,z)}{2\rho c} \qquad (4)$$

where I(x, y, z) is the intensity at point x, y, z in $W \cdot m^{-2}$.

Based on previous studies of transrectal probes, the width of the ceramic should be roughly no wider than 23 mm (Smith *et al.*, 1999). Initially the simulated design used equal size elements of 2.5 x 2.5 mm^2, and although it was capable of focusing and steering, it suffered from large grating lobes outside the focus. For example, at a focus of (x, y, z) = (5, 0, 30) mm (i.e. the 0, 0, 0 position is at the centre of the transducer face in figure 1), the grating lobe level was –3.47 dB which was not desirable since this high level can cause an increase in tissue temperature outside the focus. Removing the periodicity of the array or tapering it has been shown to reduce the grating lobe level (Hutchinson *et al.* 1995). Both dimensions of the array were chosen to be identical in order to have same focusing and steering capabilities in both x and y directions. The maximum possible steering angle was calculated to be $\tan^{-1}(1.0/4.0) = 14°$ with maximal focal depth of 40 mm. The improved tapered array design started with a 20 x 20 mm^2 piece cut into an 8 x 8 pattern with 64 individual elements with lengths (L) and widths (W) of 2.00, 2.33, 2.66, 3.00, 3.00, 2.66, 2.33, 2.00 mm for elements i = 1 through 8, respectively (figure 1). Simulations have shown that the grating lobe level of the tapered design has decreased to –8.24 dB at a similar focus location of 5, 0, 30 mm. Figure 2a shows a mesh plot for the normalized intensity as function of x and z, while figure 2b is

the corresponding contour plot with contour levels at 90, 70, 50, 30 and 10% of the maximum intensity. From the simulations, a grating lobe level of 15% of the maximum value was observed which decreased at smaller steering angles. Temperature simulations were also used to verify the potential to increase the tissue temperature to 60°C with short sonications. Figure 2c shows the temperature distribution corresponding to the pressures for figure 2a and an increase in temperature was observed at the intended location of (x, z) = (5, 30) mm.

[Insert figure 2 about here]

2.2 Transducer construction

Choosing an appropriate piezoceramic material to be used in this application is essential since it affects both electrical and acoustical properties of the array. Appropriate PZT that can be used include PZT-4, PZT-5H and PZT-8. For ultrasound imaging arrays, PZT-5H has a better performance when compared to the others, from a capacitance point of view, which is due to the fact that it has a large permittivity value, but at the same time it cannot handle the large electrical power that is used in focused ultrasound. With respect to power, PZT-4 and PZT-8 are good candidates with an advantage for PZT-8 over PZT-4 since it has an extremely high mechanical quality and extremely low loss factor. Thus PZT-8 material (TRS Ceramics, State College, PA, USA) was chosen and diced, in house, into 64 elements forming the complete array. The cuts were made by dicing the material 70% through its thickness with a kerf width of 96

μm using a dicing saw (Model 780, K & S-Kulick and Soffa Industries, Willow Grove, PA, USA) at the National Institute of Health (NIH) Medical Ultrasonic Transducer Technology Resource Centre located on The Pennsylvania State University campus (University Park, PA, USA).

For maximum acoustical power transfer from the individual elements to the tissue, a conductive matching layer was designed and fabricated. The thickness and material selection of the matching layer were designed based on the solution to a three layer problem (transducer, matching layer and tissue), which ensured the required maximum power transfer. The PZT-8 material chosen for this design had an acoustic impedance of about 33 $MPa \cdot s \cdot m^{-1}$ and the human tissue has an acoustic impedance of roughly 1.48 $MPa \cdot s \cdot m^{-1}$ (Goss *et al.* 1978, 1980). Since the input and the load impedances are not the same, the intermediate matching layer was used between the piezoelectric material and the human tissue. Analyzing a three layer problem indicated that the maximum power transmission occurs when the characteristic impedance of the matching layer equals the geometric mean of the piezoelectric characteristic impedance and the tissue characteristic impedance. With the longitudinal velocity in the matching layer material of $v_L = 1900\ m \cdot s^{-1}$ and since the resonance frequency of the array (f_o) was 1.2 MHz, the thickness of the matching layer was determined to be:

$$L = \frac{\lambda}{4} = \frac{1}{4}\left(\frac{v_L}{f_o}\right) = \frac{1}{4}\left(\frac{1900\ m \cdot s^{-1}}{1.2 \times 10^6 s^{-1}}\right) = 0.396\ mm. \qquad (5)$$

To construct the matching layer, parafilm was used to affix the piezoceramic to a glass plate with an adhesive primer poured onto the surface of the transducer face. The transducer was surrounded with a rubber dam and the silver conducting matching layer was poured onto the transducer surface. The matching layer, mixed in-housed, was a 2:1,

epoxy to silver mixture of Insulcast 501 (Insulcast, Roseland, NJ, USA) and 2-3 micron silver epoxy (Aldrich, Milwaukee, WI, USA). The whole assembly was centrifuged for 10 minutes and cured overnight. After the rubber assemble was removed, the surface was sanded and lapped to the designed thickness. For the initial prototype, the specially machined, waterproof applicator housing (90 x 60 x 60 mm^3) was made from magnet compatible acrylic.

The capacitance of each element in the array depends primarily on the thickness, permittivity and the surface area. Since the element surface area is small, the capacitance will be small and therefore the element impedance will be large which makes it necessary to find a suitable cable that has a relatively low capacitance per unit length and thus high electrical impedance. For wiring the array, a low capacitance cable (75 Ω, 15 pF/ft and 42 AWG) was used. The choice of such a cable was made based on the difficulty to electrically match small array elements to 50 Ω using high capacitance cables. Figure 3 shows a photograph of the final array.

[Insert figure 3 about here]

The connector between the cable and the amplifier used loose crimp contacts (PEI Genesis, Philadelphia, PA, USA), while the soldering between the cable and the 64 individual array elements used Indalloy #1E (Indium Corporation of America, Utica, NY, USA). This low temperature soldering material ensured that the temperature during soldering did not exceed the curie temperature for PZT-8 material. To drive the array, a specially built amplifier driving system (Advanced Surgical Systems Inc., Tucson, AZ,

USA) was used (Daum 1998). Briefly, this amplifier system was a multi-channel high power, ultrasound phased-array transducer driver for 64 elements which is capable of delivering 60 W per channel with ±1° phase resolution each. To match the impedance of the elements to the amplifier, individual LC (L = inductor and C = capacitor) circuits were built for each of the 64 elements to match each one to the common value of 50 $\Omega\angle 0°$.

2.3 Exposimetry

To determine the acoustic field generated by the array, an automated computer controlled positioning system, which could translate a hydrophone throughout the acoustic field of the array placed in a water tank, was used. The transducer was submerged in water (room temperature, approximately 20°C) in a tank (120 x 50 x 52 cm^3) made almost anechoic with sound absorbing rubber. A custom made degasser, built in-house, was used to reduce the dissolved oxygen content of the distilled water to 1-2 ppm to reduce cavitation. The system was controlled using a personal computer connected to a four-motor positioning system (Velmex Inc., Bloomfield, NY, USA) via the RS232 serial port and also connected, via the general purpose interface bus (GPIB), to a digital oscilloscope (Agilent 54622A, Agilent Technologies, Palo Alto, CA, USA) which recorded the voltage amplitudes detected by the hydrophone. Custom written, Quick Basic (Microsoft Corporation, Redmond, WA, USA) programs were used for automated control of the motors and data acquisition from the oscilloscope. Initially, multiple on-axis (i.e. where the focus is along the major z axis, z_f) exposimetry experiments were performed. With the focus set to 0, 0, z_f mm, z_f was varied from 10

mm to 40 mm with a step size of 2 mm. To determine the repeatability of the focusing, 5-10 experiments were performed at each location. For off-axis studies (i.e. where the focus not on z but aimed toward the x or y axis, x_f or y_f, respectively), the focus was located at x_f, y_f, 30 mm while the steering angle was adjusted to the desired value by choosing appropriate values for x_f and y_f. The steering angle was varied from -14° to +14° with a step size of 2° in both x and y directions with multiple experiments (5-10) performed at each angle. In both the on-axis and off-axis experiments, the scanning step size was 0.5 mm while the scanning area was 20 x 20 mm^2. The hydrophone voltage recordings were used to calculate the normalized intensities based on the pressures that were plotted as the mean and standard deviation of the results ($x \pm$ s.d.) and compared against the calculated values (AIUM 1998; IEEE 1990).

2.4 Ex vivo experiments

To test the feasibility of the array to ablate tissue, the array was submerged 3 cm in the tank aimed perpendicular to the surface of the water. Fresh porcine kidney was obtained, placed in the tank and held in front of the transducer face using metal clamps to ensure that it did not move during the experiments. A distance of 1 cm was maintained between the face of the array and the kidney to mimic the distance of a water bolus used in clinical treatments (Hurwitz *et al.* 2001). Sonication experiments drove each element at an average electrical power of 8 W for 10 seconds for both on- and off-axis focusing. For the off-axis focusing, the steering angle was at 5.7° in the x direction and 13.1° in the y direction. To examine the effects of sonication time, subsequent sonications used exposures of 15 and 20 seconds. At the end of the sonications, the kidney was carefully

removed and sliced with a scalpel to evaluate the ablated areas. Lesions were recorded several times for size using a digital caliper (Techni-Tool Inc., Worcester, PA, USA) and digitally photographed.

3. Results

To test the correlation between experimental and theoretical results, exposimetry experiments were performed. As an example of a typical result at the location (x, y, z) = (0, 3, 30) mm, figure 4a shows a comparison plot along the x axis of the calculated and experimental normalized intensities. Figure 4b plots similar theoretical and experimental data but instead along the y axis for the same focus. For both plots, the theoretical intensity data correlated well with the experimental results. From multiple experiments to evaluate the feasibility of the array to steer the focus, a typical three dimensional normalized intensity result from a focal point was aimed at -2, -0.7, 30 mm. The results were plotted as a mesh (figure 5a) or contour (figure 5b) with contour levels at 90, 70, 50, 30 and 10% of the maximum intensity with the grating lobe levels at about -7.0 dB or less.

[Insert figure 4 about here]

[Insert figure 5 about here]

Ex vivo experiments were also performed to verify the feasibility of the array to generate foci that are capable of ablating tissue. In the first sonication experiment, the

elements were driven at an average power of 8 W for 10 seconds for on-axis focusing. In the plane that was 30 mm deep in tissue and parallel to the face of the array, a cigar shaped lesion with a length of 4.5 mm, along the z axis, and a diameter of 2 mm was observed (figure 6a). Evaluation of the off-axis steering also used an average power of 8 W for 10 seconds to generate three separate lesions at locations (x, y, z) = (-3, -7, 30), (0, 0, 30) and (3, 7, 30) mm. Figure 6b shows a digital photograph of three lesions, each approximately 2 mm in diameter, which corresponded to the intended locations. To determine the effects of sonication time, the location and exposure time was focused at 0, 0, 30 mm for 10 seconds, 0, 0, 34 mm for 15 seconds 0, 0, 39 mm for 20 seconds at 8 W per element. Three lesions were observed with a diameter of 2, 2.9 and 4 mm that corresponded to the sonication times of 10, 15 and 20 seconds, respectively (figure 6c).

[Insert figure 6 about here]

4. Discussion

Intracavitary ultrasound offers an attractive means of focused ultrasound treatment for benign prosthetic hyperplasia with significant advantages over other treatment methods due to the relatively short treatment time, its noninvasive nature and reduced complications. One compelling reason for using an intracavitary device with focused ultrasound is that the prostate is easily accessible via transrectal applicators, which allow for heating of the target volume in the prostate with minimal heating of normal tissue. Using phased arrays to electrically focusing the ultrasound beam provides

a controlled localized power deposition into tissue and reduces significantly the treatment time since the focus is electronically scanned instead of manually.

Previous focused ultrasound array designs were problematic since they required complex methods to move the focus, or had linear (one dimensional) designs that were only capable of focusing along one axis. These drawbacks were the motivation to design a new array that can be used in FUS and at the same time be systematically controlled to reposition the focus throughout a specific volume with an acceptable level of grating lobes. Care was taken with this new 64 element, 8 x 8 array to account for capacitance issues between the ceramic and cables by modeling the system and impedance testing with various cables. Further improvement over this array design seems to be feasible due to recent developments in building focused transducers using piezocomposite technology (Fleury *et al.* 2002). Using piezocomposites removes the concern of low width to thickness ratios, which was an issue in this array design. A three layer PZT-8 material may also be used to increase the capacitance and thus make it easier to electrically match the small elements.

Similar to prostate cancer treatment with focused ultrasound, benign fibroadenomas in breast are currently treated clinically using multiple sonication from a single element transducer which is mechanically scanned (Hynynen *et al.* 2001). In conjunction, magnetic resonance imaging (MRI) for guidance of thermotherapy of the procedure (Quesson *et al.* 2000). Although the treatment has been shown to be effective, the process includes an unnecessary delay due to the mechanical scanning protocol. When closely spaced locations are targeted with focused ultrasound, thermal buildup results from the accumulation of neighboring sonications and the near field heating. As a

result, a lengthy delay between sonications (cooling time) is required to reduce thermal buildup. Investigators have shown that a cooling time of 50-60 seconds was necessary to reduce the heat from the near neighbor sonications (McDannold *et al.* 1999) however this can add considerable time to the procedure and initiate inaccuracies to the MR thermometry through patient motion. With phased arrays a focal pattern can be arranged such that there is enough time for the heat to dissipate by sonicating non-neighboring regions within the tumor (Daum and Hynynen 1998). A treatment planning routine can be plotted over the entire tumor region such that the volume is ablated through distant and non-adjacent ablations to avoid thermal buildup yet destroy the volume in the least amount of time. This research demonstrates the feasibility of an electrically steered array which can be used to ablate tissue for the intended treatment of benign prosthetic hyperplasia. Future plans for will advance this design to a clinical model to be used for *in vivo* studies.

Acknowledgements

This work was supported by the Whitaker Foundation (RG-00-0042) and the Department of Defense Congressionally Directed Medical Prostate Cancer Research Program (DAMD17-0201-0124).

Figure Legends

Figure 1.

Based on the simulations, a diagram of the two dimensional 64 element (8 x 8) tapered array with total size of 20 x 20 mm^2 with the proportions of the ceramic and matching layer illustrated. The diced face of the ceramic was cut 70% through and each individual element was attached to the electrical cabling using low temperature soldering material.

Figure 2.

Before the construction of the array, simulations of the acoustic field were performed to evaluate the focusing of the elements and reduce potential grating lobes. Shown is the normalized intensity (a) in the x and z directions for a focal point at (x, y, z) = (5, 0, 30) mm along with a (b) contour plot values taken at 90, 70, 50, 30, 10% of the normalized intensity with a grating lobe level of 15% of the maximum intensity. A temperature map (c) corresponding to the pressures generated in (a) was numerically solved using the bioheat transfer equation. This simulated figure shows an increase in tissue temperature to the target of 60°C at the focal point using 10 second sonication while outside the target region the temperatures were normal as indicated from the temperature colour bar.

Figure 3.

Photograph of the constructed, waterproof array machined from acrylic with 2.3 m low capacitance cable which connected to the amplifier system.

Figure 4.

Comparison of calculated and experimental normalized intensities for a focus at 0, 3, 30 mm plotted along the (a) x axis and (b) y axis.

Figure 5.

Exposimetry results of the normalized intensity for off-axis focusing with the focal point aimed at -2, -0.7, 30 mm plotted as a (a) mesh or (b) contour with levels indicated at 90, 70, 50, 30, 10%. These results indicate acceptable grating lobes of less than –7.0 dB.

Figure 6.

Ex vivo experimental results of lesions created with on and off-axis focusing with the array driven at an average of 8 W per element for various sonication times. (a) Focusing 30 mm into the tissue, a cigar shaped lesion was created from a 10 second sonication. (b) Evaluation of the electrical steering at (x, y, z) = (-3, -7, 30), (0, 0, 30) and (3, 7, 30) mm created 2 mm diameter lesions. (c) Effects of the sonication time variation are illustrated from exposure times of 10, 15 and 20 seconds.

Reference List

[1] Stephens F. All about prostate cancer. South Melbourne, Australia; New York: Oxford University Press, 2000.

[2] Tan JS, Frizzell LA, Sanghvi NT, Seip R, Wu JS, Kouzmanoff JT. Design of focused ultrasound phased arrays for prostate treatment. *IEEE Ultrasonics symposium* 2000:1247-51.

[3] Seip R, Sanghvi NT. Comparison of split-beam transducer geometries and excitation configuration for transrectal prostate HIFU treatments. *IEEE Ultrasonics symposium* 2001:1343-46.

[4] Ebbini ES, Bischof JC, Coad JE. Lesion formation and visualization using dual-mode ultrasound phased arrays. *IEEE Ultrasonics symposium* 2001:1351-54.

[5] Yao H, Phukpattaranont P, Ebbini ES. Enhanced lesion visualization in image-guided noninvasive surgery with ultrasound phased arrays. *23rd annual EMBS international conference, IEEE* 2001:2492-95.

[6] Barrett DM. Mayo Clinic on prostate health. 1st ed. Rochester, Minn.: Mayo Clinic; New York, 2000.

[7] Hutchinson EB, Hynynen K. Intracavitary phased arrays for non-invasive prostate surgery. *IEEE Trans Ultrason Ferroelectr Freq Control* 1996;43:1032-42.

[8] Sokka S, Hynynen K. The feasibility of MRI guided whole prostate ablation with a linear aperoidic intracvitary ultrasound phased array. *Phys Med Biol* 2000;45(11):3373-83.

[9] Buchanan MT, Hynynen K. Design and experimental evaluation of intracavitary ultrasound phased array system for hyperthermia. *IEEE Trans Biomed Eng* 1994;41:1178-87.

[10] Zemanek J. Beam behavior within the nearfield of a vibrating piston. *J Acoust Soc Am* 1971;49:181-91.

[11] Pennes HH. Analysis of tissue and arterial blood temperatures in the resting human forearm. *J Appl Physiol* 1948;1:93-122.

[12] Nyborg WL. Heat generation by ultrasound in a relaxing medium. *J Acoust Soc Am* 1981;70:310-12.

[13] Smith NB, Buchanan MT, Hynynen K. Transrectal ultrasound applicator for prostate heating monitored using MRI thermometry. *Int J Radiat Oncol Biol Phys* 1999;43:217-25.

[14] Hutchinson EB, Buchanan MT, Hynynen K. Evaluation of an aperiodic phased array for prostate thermal therapies. *IEEE Ultrasonics symposium* 1995:1601-04.

[15] Goss SA, Johnston RL, Dunn F. Comprehensive compilation of empirical ultrasonic properties of mammalian tissues. *J Acoust Soc Am* 1978;64:423-57.

[16] Goss SA, Frizzell LA, Dunn F. Ultrasonic absorption and attenuation in mammalian tissues. II. *J Acoust Soc Am* 1980;68:93-108.

[17] Daum DR. A large scale phased array ultrasound system for non-invasive surgery of deep stated tissue [PhD dissertation]. Cambridge (MA): Massachusetts Institute of Technology; 1998.

[18] Hurwitz MD, Kaplan I, Svensson GK, Hansen J, Hynynen K. Feasibility and patient tolerance of a novel transrectal ultrasound hyperthermia system for treatment of prostate cancer. *Int J Hyperthermia* 2001;17(1):31-7.

[19] Fleury G, Berriet R, Le Baron O, Huguenin B. New piezocomposite transducers for therapeutic ultrasound. *Workshop on MRI-guided focused ultrasound surgery* 2002:39.

[20] Hynynen K, Pomeroy O, Smith DN, Huber PE, McDannold NJ, Kettenbach J, *et al.* MR imaging-guided focused ultrasound surgery of fibroadenomas in the breast: a feasibility study. *Radiology* 2001;219:176-85.

[21] Quesson B, de Zwart JA, Moonen CT. Magnetic resonance temperature imaging for guidance of thermotherapy. *J Magn Reson Imaging* 2000;4:525-33.

[22] McDannold NJ, Jolesz FA, Hynynen KH. Determination of the optimal delay between sonications during focused ultrasound surgery in rabbits by using MR imaging to monitor thermal buildup in vivo. *Radiology* 1999;211:419-26.

[23] Daum DR, Hynynen K. Thermal dose optimization via temporal switching in ultrasound surgery. *IEEE Trans Ultrason Ferroelectr Freq Control* 1998;45(1):208-15.

Figure 1

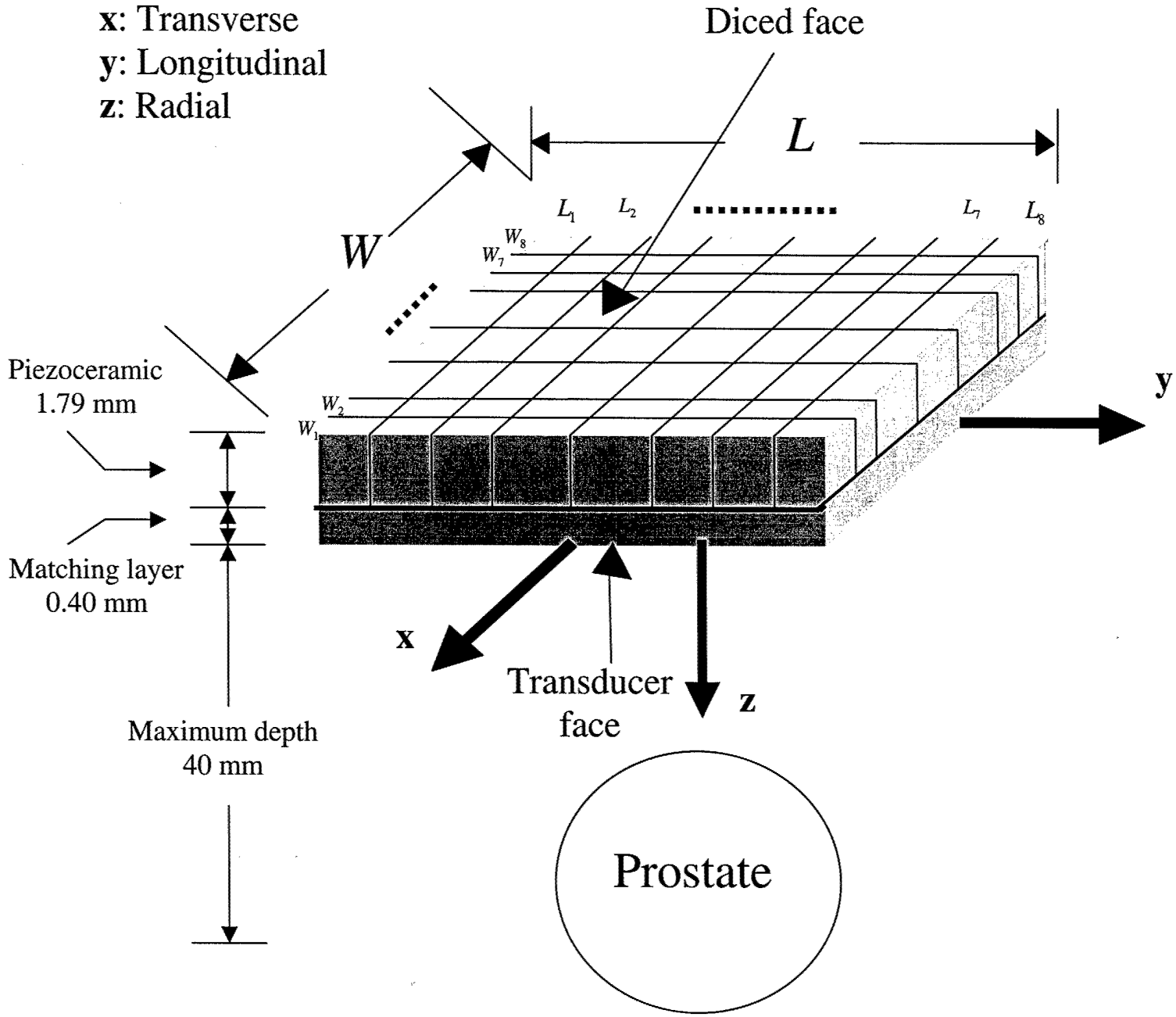
x: Transverse
y: Longitudinal
z: Radial
Diced face
L
W
L_1
L_2
L_7
L_8
W_8
W_7
W_2
W_1
y
Piezoceramic
1.79 mm
Matching layer
0.40 mm
x
Transducer
face
z
Maximum depth
40 mm
Prostate

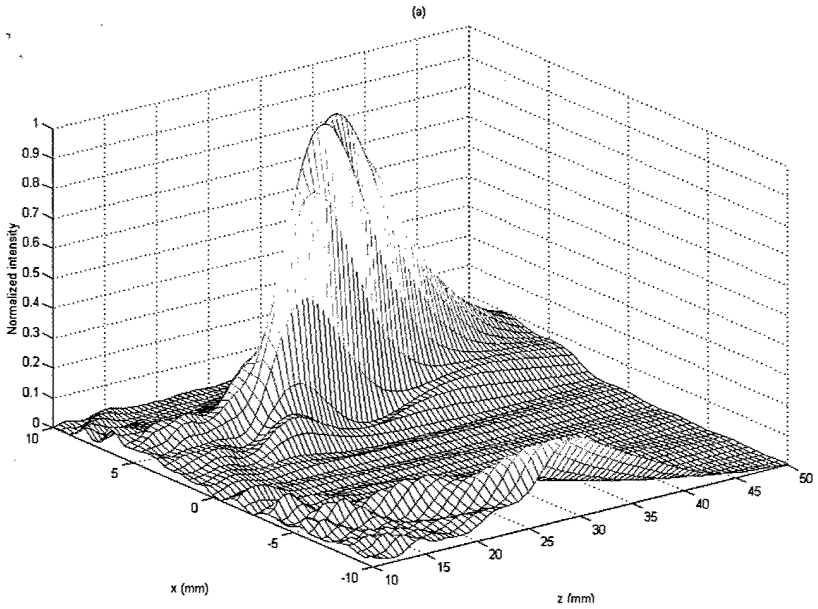

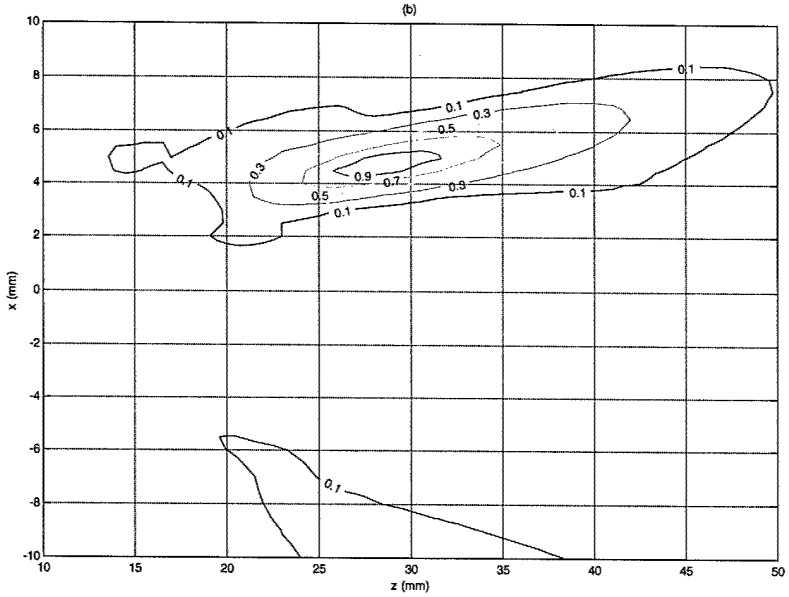

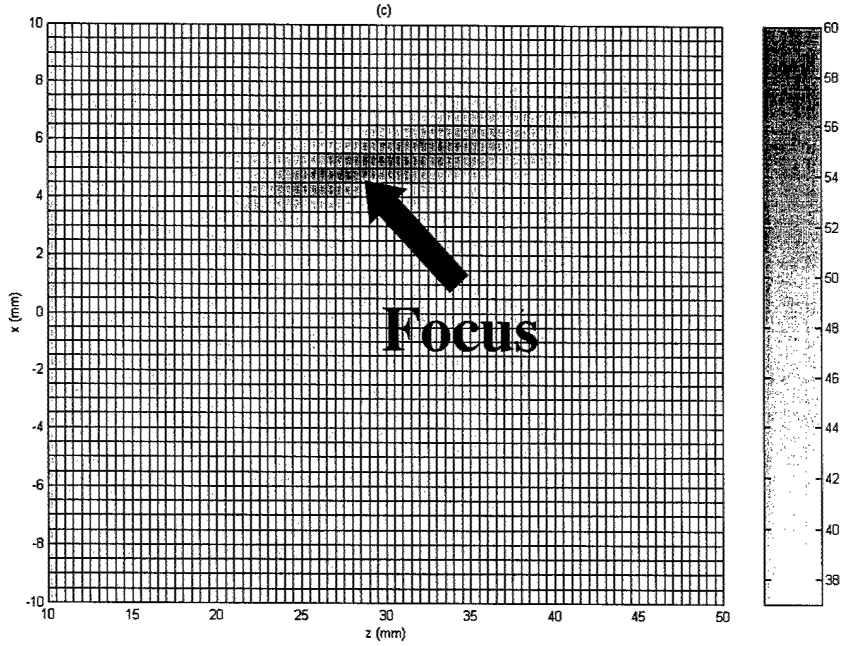

Figure 2

Figure 3

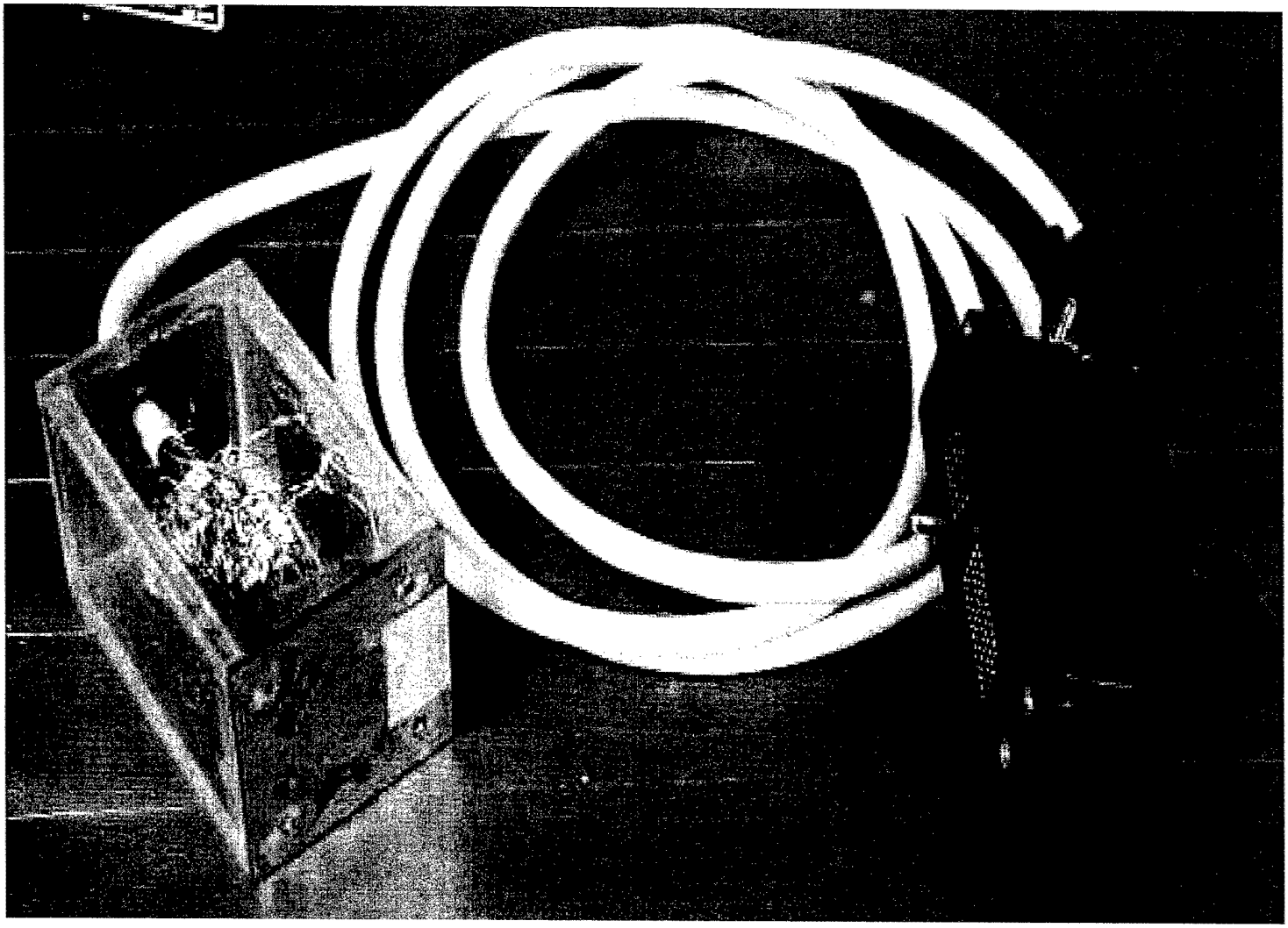

Figure 4

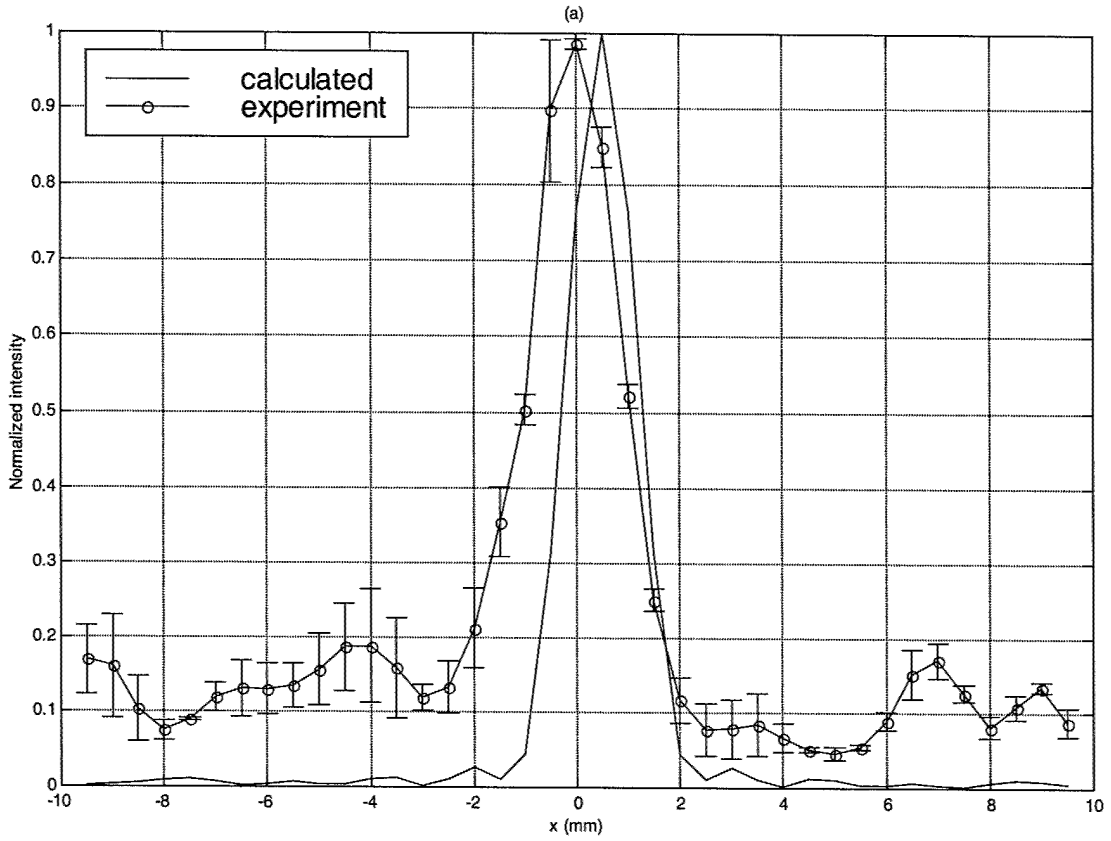
(a)
calculated
experiment
Normalized intensity
x (mm)

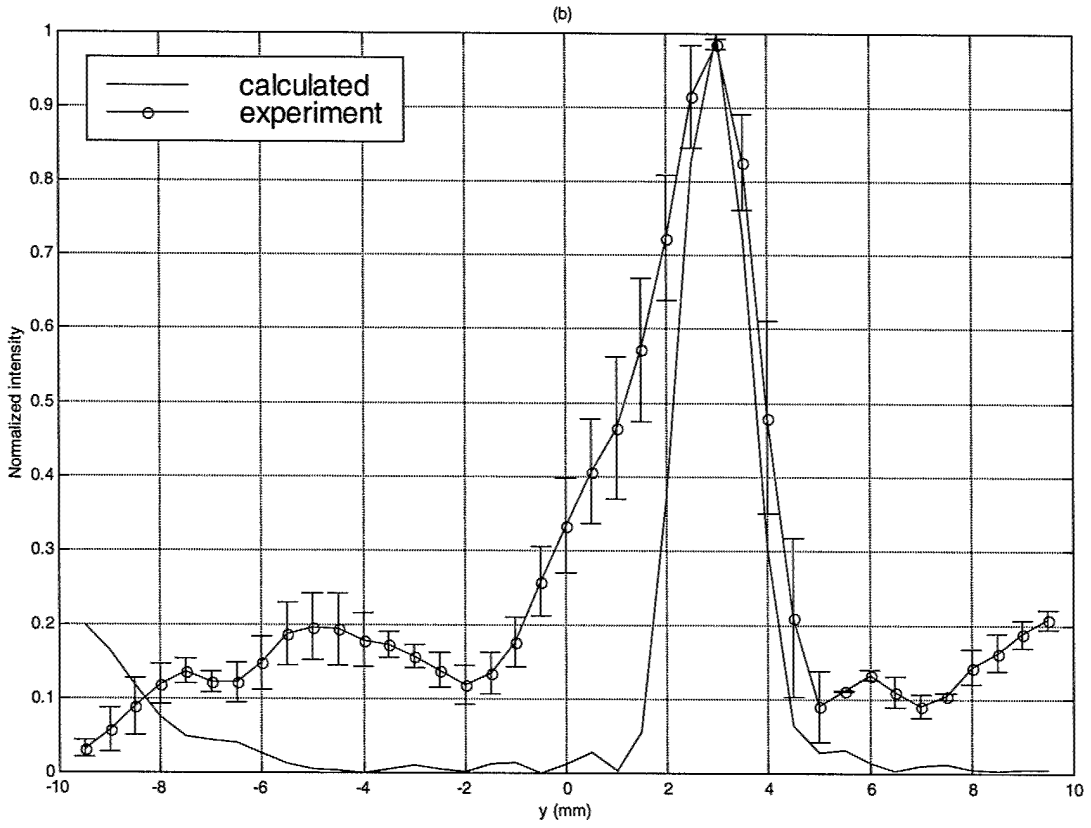
(b)
calculated
experiment
Normalized intensity
y (mm)

Figure 5

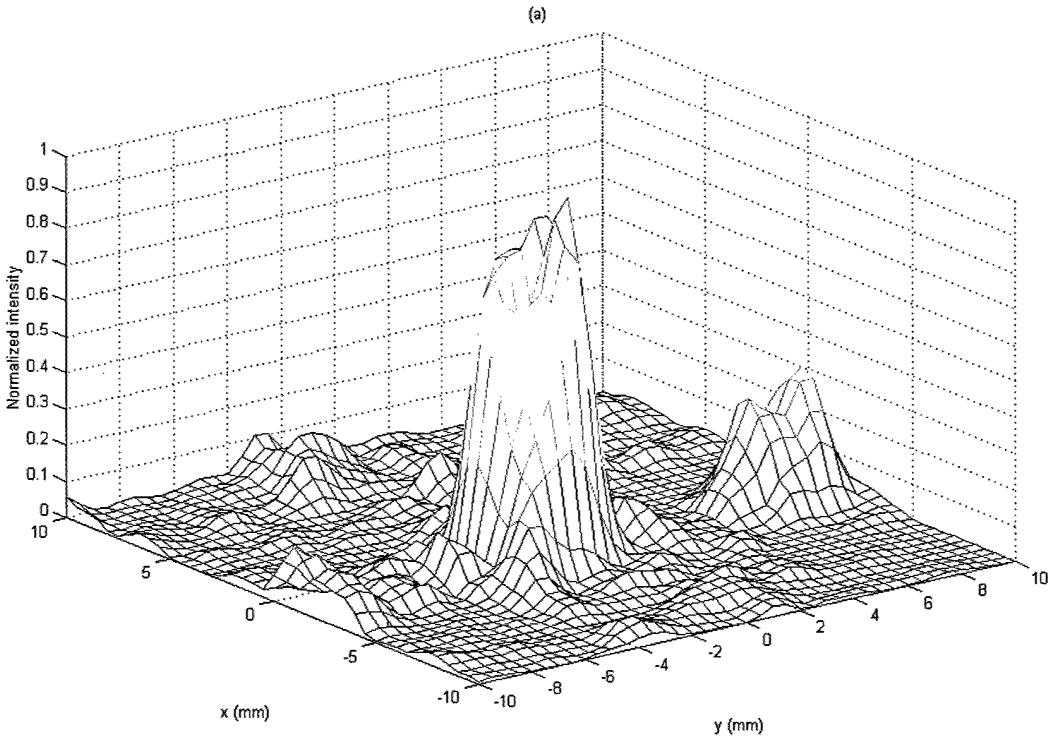
(a)
Normalized intensity
1
0.9
0.8
0.7
0.6
0.5
0.4
0.3
0.2
0.1
0
10
5
0
-5
-10
x (mm)
-10
-8
-6
-4
-2
0
2
4
6
8
10
y (mm)

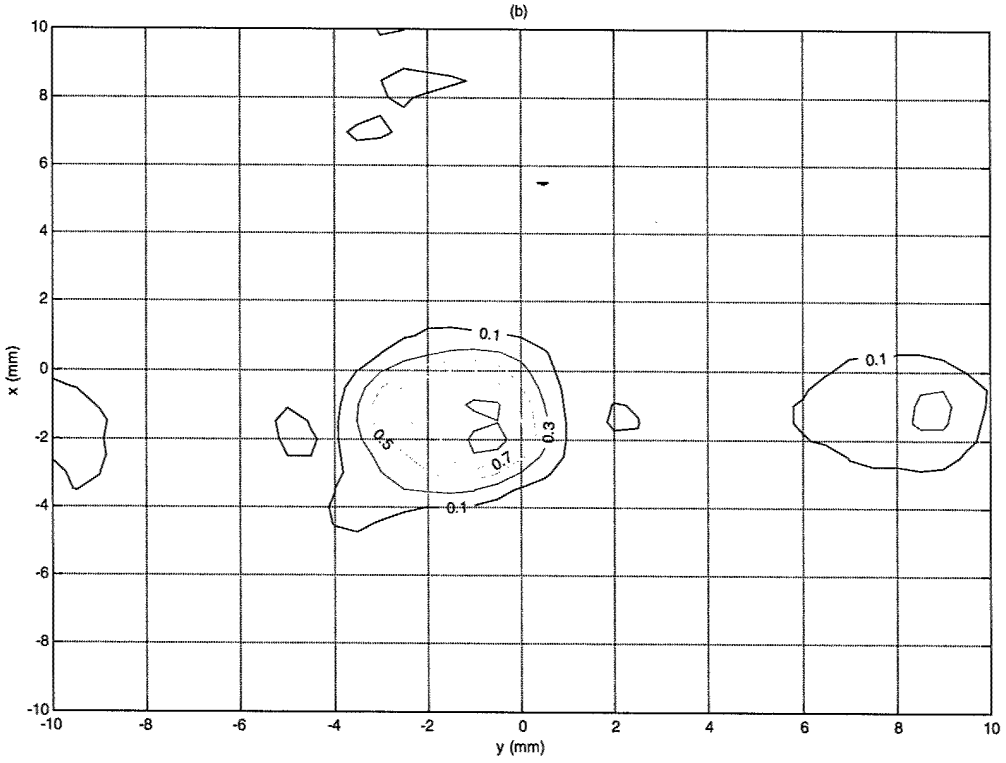
(b)
x (mm)
10
8
6
4
2
0
-2
-4
-6
-8
-10
-10
-8
-6
-4
-2
0
2
4
6
8
10
y (mm)
0.1
0.1
0.3
0.5
0.7
0.1

Figure 6a

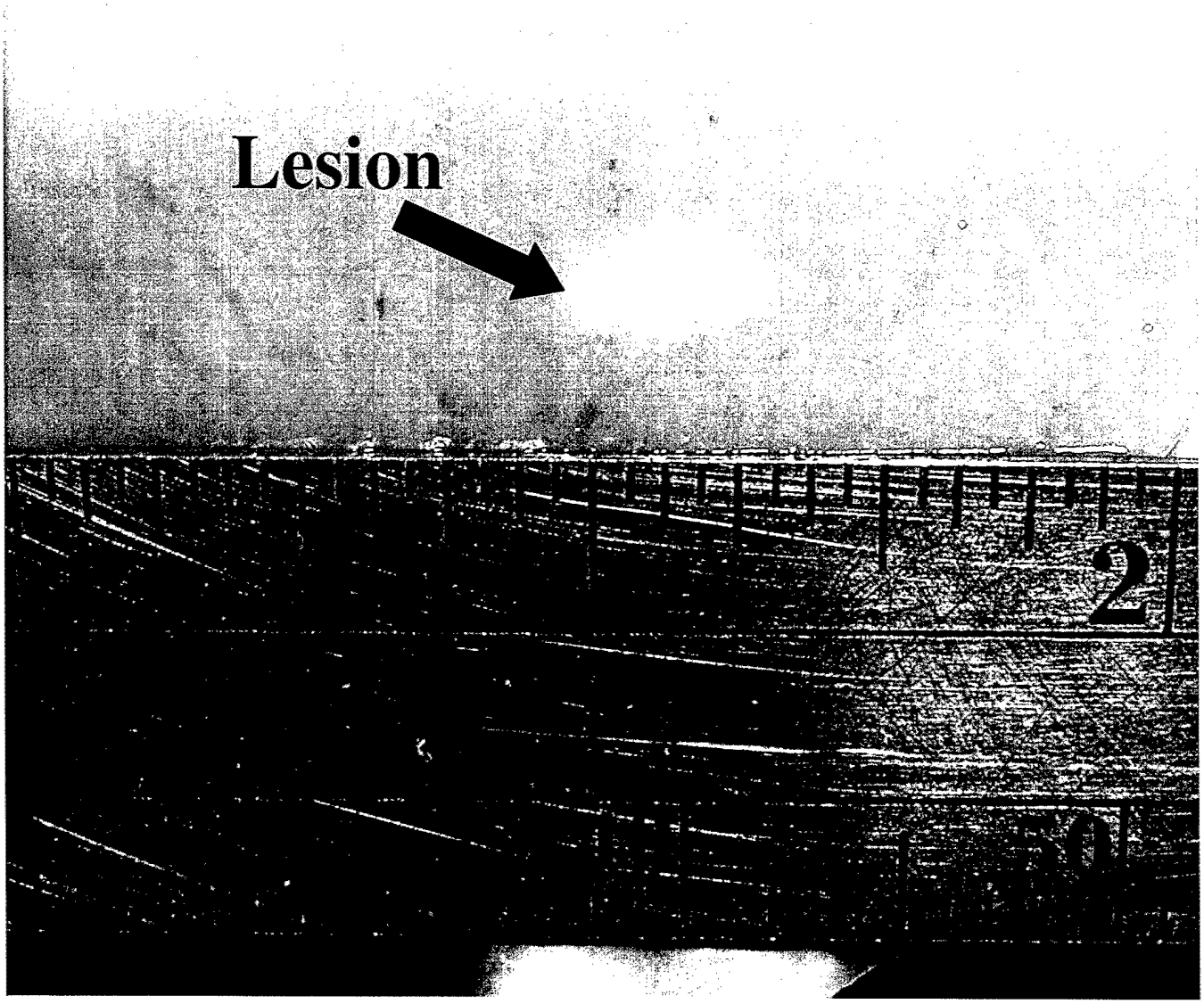

Figure 6b

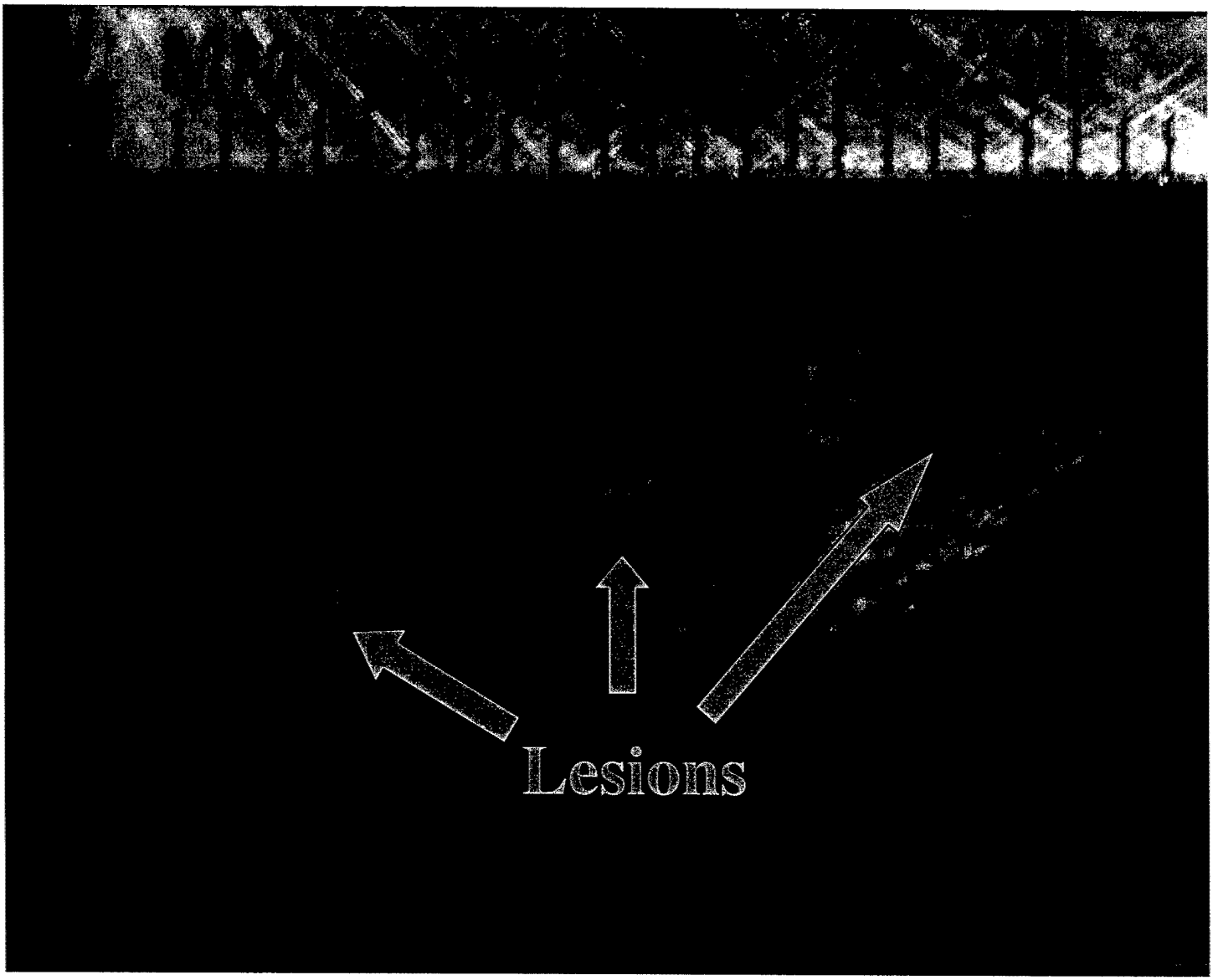

Figure 6c

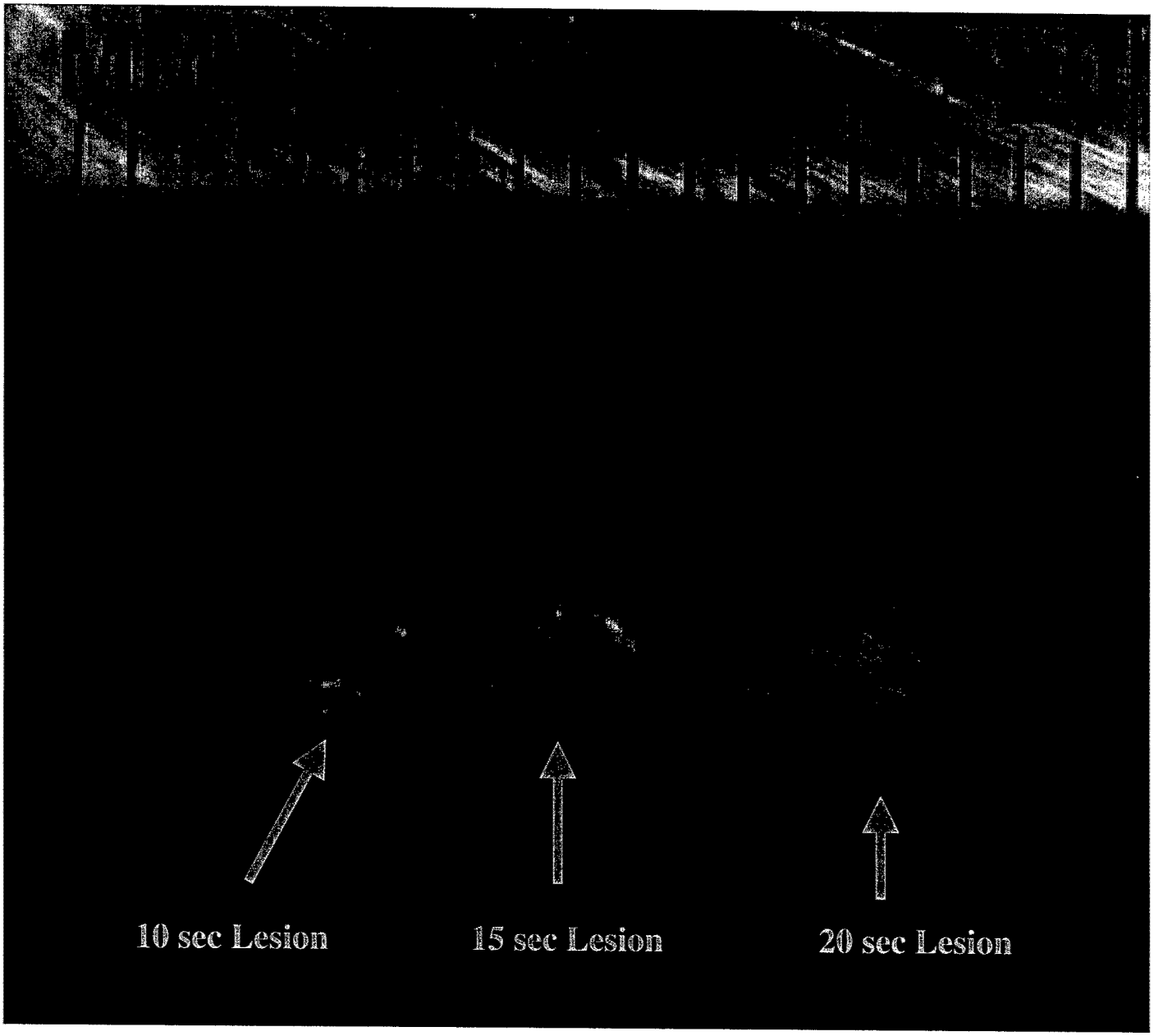

Workshop on

MRI-Guided: Focused Ultrasound Surgery

SYLLABUS

19-21 June 2002

Cambridge, Massachusetts, USA

INTERNATIONAL SOCIETY FOR
ISMRM
MAGNETIC RESONANCE IN MEDICINE

Two Dimensional Array Design for Tissue Ablation for Treatment of Benign Prosthetic Hyperplasia

[1] Khaldon Y. Saleh and [2] Nadine Barrie Smith
Department of Bioengineering, The Pennsylvania State University, University Park, PA 16802
[1] kysbio@engr.psu.edu (presenter), [2] nbs@engr.psu.edu
814-865-8087(office) 814-863-0490 (fax)

Abstract

For treating prostate disease such as benign prosthetic hyperplasia, a two dimensional ultrasound array has been designed and constructed. Intracavitary ablation of tissue requires an array be small in size and be able to electrically steer the focus within the prostate volume without physically moving the device. The goal of this research was to design and construct an ultrasound array that will be capable of focusing and steering in a three dimensional volume. After theoretically designing the array using the calculated pressure field and the bioheat transfer equation, a small two dimensional array was cut 70% through the ceramic (PZT-8) using a dicing saw into an eight by eight aperoidic design (total size, 2 x 2 cm^2). The structural integrity of the array face was fortified with a unique matching layer for maximum acoustic power transfer to tissue. With regards to the cabling of a multi element device, analysis of the transducer ceramic and cable impedance has been designed for maximum power transfer with minimal capacitance and diameter. For this initial prototype, the final construction used MRI compatible housing and cabling. From the numerical analysis, array has the capability of focusing and steering in a three dimensional volume with a steering angle of ±14° and has the ability to necrose tissue.
key words: transducer design, two dimensional array, beamsteering, matching layer

Introduction

Focused ultrasound has been shown to give promising results in treating benign prosthetic hyperplasia (BPH). Although BPH is not life threatening, treatment is necessary since normal urine flow can be blocked as a result of prostate pushing against the urethra and the bladder. The goal of this research is to construct, computationally and experimentally, a two-dimensional intracavitary phased array suitable for tissue ablation in the prostate. Part of the design criteria is that a specific region in a target volume will be ablated by focusing the ultrasound beam at that region using short high temperature sonications. A magnetic resonance imaging (MRI) compatible, ultrasound phased array will be presented for the treatment of BPH.

Previous one dimensional prostate array transducer geometries include a 64 x 1 aperiodic, linear array which reduced grating lobes and could electrically adjust the focus at distal and proximal locations along the urethra [1], and a 60 x 1, linear array with a mechanical rotation which could electrically steer the focus along the urethra and mechanically steer left and right of the mid-saggital urethra [2]. The drawbacks behind these prostate arrays are that they can only focus at distal or proximal locations along the urethra or complex mechanics which move the focus. The advantage with a two dimensional array is that it can electrically focus at distal and proximal locations along the urethra and left and right of the mid-saggital line by changing the phase to the elements. The difficulty with designing a two dimensional array is the dicing of the ceramic while maintaining a structural grounding plane for the individual elements. To overcome this problem, the elements of the ceramic can be partially diced and the structural integrity of the transducer face can be maintained with an acoustic matching layer. An additional problem is the impedance matching to 50 ohms for a ceramic diced into small elements. This research presents a small, eight by eight two dimensional ultrasound array designed to ablate tissue while overcoming many problems involved with transducer fabrication.

Materials and Methods

Array Design:

A two dimensional ultrasound phase array has been designed to be able to focus, and thus ablate tissue, and steer inside a volume of interest. The array was designed to heat the entire prostate from the limited confines of the rectum. As with previous array designs, Huygen's principle, which models each surface element as a grid of simple sources and then sums the contribution from the field, was used to

model the pressure field [3]. From the pressure field, the temperature increase in the tissue volume was determined using the bioheat transfer equation [4]. Based on the computational results, a two dimensional (8 x 8) design using 64 elements was chosen (Fig. 1). The size was a 2 x 2 cm^2 array, with individual elements with equal lengths and widths of 2.00, 2.33, 2.66, 3.00, 3.00 , 2.66, 2.33, 2.00 mm for elements 1, 2, ..., 8, respectively. All ceramics were cut using a dicing saw (Model 780, K & S-Kulick and Soffa Industries, Willow Grove, PA) at the NIH Medical Ultrasonic Transducer Technology Resource Center (University Park, PA, USA).

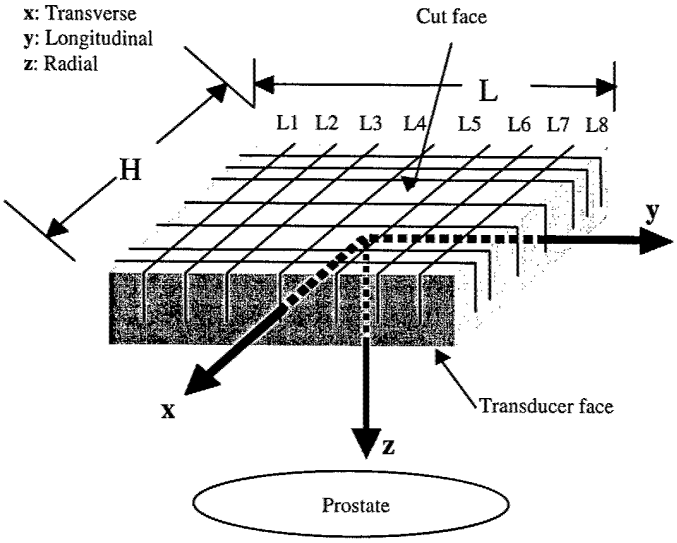

Fig. 1. The upper face is the cut face of the transducer in which the 70% cut through is made, in this face, the 64 elements are visible. The other side of the array is the transducer face, which radiates the ultrasound wave into the prostate.

From the analysis, this array was capable of focusing and steering with a steering angle of 14° with maximum focal depth of 4 cm. For off-axis focusing, Figure 2a shows the normalized pressure field in the x, z plane (x = transverse, z = radial) locations of 5, 30 mm, respectively, while Figure 2b shows the temperature distribution at the same location. In the y, z plane (y = longitudinal, z = radial), Figure 2c shown the pressures at -5, 30 mm, respectively, with the temperature rise at this locations also plotted (Fig. 2d).

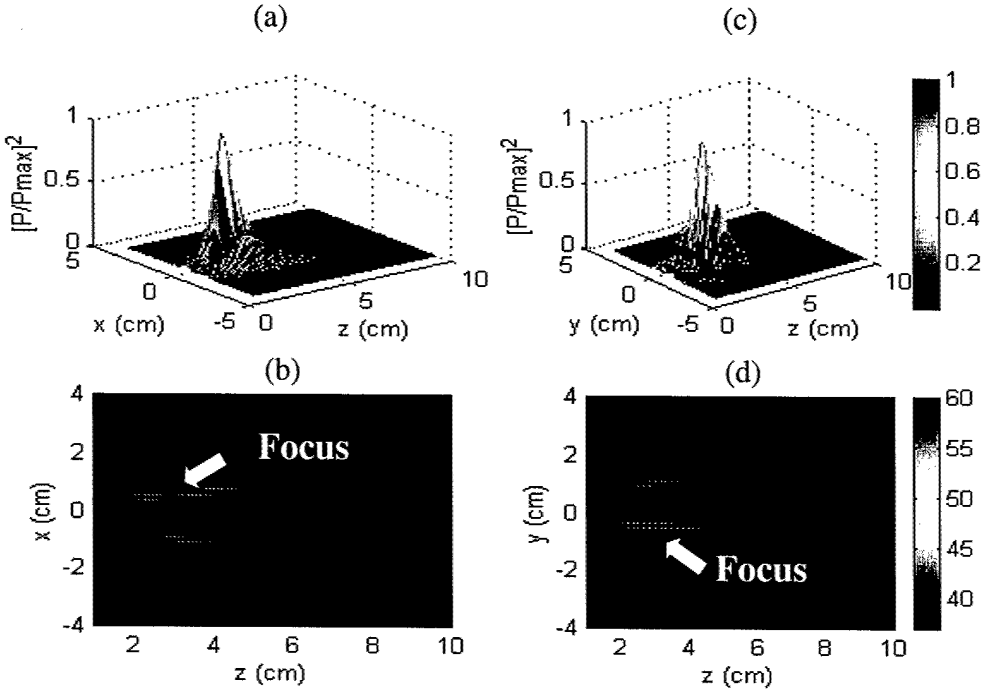

Fig. 2. Pressure field distribution was calculated using Rayleigh-Sommerfeld equation for a focus at (5, -5, 30) mm in the (a) x, z plane (c) y, z plane, and the temperature distributions corresponding to (a) and (c) in (b) and (d) respectively.

Matching layer:

The piezoelectric material has an acoustic impedance of about 33 MPa·s/m and the human tissue (also water) has an acoustic impedance of about 1.48 MPa·s/m [5]. Based on the maximum power transfer, the load (human tissue) must have the same acoustic impedance as the input impedance (piezoelectric impedance). Since the input and the load impedances are not the same, an intermediate layer (matching layer) must be put between the piezoelectric material and the human tissue thereby becoming a three layer problem to be solved. Applying the continuity of normal specific acoustic impedance at the boundaries with some algebraic manipulation yields that the maximum intensity transmission coefficient, T, (and thus the power transmission coefficient since the surface area is the same at both the transmitting and receiving sides) occurs when the thickness of the matching layer equals an integer multiple of quarter a wavelength [$L = (2n-1)\lambda/4$ n = 1, 2, 3, ...].

To construct the matching layer, parafilm was used to wax the ceramic to a glass plate. Adhesive primer was poured into the surface of the transducer face. The transducer was surrounded with a rubber dam and the silver conducting matching layer was poured onto the transducer surface. The matching layer (mixed in-housed) was a 2:1, epoxy to silver mixture of Insulcast 501 (Insulcast, Roseland, NJ, USA) and 2-3 micron silver epoxy (Aldrich, Milwaukee, WI, USA). The whole assembly was centrifuged for 10 minutes and cured overnight. After the rubber assemble was removed, the surface was sanded and lapped to the designed thickness.

Cable impedance:

Permittivity is an important factor in determining the electrical performance of a lead zirconate titanate (PZT) ceramics. The effect of permittivity becomes more evident when the surface area of the individual elements of the array are small, which is the case in this design. For a PZT-8 material, element with dimensions of 2 x 2 mm^2 dimensions and resonance frequency of 1.5 MHz, the element capacitance was found to be 20.63 pF, which means an element impedance of 5.14 kΩ magnitude. Since the load impedance (element impedance) was high, the cable has to be a low capacitance cable which effectively means high cable impedance, so a cable with high characteristic impedance is necessary for our requirement. It has been found that a cable with a characteristic impedance of 75 Ω was suitable. A 75 Ω, 15 pF/ft and 42 AWG was used. The electrical connection to the amplifier side was done using loose crimp contacts (PEI Genesis, Philadelphia, PA), while the connection to the PZT was using Indalloy # 1E (Indium Corporation of America, Utica, NY), which is a low temperature soldering material that was used to be sure that the temperature during soldering did not exceed the curie temperature for PZT-8 material.

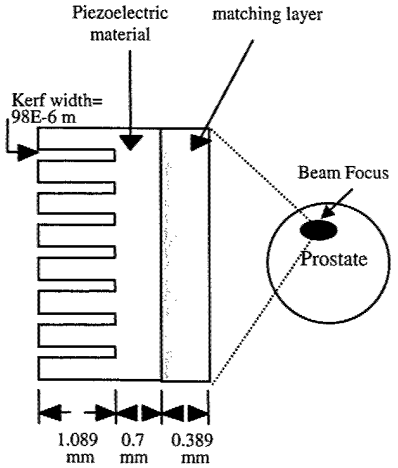

Fig. 3. Side view of the piezoelectric material and the matching layer, which shows the 70% cut through ceramic. The layer acoustically matches the high characteristic impedance piezoelectric material to the low characteristic impedance human tissue.

Results

Based on the design criteria, lead zirconate titanate type 8 (PZT-8) ceramic was chosen for the final design based on its efficiency as a high power device. The PZT-8 material (TRS Ceramics, State College, PA, USA) was cut 70% through the ceramic with a kerf width of 98 μm on the dicing saw (Fig. 3). Although many computational transducer designs account for element size, very few take into account the final effect of the kerf size between each element. For this design, total of kerfs would be about 0.7 mm from the original array layout which can potentially effect the ability to properly steer the beam.

To give maximum acoustic transmission from the ceramic to the tissue and maintain the integrity of the two dimensional design, a matching layer was placed onto the transducer surface with a thickness

of L = 0.389 mm (Fig. 3). The matching layer was found to firmly hold the array together while attaching the electrodes (Fig. 4a) to the individual element and be submerged for in indefinite length underwater without any leakage problems at the array face.

As an early phase prototype and not a clinical device, a water tight magnet compatible assembly for the 64 element phased array is shown in Fig. 4b. The array is shown connected to a 2.3 m long DL cable connector cable. The DL connector can easily be attached to a specially built amplifier driving system (Advanced Surgical Systems, Inc, Tucson, AZ). With this design, each element of the transducer was matched to the 50 ohm impedance of the amplifier.

(a) (b)

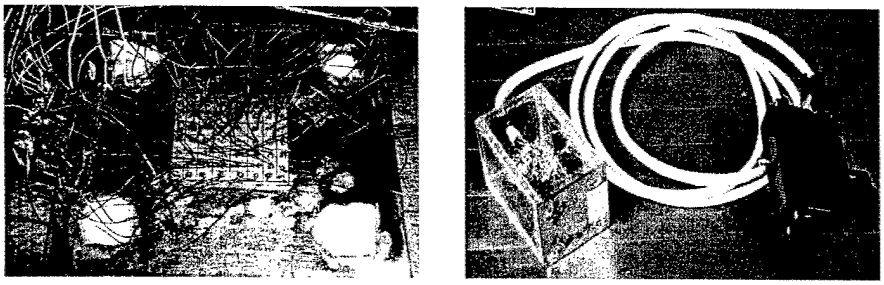

Fig. 4. The actual array (a) after finishing soldering the coaxial cable to the array (b) the final array that includes a 2.3 m coaxial cable and a water proof housing to be used in water.

Discussion

Exposimetry of a previously constructed four by five array had very good agreement between the theoretical and experimental results [6]. Unfortunately the earlier array suffered from power mismatch between the transducer elements and the cabling. Greater care was taken with this new 64 element, eight by eight array to account for capacitance issues between the ceramic and cables by modeling the system and impedance testing with various cables. Moreover, earlier array designs also had problems with water leakage into the interior housing of the array however the matching layer has solved this situation.

To choose an appropriate PZT material to be used in such an application is an issue of great importance, Although PZT-5H has a better performance if compared to PZT-4 and PZT-8, from a capacitance point of view, it cannot handle the large power that is used in tissue ablation. PZT-4 and PZT-8 are good candidates concerning power, with an advantage for PZT-8 over PZT-4. Following designs may use three layer PZT-8 material to increase the capacitance, and thus make it easier to electrically match. The matching layer helped to mechanically match the PZT material to the load, while the impedance matching circuits helped to electrically match the electrical impedance of the cable and load to the amplifier.

Acknowledgments: This work was supported by the Whitaker Foundation (RG-00-0042) and the Department of Defense Congressionally Directed Medical Prostate Cancer Research Program (DAMD 17-0201-0124).

References

[1] Hutchinson, E. B., Buchanan, M. T., and Hynynen, K., "Design and optimization of an aperiodic ultrasound phased array for intracavitary prostate thermal therapies," *Med.Phys.*, vol. 23, no. 5, pp. 767-776, May1996.

[2] Sokka, S. and Hynynen, K. "The feasibility of MRI guided whole prostate ablation with a linear aperoidic intracvitary ultrasound phased array" Phys. Med. Biol., 45 (11), 3373-3383, 2000.

[3] Zemanek, J., "Beam behavior within the nearfield of a vibrating piston," *J Acoust Soc Am*, vol. 49 pp. 181-191, 1971.

[4] Pennes, H. H., "Analysis of tissue and arterial blood temperatures in the resting human forearm.," *Journal of Applied Physiology*, vol. 1, no. 2, pp. 93-122, 1948.

[5] Kinsler, L. E., Frey, A. R., Coppens, A. B., and Sanders, J. V., *Fundamentals of Acoustics*, 3rd ed. New York: John Wiley & Sons, 1982.

[6] Helser, J. L., Sparrow, V. W., and Smith, N. B., "Two-dimensional ultrasound phased array for treatment of benign prostatic hyperplasia," *J Acoust Soc Am*, vol. 5 pp. 2546, 2000.

PENNSTATE

Department of Bioengineering

Two Dimensional Array Design for Tissue Ablation for Treatment of Benign Prosthetic Hyperplasia

Khaldon Y. Saleh and Nadine Barrie Smith
College of Engineering
The Pennsylvania State University
University Park, PA 16802

Outline

- Introduction.
- Proposed design.
- Simulation results.
- Construction issues.
- Exposimetry.
- Conclusion.

Introduction

- ✓ 2-D array design.
- ✓ Focusing and Steering in a 3-D volume.
- ✓ Matching layer to increase acoustical transmission.
- ✓ Low capacitance cable to be able to match.
- ✓ Matching circuits to increase electrical transmission.

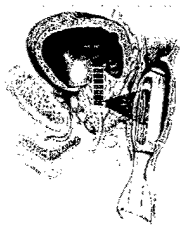

http://www.focus-surgery.com

Proposed design

8 x 8 two dimensional phased array.

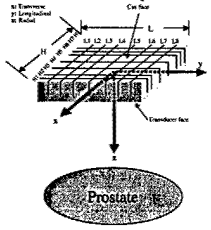

Frequency: 1.2 MHz.
Ceramic: PZT-8.

Li = [2.00 2.33 2.66 3.00 3.00 2.66 2.33 2.00]
Hi = [2.00 2.33 2.66 3.00 3.00 2.66 2.33 2.00]

Simulation results

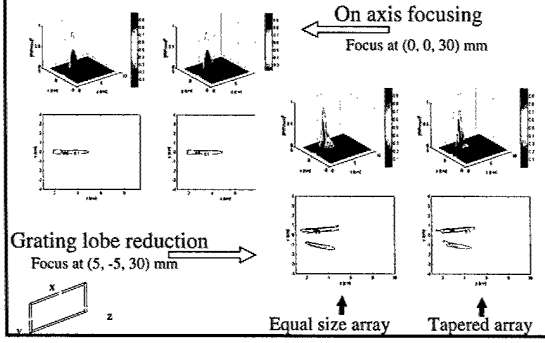

Simulation results

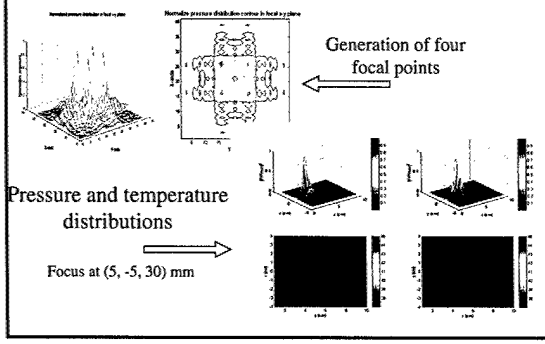

Construction issues – *Ceramic types*

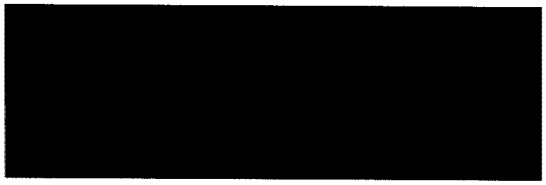

Construction issues - *Transducer Dicing*

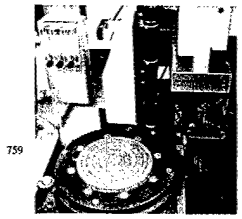

Dicing saw model 780, K & S-Kulick and Soffa Industries (Willow Grove, PA)
The NIH Medical Ultrasonic Transducer Technology Resource Center (University Park, PA, USA)

Construction issues - *Matching layer*

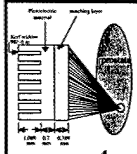

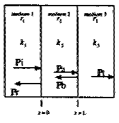

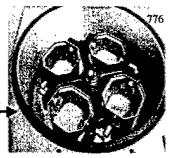

$$T = \frac{4r_{13}}{(r_{12} + r_{23})^2} \quad \text{where} \quad r_{ij} = r_i / r_j$$

$T = 1.0$ *occurs when*

$r_2 = \sqrt{r_1 r_3}$ *and* $L = (2n-1)\lambda/4$

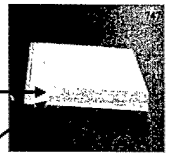

Construction issues - *Cable impedance*

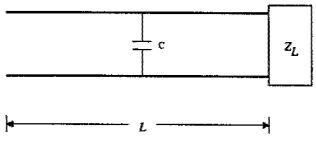

$$C_e = \frac{\varepsilon_{33} A_e}{t} = 20.63 \text{ pF} \qquad C = C_m[pF/m] \text{ x } L[m]$$

$$Z_{cable} = \frac{1}{j\omega_0 C} \qquad Z_{in} = \frac{Z_0}{j\tan(\beta L)}$$

Construction issues - *Impedance matching*

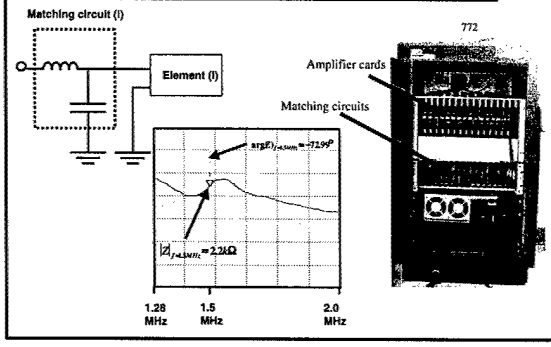

Construction

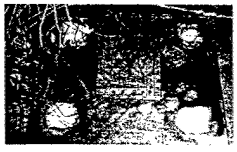

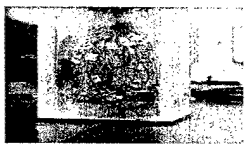

- Water proof.
- MRI compatible.

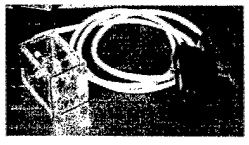

Exposimetry

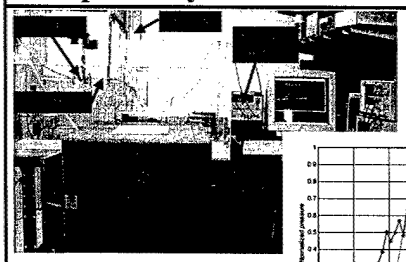

Focus at (0, 0, 30) mm

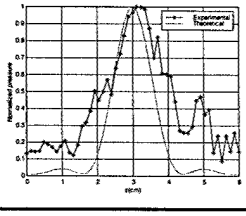

Conclusion

- A 2-D phased array capable of focusing and steering in a volume.
- Matching layer to acoustically match.
- Matching circuits to electrically match.
- Low capacitance cable to prevent loss of power due to the high element impedance.
- The final array was water proof and MRI compatible.
- Initial experimental data was taken.

Acknowledgments

- Whitaker Foundation.
- Department of Defense Congressionally Directed Medical – Prostate Cancer Research Program – Idea Development Award.

Thesis Proposal for the Ph.D. Degree
in
Bioengineering

Optimized Hyperthermia Treatment of Prostate Cancer Using a Novel Intracavitary 2D Ultrasound Array

Submitted by: O. Al-Bataineh Date: JAN 03

Proposed Duration of studies: Starting: JAN 03 Ending: JAN 05

Thesis Advisor: Name: Dr. Nadine Barrie Smith
Title: Assistant Professor, Bioengineering Department

Thesis Committee Approval:

Members:	Approval
Nadine Barrie Smith, Advisor Assistant Professor, Bioengineering Department	---------- Signature Date
Roger Gaumond Associate Professor, Bioengineering Department	---------- Signature Date
Robert Keolian Associate Professor, Graduate Program in Acoustics	---------- Signature Date
Victor Sparrow Associate Professor, Graduate Program in Acoustics	---------- Signature Date
Jeffry D. Zahn Assistant Professor, Bioengineering Department	---------- Signature Date

Department Approval:

Chairman, Bioengineering Department Professor Herbert H. Lipowsky	---------- Signature Date

Outline

Abstract

Cancer of the prostate is the most commonly diagnosed non-skin cancer in America and tends to disproportionately affect men who are members of minority groups (Fig. 1). An estimated 190,000 men are diagnosed with prostate cancer, and 37,000 are dieing of it every year. Localized hyperthermia is a useful adjuvant to chemotherapy and radiotherapy in treatment of prostate cancer. Intracavitary ultrasound offers an attractive means of noninvasive localized hyperthermia treatment for prostate cancer with reduced side effects compared to competing modalities. In a hyperthermia treatment, the entire prostate gland is typically heated to about 43°C for times up to 1 hour. This could be done if the applied ultrasonic wavefields are optimized to specifically target prostate tissue. Recent advances in tissue modeling, numerical methods for ultrasound simulation, and magnetic resonance (MR) thermometry can now be employed to achieve this optimization of ultrasound hyperthermia treatment. Application of ultrasound therapy specifically tailored to the physiological characteristics of the prostate and surrounding tissue will result in a uniform hyperthermia treatment with minimal effects elsewhere. The goals of the proposed research are to determine optimal wavefield characteristics for specific thermal treatment of the prostate, to design and implement an optimized transducer for prostate hyperthermia, and to confirm the new transducer's performance through *ex vivo* and *in vivo* experiments.

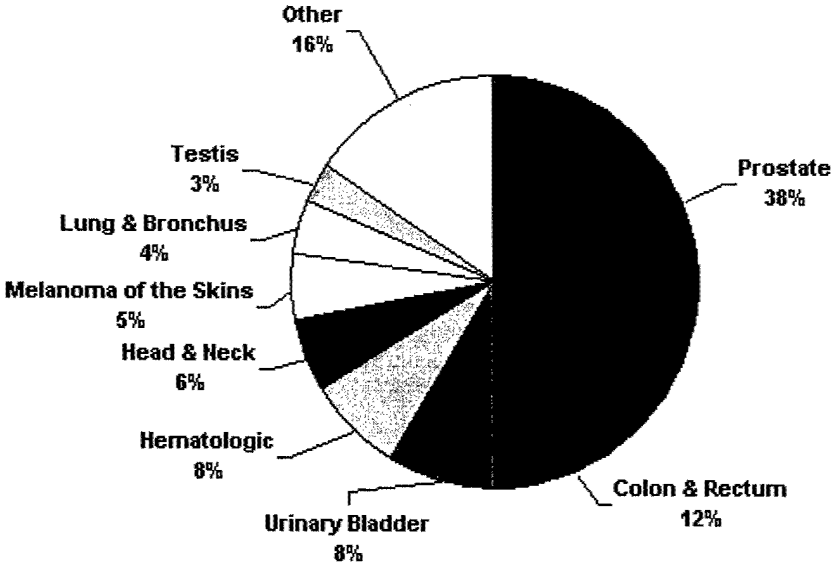

Fig. 1. The percentage of diagnosed cancers among males as reported by the National Cancer Institute, 2000.

A. Specific Aims

A two-dimensional ultrasound array will be designed and optimized depending on a realistic modeling of the prostate cancer. The proposed array is supposed to elevate the temperature of the whole prostate gland to a nontoxic thermal level to disrupt the biological activity of the cancer's cells while treated with radiotherapy or chemotherapy. To achieve this goal, the specific aims are:

Specific aim (1): Realistic modeling of ultrasound prostate hyperthemia

Detailed 3D MRI image of the prostate and the surrounding tissue will be obtained from the Visible Human Project to help building an accurate simulation model for ultrasound propagation and temperature elevations. The model is supposed to reflect the accurate tissue structures and acoustical parameters, which will incorporate scattering and diffraction effects, acoustic nonlinearity, absorption, heat transfer and perfusion of the blood. This accurate model will help in optimizing the acoustical parameter as well as the geometry of the array in order to get uniform heating all over the prostate volume.

Specific aim 2: Beam design and optimization

Using the realistic model of prostate ultrasound interaction, optimal sonications will be determined to satisfy the hyperthermia conditions for the whole prostate volume. The main parameters to be studied are: ultrasonic resonance frequency, energy level, pulse duration, and beam shape.

Specific aim 3: Hyperthermia array design and fabrication

A two-dimensional array transducer will be designed for practical experiments and hyperthermia realization. The optimal acoustical depending on the accurate simulation method will be the major guidance rules for this array design. Array prototypes will be constructed and tested. Exposimetry of the ultrasound pressure field will be used to compare the theoretical with the experimental results.

Specific aim 4: In vitro and in vivo hyperthermia monitored with MR thermometry

Evaluation of the two-dimensional array will be conducted using MR thermometry. The proton resonance frequency (PRF) shift technique will be used to monitor the temperature rise non-invasively. Initially the experiments will be conducted in a perfused phantom and rabbit muscle. These experiments will test the prototype in real life to compare simulation with in vivo results.

Specific aim 5: in vivo prostate hyperthermia and evaluation

Final experiments will be conducted using the 2D prototype array on dogs while monitoring the temperature non-invasively using MRI images. The optimal sonications will be conducted using the optimized beam pattern to uniformly heat the prostrate to the desired thermal dose. Histologic study of the prostate, rectum, and surrounding tissue will provide final assessment for performance of the optimized treatment.

B. Background and significant

B.1. Prostate gland and prostate cancer

The prostate gland is a single doughnut-shaped gland about the size of a chestnut. It encircles the part of the urethra just inferior to the bladder (Fig. 2). Enclosed by a thick connective tissue capsule, it is made up of 20 to 30 compound tubular-alveolar glands embedded in a mass of smooth muscle and dense connective tissue. When prostate cells fail to honor normal controls of cell division and multiply excessively, an up normal mass of proliferating cells called a neoplasm results. Neoplasms are classified as benign or malignant. A benign neoplasm, commonly called a tumor, is strictly a local affair. Its cells remain compacted, are often encapsulated, tend to grow slowly, and seldom kill their hosts if they are removed before they compress vital organs. In contrast, cancers are malignant neoplasms, non-encapsulated masses that grow relentlessly and may become killers. Their cells resemble immature cells, and they invade their surroundings rather than pushing them aside. Malignant cells can also break away from the parent mass, the primary tumor, and travel via blood or lymph to other body organs, where they form secondary cancer masses. This capability for traveling to other parts of the body is called

metastasis. Metastasis and invasiveness distinguish cancer cells from the cells of benign neoplasms (Maurieb E.N., 1999).

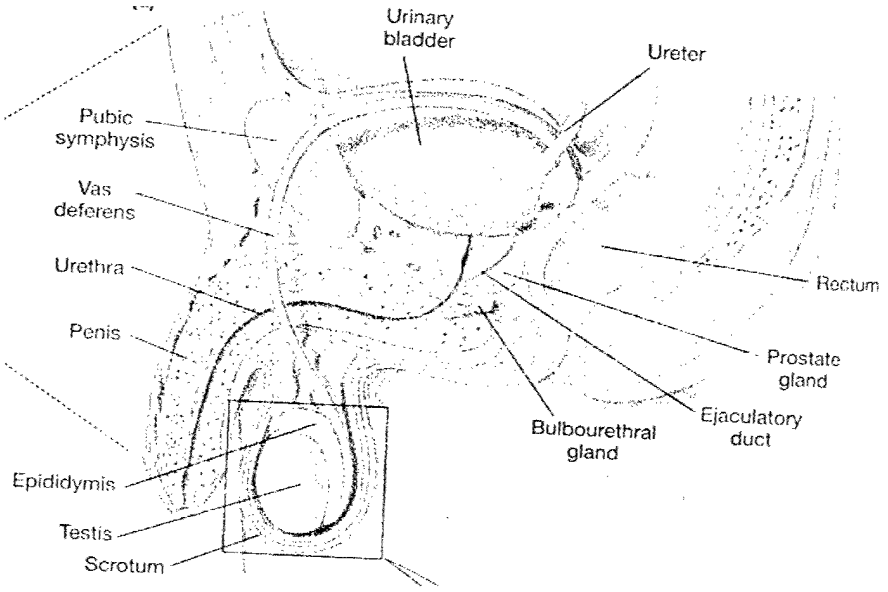

Fig. 2. Anatomy of the male reproductive system showing the prostate gland {Silverthorn D.U. 2001 56 /id}.

Thermal treatment has proven to treat both benign and malignant growths in the prostate. Localized hyperthermia is useful adjuvant to chemotherapy (Bornstein B.A. et al, 1993) and radiotherapy (Overgaard et al, 1996) in the treatment of prostate cancer. It also slows the growth of some tumors and increases antibody production. Changes in cells' temperature can disrupt the bonds that hold a protein in its tertiary configuration, causing the protein to lose its shape (Fig. 3). Small changes in temperature can increase or decrease the activity of enzymes (Silverthorn D.U., 2001), however, once the changes exceed some critical point, the structure of the enzyme is altered so much that its activity is destroyed. When this occurs, the enzyme is said to be denatured. The potential disastrous influence of temperature on enzymes and other proteins is the reason that the body so closely regulates this factor.

B.2. Ultrasound Hyperthermia

For the clinical management of prostate cancer, localized hyperthermia has been successful as an adjuvant to chemotherapy (Bornstein B.A., Zouranjian P.S., Hansen J.L., Fraser S.M., Gelwan L.A., Teicher B.A., and Svensson G.K., 1993) and radiotherapy (Overgaard J., 1989;Sneed and Phillips, 1991;Overgaard, Gonzalez, Hulshof, Arcangeli,

Dahl, Mella, and Bentzen, 1996). In a hyperthermia treatment, a large tissue volume (the whole prostate gland) is typically heated to about 43°C for times up to 1 hour, although use of higher temperatures for shorter times may also be beneficial (ter Haar, 2001). Hyperthermia acts as a radiosensitizer that increases radiation damage and prevents subsequent repair. In the environment of a malignant tumor with a low blood supply, hypoxia and low pH, hyperthermia is directly cytotoxic (Overgaard J., 1989). Methods for application of hyperthermia include microwaves (Leyons B.E. et al, 1984;Astrahan M.A. et al, 1989), radiofrequency EM radiation (Hall et al, 1990), and ultrasound (Cain C.A. and Umemura S.A., 1986;Diederich and Hynynen, 1990;Ebbini E.S. and Cain C.A., 1991;Ebbini E.S. and Cain C.A., 1991;Tu et al, 1994;Lee R.J. et al, 1999).

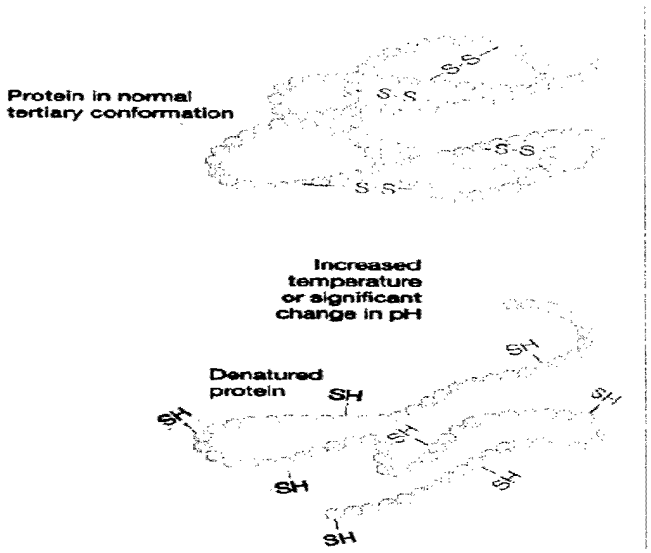

Fig. 3. Heat and acid can break the sulfur-sulfur or hydrogen bonds that hold a protein in its three-dimensional shape. When this happens to an enzyme, it loses its activity (Silverthorn D.U., 2001).

Intracavitary ultrasound offers a means of noninvasive localized hyperthermia treatment for tumors of the prostate, with significant advantages over other hyperthermia methods (Table 1). The prostate is easily accessible via intracavitary (transrectal) applicators, which allow for heating of the prostate with minimal heating of normal tissue (Buchanan M.T. and Hynynen K., 1994;Hutchinson E.B. and Hynynen K., 1996;Sanghvi N.T. et al, 1996). Intracavitary ultrasound arrays allow for deep localized heating with power control and capable of generating sufficient power for hyperthermia.

Applicator / Design	Advantages	Disadvantages
Interstitial / Perineal Implant (Prionas et al, 1994;Kaplan et al, 1991)	• Good heat coverage • Used with radiotherapy	• Ionizing radiation & invasive • Requires anesthesia
Intracavitary / Transurethal (Astrahan M.A. et al, 1991)		• Most tumors are posterior; insufficient surface area to provide adequate heating
Intracavitary / Microwave (Servadio and Leib, 1991;Montorsi et al, 1992)	• Adequate coverage of the gland with 915 MHz microwave radiation	• Difficult controlling the heating field • Invasive optical thermometry • Treatment time up to 8 hours
Intracavitary / Ultrasound (Fosmire et al, 1993;Smith et al, 1999;Hurwitz et al, 2001)	• Can control power deposition • Angular control of power field • Good penetration	• Invasive transperineal thermocouple temperature monitoring

Table 1. Comparison of the techniques for hyperthermia heating of the prostate

B.3. Modeling of tissue-ultrasound interaction

Development of more effective methods for ultrasonic hyperthermia will require more complete understanding of the physical mechanisms for heating of human tissue by ultrasound. Previous simulation studies of ultrasound-induced tissue heating have not considered anatomically realistic tissue structure, and most have not considered important propagation effects such as acoustic nonlinearity. These previous studies offer only limited insight for design of new hyperthermia methods.

Accurate modeling of large-scale ultrasound tissue interactions has only recently become feasible. The first numerical studies of full-wave ultrasonic propagation in anatomically realistic tissue models were recently conducted (Mast T.D. et al, 1997;Mast et al, 1999). These studies of ultrasonic propagation, which have previously considered the abdominal wall (Mast et al, 1998), the chest wall (Mast, Hinkelman, Metlay, Orr, and Waag, 1999), and the breast, have shown that simple models such as phase screens (Hirama M. et al, 1982;O'Donnell M. and Fleming R.Y., 1988;Nock L. et al, 1989), refraction by homogeneous layers (Robinson D.E. et al, 1981;Manry, Jr. and Broschat, 1996), scattering by irregular interfaces (Berkhoff A.P. et al, 1994), and weak scattering approximations (Waag R.C. et al, 1983;Lizzi F.L. et al, 1992) are all inadequate to explain complex *in vivo* interactions between ultrasound and soft tissues. However, full-

wave scattering models incorporating realistic tissue structure produce simulated ultrasound-tissue interactions that agree well with experimental measurements on human tissues (Hinkelman et al, 1998;Mast, Hinkelman, Orr, and Waag, 1998).

Recently, a new k-space method ideal for computation of ultrasonic propagation through soft tissues has been developed (Mast T.D. et al, 2001). For soft tissue computations, the k-space method provides higher efficiency and accuracy than finite difference, finite element, and psuedospectral methods. Thus, the k-space method allows very high accuracy to be obtained using coarse spatial and temporal discretization, so that ultrasound interactions with large 3D tissue models can now feasibly be computed.

In addition to scattering diffraction, and realistic anatomy, accurate modeling of ultrasonic hyperthermia requires inclusion of frequency-dependent absorption, acoustic nonlinearity, and heat transfer effects. The k-space method is sufficiently general to be extended in this manner. Frequency-dependent absorption is most realistically modeled as a combination of relaxation processes (Nachman A.I. et al, 1990); multiple-relaxation process absorption has recently been added to the k-space method (Tabei et al, 2002) using an efficient approach that also incorporate perfectly-matched-layer absorbing boundary conditions (Yuan X. et al, 1999). Heat generation and transfer due to absorption of ultrasound can be modeled using bio-heat transfer equation, which can be solved simultaneously with acoustic propagation equations (Bardati F. and Gerosa G., 1990;Damianou C.A. and Hynynen K., 1993;Hallaj and Cleveland, 1999). Acoustic non-linearity and the resulting harmonic generation can be incorporated by inclusion of nonlinear terms in the propagation equations employed (Hallaj and Cleveland, 1999;Sparrow V.W. and Raspet R., 1991).

B.4. Noninvasive MR temperature mapping

Precise determination of energy deposition and tissue temperature in 3D space has been a recurring problem with hyperthermia. Methods for monitoring temperature changes *in vivo* have traditionally used invasive probes (Young I.R. et al, 1995). Yet, this technique only provides temperature measurement at certain points in the target volume. Thermocouples can potentially bypass the regions of greatest temperature elevation, or might miss large under-heated regions. Another problem with invasive thermometry is

the uncertainty of the location of the thermocouple relative to the heating device. Recent advances in non-invasive magnetic resonance (MR) thermometry techniques have used the temperature dependence of the proton resonance frequency (PRF) (DePoorter J., 1994). Many studies have successfully used the PRF shift to localize and monitor ultrasound hyperthermia (Caretr D.L. et al, 1999;Smith, Buchanan, and Hynynen, 1999). Use of MRI provides not only quantitative 3D temperature measurements, but also precise locations of the heating device and the target area.

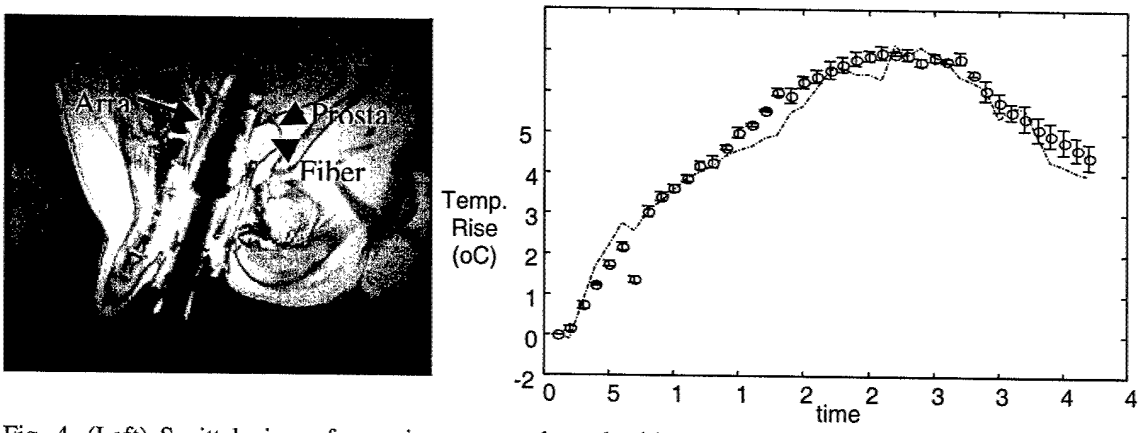

Fig. 4. (Left) Sagittal view of a canine prostate heated with a 16-element unfocused ultrasound array. (Right) Non-invasive MR temperature measurements (mean ± s.d.) correlated with invasive fiber optic temperature (dashed line).

C. Preliminary studies

C.1. Prostate hyperthermia with a 16 element array monitored with MR thermometry

In order to show the feasibility of in vivo temperature monitoring of prostate hyperthermia, preliminary results from an unfocused array in a clinical General Electric (GE) 1.5 Tesla (T) magnet heating canine prostate are presented. Figure 4 shows a magnitude image of the array in the prostate of a dog. The array was designed to heat the entire prostate from the limited confines of the rectum, and was constructed using one-third cylindrical sections from PZT-8 material. The partial-cylindrical intracavitary array consists of 16 elements in a 4x4 pattern, each of which can be powered individually or in any combination by a 16-channel amplifier system designed to operate between 1-2 MHz and to deliver 60 W per channel.

Phase-difference imaging was used to determine temperature rise by proton resonant frequency (PRF) shifts. Reference (baseline) and measurement scans were obtained and phase subtraction was carried out to compute the PRF shift (Chung A. et al, 1996;Ishihara et al, 1995). The temperature dependence for rabbit muscle was used for calculating the temperature elevation using a spoiled gradient echo sequence (Kuroda et al, 1998). Figure 5(b) shows a comparison of the results from the MR temperatures (x ± s.d.) in a region of interest (ROI) to temperatures measured with a fiber-optic temperature probe embedded in the prostate (dashed line).

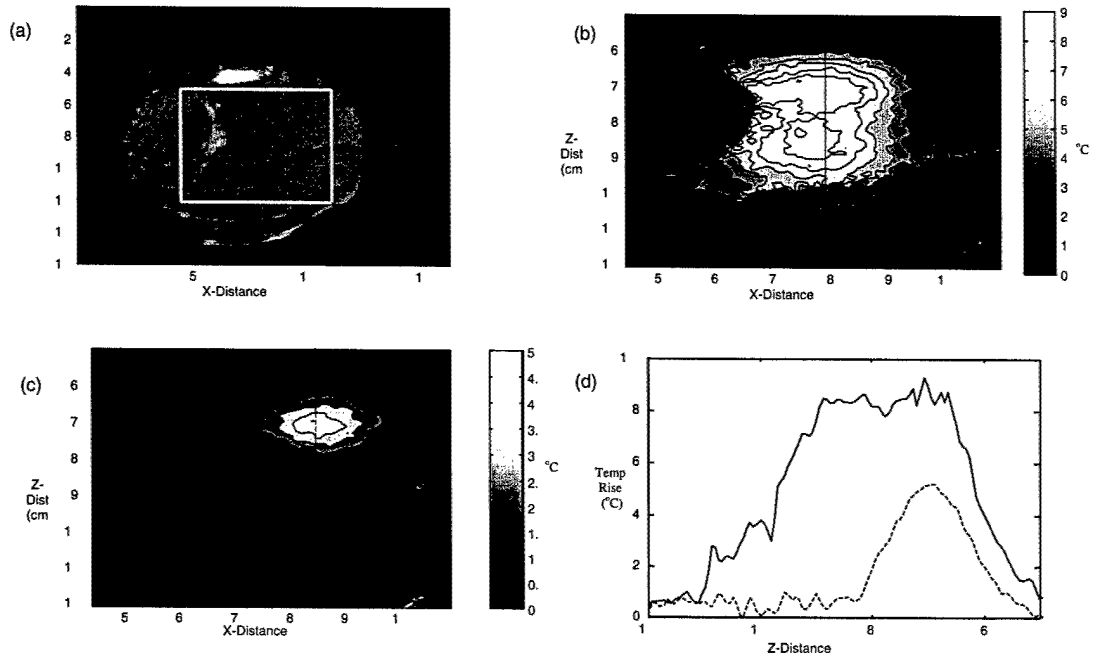

Fig. 5. (a) MRI taken 1 cm within the rabbit, parallel to the skin surface with the array located beneath the center of the marked ROI. (b) Spatial temperature map for four elements in the center of the array driven at 3.7 W for 10 min. (c) Temperature map obtained for one element operating at 5 W for 10 min. (d) Temperature profiles along the solid line from (b) and dashed line from (c).

Experimental evidence, obtained using the array described above, shows that highly localized heating patterns can be obtained using ultrasonic hyperthermia in living tissue, and that the specific spatial heating patterns depend strongly on the beam characteristics of the transducer employed. Figure 5 shows MRI-measured temperature maps for heating of *in vivo* rabbit muscle using a prototype prostate hyperthermia probe. Here, the only beam characteristics changed were the number of array elements employed. Both cases shown in Figure 5 show highly localized heating; however, the size of the significantly heated region varies greatly depending on the array characteristics.

The specific geometry of the region heated stems from a number of factors including not only the initial ultrasonic beam characteristics, but also tissue-dependent absorption, scattering, heat transfer, and perfusion properties.

The results shown in Figure 5 indicate that ultrasonic arrays for prostate hyperthermia can be designed to achieve spatial heating distributions of size appropriate for uniform treatment of the prostate. Although a single fixed region of interest may not be sufficient for the range of anatomical geometries encountered in prostate cancer patients. Variable focal characteristics would allow the region of interest to be sized appropriately for each patient. The locality of the heating will be further improved by optimization of beam characteristics to specifically target prostate tissue.

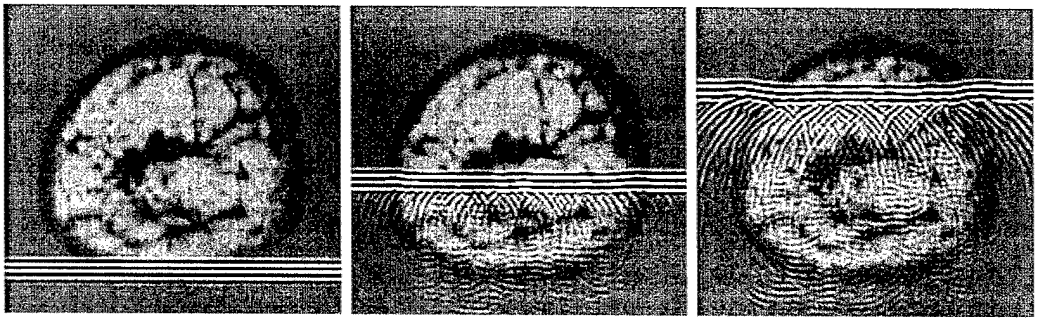

Fig. 6. Simulated propagation of a 1.25 MHz pulse through a human breast model based on the Visible Woman data set. The area shown in each frame is 55.5 mm in height and 77.7 mm in width. The temporal interval between frames is 5.3 μs. the breast tissue model employed is superimposed on each frame, with subcutaneous fat appearing light gray, skin and glandular tissue appearing medium gray, and connective tissue appearing dark gray.

C.2. Modeling of tissue-ultrasound interaction

The Visible Human data set (National Library of Medicine (US) Board of Regents 1990) provides three dimensional volumetric image data for one male and one female subject. These three-dimensional data, which include layer-by-layer photographic, CT and MRI images, can be processed to obtain detailed three-dimensional tissue maps appropriate for modeling of ultrasonic propagation. A cross section of one such map, for female breast tissue, is shown in Figure 6. This map was obtained by a new computer segmentation method, in which the hue, saturation and value of photographic image data were mapped to tissue type using empirically determined relations between the local mass density and the optical properties of soft tissue. The resulting map accurately delineates skin. Subcutaneous fat, connective tissue (septa), and glandular tissue. Because

empirical relationships also have been found to hold between density and sound speed, absorption, and nonlinearity parameters for human soft tissue (Mast T.D., 2000), this method can be used to realistically map multiple parameters affecting ultrasonic propagation and heat transfer. Since the tissue segmentation is performed automatically based on the predetermined empirical relationships, high-resolution three-dimensional maps, as will be needed for the prostate hyperthermia modeling described below, can be easily obtained.

Propagation of a 1.25 MHz ultrasonic pulse through this breast model has been computed using the k-space (Mast T.D., Souriau L.P., Liu D., Tabei M., Nachman A.I., and Waag R.C., 2001). Three snapshots of the resulting pressure field are shown in Figure 6 superimposed on an image of the tissue model's sound speed variation. The computed fields show scattering and diffraction effects consistent with experimentally measured propagation effects in human breast tissue (Hinkelman et al, 1995).

Other preliminary simulation results have shown the potential for specifically targeting prostate tissue in hyperthermia treatments. The example, shown here illustrates how optimization of the beam amplitude and frequency can allow prostate tissue to be specifically targeted relative to surrounding tissues. The prostate is a dense, protein-rich organ (density 1045 kg/m^3, protein content 15%, lipid content 1.2%)(Duck F.A., 1990) that is adjacent to the bladder and surrounded primarily by fatty tissue (Gray H., 2000). Thus, the acoustic and thermal properties of the prostate and surrounding tissues are reasonably estimated by nominal values for fatty and non-fatty soft tissues (ICRU, 1999). Typical fatty tissue has lower absorption, particularly at high frequencies, but a larger coefficient of nonlinearity B/A.

To obtain a preliminary estimate of power deposited into the prostate and surrounding fatty tissue, each tissue was assumed to be sonicated by a plane wave of specified initial amplitude and frequency. Using estimated values for the nonlinearity parameter (ICRU, 1999), amplitudes of the fundamental and first harmonic of the ultrasound beam were computed using the Fubini-Ghiron solution for nonlinear plane wave propagation (Pierce A.D., 1989). Amplitudes of the fundamental and first harmonic were then corrected using a power-law model of the frequency-dependent absorption (ICRU, 1998), and the power deposited into each tissue type was computed using the

formula given by Eq. 1 below (Nyborg W.L., 1981). The ratio of the power deposited in the prostate relative to that deposited in the surrounding fatty tissue gives a simple quantitative measure of the treatment specificity.

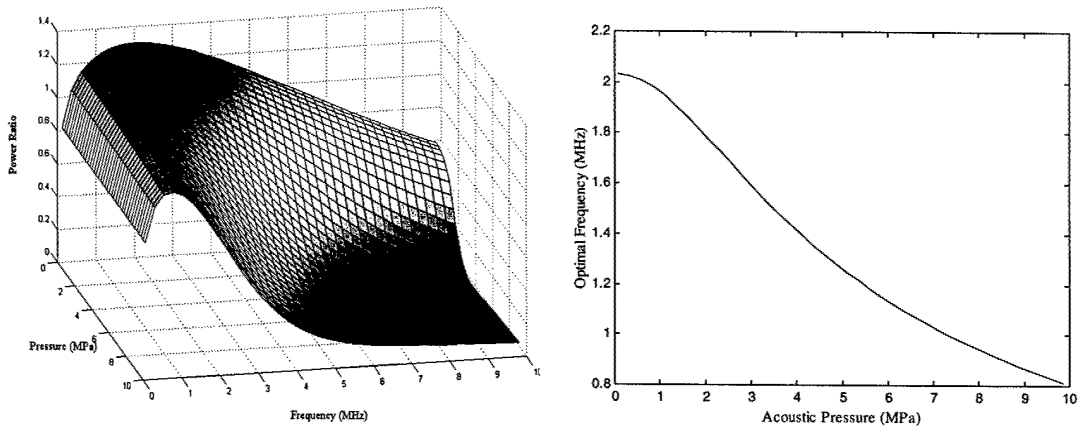

Fig. 7. (Left) Simulated ratio of power deposited into the prostate relative to surrounding tissue. Ratios above 1 indicate that more power is deposited into the prostate for the given amplitude and frequency. (Right) Optimal beam frequency as a function of amplitude.

The relative power deposited into the prostate and surrounding tissue, Figure 7, shows that the beam amplitude and frequency can be optimized to cause significantly more heating in the prostate than surrounding tissue. However, this situation only occurs for a fairly narrow range of amplitudes and frequencies. For a given beam amplitude, there exists an optimal frequency (associated with tradeoffs between absorption and nonlinearity) that maximally targets the applied thermal dose to the prostate, resulting in energy deposition up to 30% greater than in surrounding tissues. The increase in differential heating of the prostate will be even greater, due to its larger heat capacity, thermal conductivity, and thermal diffusivity relative to fatty tissue. Suboptimal choices of the beam parameters, however, can result in excessive heating of surrounding tissue. For example, beam amplitude of 10 MPa at a center frequency of 3 MHz would deposit about twice as much power into surrounding fatty tissue than into prostate.

Although these preliminary results indicate that the prostate can be specifically targeted for hyperthermia therapy, beam characteristics appropriate for clinical treatment cannot be accurately determined from such a simple model. The detailed modeling approach proposed, which considers important factors such as three-dimensional tissue structure, heat transfer characteristics including perfusion, realistic beam shapes, and

higher order nonlinearity coupled with relaxation absorption, will provide much more precise optimization suitable for design of clinical hyperthermia instruments.

D. Research design and methods

The goal of prostate-specific ultrasonic hyperthermia treatment will be achieved by the design of optimal beams and treatment strategies and by implementation of a new two-dimensional intracavitary array to realize the optimal ultrasonic treatment. Detailed simulations of ultrasonic prostate hyperthermia incorporating detailed anatomical structure corresponding to the specific aims, will guide the design, implementation, and refinement of the optimal treatment method.

D.1. Specific aim 1: Realistic modeling of ultrasound prostate hyperthermia

To obtain a computational method suitable for large-scale three-dimensional models of prostate hyperthermia, the k-space method (Mast T.D., Souriau L.P., Liu D., Tabei M., Nachman A.I., and Waag R.C., 2001), which incorporates absorption from multiple relaxation processes (Tabei, Mast, and Waag, 2002) will be extended to incorporate finite amplitude effects (Hallaj and Cleveland, 1999;Sparrow V.W. and Raspet R., 1991) and heat transfer effects including perfusion (Damianou C.A. and Hynynen K., 1993;Hallaj and Cleveland, 1999). Numerical results will be compared with analytic solutions for canonical problems to confirm accuracy, as in (Mast T.D., Souriau L.P., Liu D., Tabei M., Nachman A.I., and Waag R.C., 2001). These comparisons will allow assessment of the optimal discretization schemes to minimize computation time for large 3D models while accurately representing ultrasound-induced heat generation.

The time-domain acoustic pressure p, at any point r in the field, will be computed by solution of the nonlinear, absorbing wave equation

$$\nabla \cdot \left[\frac{\nabla p(\vec{r},t)}{\rho(\vec{r})} \right] - \kappa(\vec{r},t) \otimes \frac{\partial^2 p(\vec{r},t)}{\partial t^2} + \frac{\beta(\vec{r})}{\rho(\vec{r})c(\vec{r})} \frac{\partial^2 p(\vec{r},t)^2}{\partial t^2} = 0$$

where ρ is the density, κ is the compressibility, which includes a time-dependent part due to relaxation absorption, β is the coefficient of nonlinearity, and c is the speed of sound.

The nonlinear, absorbing wave equation will be solved simultaneously with Pennes' bioheat transfer equation (Pennes H.H., 1948),

$$\rho(\vec{r})c_t(\vec{r})\frac{\partial T(\vec{r},t)}{\partial t} = k\nabla^2 T(\vec{r},t) - w(\vec{r})c_b[T(\vec{r},t) - T_a] + q(\vec{r},t)$$

where c_t is the specific heat of the tissue, k is the thermal conductivity, T is the tissue temperature, T_a is the arterial blood temperature (37°C), w is the tissue perfusion (in kg/m^{3}s), c_b is the specific heat of blood (3770 J/kg°C), and q is the power deposited locally in the tissue, given by (Nyborg W.L., 1981)

$$q(\vec{r},t) = \frac{\alpha(\vec{r})\left|p(\vec{r},t)\right|^2}{\rho(\vec{r})c(\vec{r})}$$

where α is the relaxation absorption coefficient at the center frequency and $|p|$ is the magnitude of the acoustic pressure's analytic envelope.

Initial models of prostate, rectal wall, and surrounding tissues will be developed using image data from the Visible Human (National Library of Medicine (US) Board of Regents 1990). Tissue will be algorithmically mapped by empirical correlation of image parameters (*e.g.*, optical hue, saturation, and brightness as well as CT and MRI image amplitude) with tissue type. Wherever possible, required parameters (*e.g.*, speed of sound, density, absorption characteristics, nonlinearity coefficient, specific heat capacity, and thermal conductivity) will be obtained from the available literature (Duck F.A., 1990;ICRU, 1998). When specific parameters are not available for a given tissue type, estimates will be made based on the tissue constituents and mixture laws (Goss et al, 1978;Goss et al, 1980;Apfel R.E., 1986) as well as on empirical relationships between properties of various tissues (Mast T.D., 2000). Additional tissue models, with variable size and geometry for the prostate and surrounding tissues, will be made based on ultrasonic B-scans and other available image data.

D.2. Specific aim 2: Beam design and optimization

Thermal dose will be computed, using the realistic tissue modeling approach described above, for a range of beam and waveform parameters. The thermal dose is given, for a particular temperature field, by the method of (Sapareto S.A. and Dewey

W.C., 1984). During hyperthermia treatments, tissue is heated for long periods of time at low temperature elevations (approximately 30 minutes at 43°C). At a temperature of 43°C, a treatment must be shorter than 240 minutes to avoid tissue necrosis. The dose accumulated by a treatment is calculated numerically and referenced to an equivalent treatment at 43°C in the following manner:

$$Dose(T_{ref}, \vec{r}) = \int_0^{t_{final}} R^{43-T(\vec{r},t)} dt \approx \sum_{t=0}^{t_{final}} R^{43-T_{\Delta t}} \Delta t$$

where T_{ref} is the reference temperature for the treatment, T is the local temperature, Δt is the time interval, $T_{\Delta t}$ is the temperature at time interval Δt, t_{final} is the total time of elevated temperature (both heating and cooling), and R = 0.5 if T(r,t) > 43°C and R = 0.25 if T(r,t) ≤ 43°C. The definition of thermal dose employed here depends on spatial position. That is, the thermal dose is computed locally for a number of small regions inside and outside the prostate, based on the local time-dependent temperature, rather than for the prostate as a whole. Spatially dependent thermal doses will be systematically determined for ranges of pulse lengths, duty cycles (Smith N.B. and Hynynen K., 1998), switching patterns (Daum D. and Hynynen K., 1996), center frequencies (1.2-1.8 MHz), and signal amplitudes. The effects of a variety of beam characteristics, including variations in focal depth, focal width, and apodization, will also be systematically investigated.

For each simulation, the effectiveness of sonication will be quantified a figure of merit (FOM) that indicates the deviation of the achieved thermal dose from the ideal, i.e.,

$$FOM = \frac{\left\| Dose(\vec{r}) - Dose_{ideal}(\vec{r}) \right\|}{\left\| Dose_{ideal}(\vec{r}) \right\|}$$

where $Dose_{ideal}$, the ideal spatially dependent thermal dose, corresponds to a uniform, optimal thermal dose (*e.g.*, the dose corresponding to 30 minutes at 43°C) within the prostate and zero thermal dose outside the prostate. The same optimal thermal dose could also be achieved by uniformly heating the prostate to a higher temperature for a shorter period of time. Our figure of merit can be thought of as an error term that is zero for an optimal treatment. The FOM is nonzero for any suboptimal thermal dose, whether due to heating outside the prostate, nonuniform heating inside the prostate, or a quantity of

heating inside the prostate that differs from the desired dose. Thus, minimization of this FOM provides a quantitative approach to optimization of ultrasonic prostate hyperthermia.

This figure of merit will be determined as a function of each parameter investigated. Of particular importance is the capability of exploiting differences between the acoustic and thermal properties of the prostate gland and surrounding tissues. For example, differences in acoustic nonlinearity and absorption motivate investigation of effects of signal amplitude and frequency, while difference in specific heat capacity, thermal conductivity, and perfusion will guide investigations of spatial and temporal beam characteristics. To further refine the parametric investigation of hyperthermia performance, beam parameters found to have the greatest effect on the FOM will be systematically varied in combination to obtain quantitative relationships between therapeutic effectiveness and design parameters. These results will directly guide the array design.

D.3. Specific Aim 3: Hyperthermia array design and fabrication

The optimal beam characteristics determined in the simulation study will be employed to design a hyperthermia probe that produces near-optimal beams at a reasonable cost. The piezoelectric elements' resonance frequency and damping factor will be chosen to match the optimal center frequency and bandwidth found for prostate hyperthermia from the simulation studies described above. Incident pressure wavefields for practical transducer designs will be computed using Huygens' principle, which models each surface element as a grid of simple sources and then sums the contribution from the field (Zemanek J., 1971). The number of elements, element geometry, size, and pitch will be specified so that optimal beam patterns can be matched as closely as possible, within design and cost constraints.

Once a practical transducer design is obtained, simulations of the transducer's wavefield will be made to confirm its hyperthermia performance before fabrication. Since the ultimate aim of this research is to address prostate cancer in humans, the geometry of the array will be designed for use in humans. The array will be designed to heat the entire prostate from the limited confines of the rectum, based on computed tomograpghy (CT)

data of several prostate cancer patients, the applicator diameter must be 23 mm or less . From analysis of the same CT data, it was determined that to heat the entire gland, including the seminal vesicles, an applicator with 120° angular beam field would be necessary, with a length about 6 cm. For the transducer proposed for this research, the new design will be a two dimensional array.

The proposed transducer design, together with controlling electronics and other components of the experimental system, is sketched in Figure 8. An 8x8 (64 element square) two-dimensional array will be the initial design. Based on the results of the simulation studies and experimental experience, the initial design will be modified for the frequency, efficiency, element configuration, and beamforming characteristics necessary to realize optimal hyperthermia treatment. Once an array design is established, the prototype array will be manufactured using the facilities on the penn state campus. Exposimetry will be performed to determine the experimental pressure field and will be compared to theoretical results.

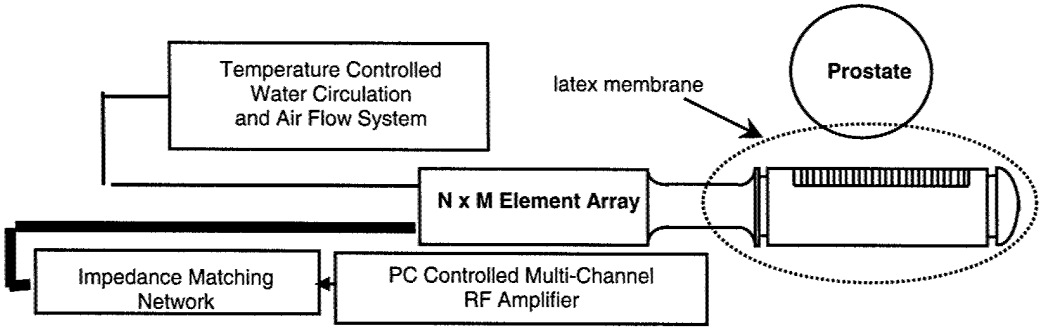

Fig. 8. A multi-element, two-dimensional array will be used to uniformly heat the prostate for hyperthermia treatment.

Although the propagation model described above should provide excellent estimates of the temperature changes caused by a particular ultrasound array design, this model may be limited by available knowledge of tissue structure and characteristics. Furthermore, the simulations described above will provide theoretical thermal dose information, but will not directly predict tissue damage. Thus, experimental studies will be crucial to provide a complete depiction of expected effects on the human prostate. These experiments, which will employ perfused phantoms and *in vivo* animal models, are described in the following sections.

D.4. Specific aim 4: *In vitro* and *in vivo* hyperthermia monitored with MR thermometry

After extensive exposimetry of the array in a water tank verifying the intended array pressure fields, temperature rises and corresponding thermal doses induced by the optimized array will be quantified using the array in a MRI facility. For evaluation of the array for hyperthermia, the goal is for the array to uniformly heat the size of a prostate, as quantified by the figure of merit defined above. The optimal activation, power, and phase of the array elements, computationally determined in the previous section, are tested at this stage. The proton reference frequency shift method will be used to monitor the temperature changes in the phantom or animal. Processing software has been previously coded on a PC, which can display temperature maps after image acquisition and reconstruction. For hyperthermia evaluation, 3 oil phantoms are placed on the outside of the phantom/animal to correct for the drift of the main magnetic field. In case of animal motion during a hyperthermia treatment, utilization of spectroscopic techniques, which are less sensitive to motion, will be tested (Mulkern et al, 1998). Motion sensitivity can be suppressed using a multi-echo sequence instead of a single-echo sequence. These experiments will be carried out at the university of Illinois at Urbana Champaign in a 1.5 T, 33 cm bore animal magnet.

Initial experiments will involve heating a dynamic two-dimensional phantom with thermal characteristics designed to precisely follow pennes bio heat transfer equation including perfusion effects (Payne et al, 2001). For *in vivo* experiments, anesthetized New Zealand white rabbits (3-4 kg) rabbits will be used since this is a well-studied system in previous hyperthermia and focused ultrasound investigations and since rabbit muscles are large enough to simulate human tissues for thermal surgery. Smaller animals cause problems because the boundary conditions dominate the temperature elevation. Approximately 10 rabbits will be used for these experiments. While under general anesthesia throughout the entire procedure, the thigh will be used for a hyperthermia. A 22-gauge catheter needle will be introduced into the phantom or thigh muscle and the tip located by the susceptibility artifact induced in a T2 weighted image. A fiber optic thermocouple (Luxtron) will be introduced into the catheter, and the needle withdrawn. The plane in which independent temperature measurements can be obtained via the fiber

optic thermocouple is therefore defined. For coupling the array to the tissue, a 37°C, circulating water bolus is placed around the transducer. For hyperthermia evaluation, therapeutic temperatures between 43 and 45°C will be maintained for 20-60 min. The temperature decay will be monitored until the baseline temperatures have reached. Tissue changes will be followed by repeating the T1-and T2-weighted images. After this, a contrast agent bolus will be injected and the dynamic changes monitored. Finally, high-resolution contrast-enhanced images will be obtained to evaluate tissue damage. Following the sonications, rabbits will be sacrificed while under anesthesia (pentobarbital 130 mg/kg) and the snoicated area will be harvested for histological evaluation.

This first in vivo experimental study will allow initial evaluation of the prototype arrays performance in perfused tissue. Based on this initial data and complementary simulation, parameters such as the beam focal characteristics, duty cycle, pulse center frequency, and amplitude will be further refined before the next stage of in vivo experiments. For example, if the ultrasound-induced temperature rise is found to be more or less than optimal, the duty cycle and switching characteristics and temperature rise determined from the initial simulation. Similarly, if the spatial extent of the applied thermal dose differs significantly from expectation, beam parameters will be adjusted with guidance from the initial simulation results. Such adjustments could include additional focusing or defocusing of the beam to modify the azimuthal extent of the thermal dose, and adjustments in amplitude or frequency to modify the axial extent based on tradeoffs between absorption and nonlinearity.

D.5. Specific aim5: in vivo prostate hyperthermia and evaluation

To confirm and evaluate the performance of the optimal hyperthermia array for *in vivo* prostate hyperthermia, the multiple element ultrasound array will also be used for *in vivo* experiments with canines in an MRI scanner. For the hyperthermia treatment, the ultrasound will uniformly heat the prostate to the desired thermal dose using the optimal beams and temporal sonication patterns developed earlier. Approximately 6 canines will be used; the animal handling procedure will be similar to that described above. Canine prostate hyperthermia will be performed in a T2, whole body magnet. Several canines will be anesthetized using an IM injection into the caudal thigh using ketamine (5 mg/kg)

and xylazine (0.6-2 mg/kg). The rectum will be cleaned and then the animal will be moved to the MRI suite and placed on a standard MRI table. The prostate will be imaged and the temperature sensors will be inserted in the target volume using the image information. The rectum will be filled with degassed acoustic coupling gel and the array will be inserted. Good contact will be verified by MRI images. Baseline temperature sensitive MR images will be collected.

During the hyperthermia treatment, temperature maps will be produced approximately every minute and viewed directly on the PC. Therapeutic temperatures between 43 and 45°C will be uniformly maintained for 20-60 minutes. Built-in controls will shut the transducer amplifiers down if the temperature rises above a certain threshold value during the treatment. In the case of motion, multiple echo sequences will be used to reduce artifact. Tissue changes will be followed by repeating the T1- and T2- weighted images. After this a contrast agent bolus will be injected and the dynamic changes monitored. Finally, high-resolution contrast-enhanced images will be obtained to evaluate tissue damage. Special care will be taken to evaluate locations that appeared to have hot spots based on the MR information.

Following the hyperthermia, canines will be sacrificed while under anesthesia (pentobarbital 130 mg/kg). The prostate, rectum, and surrounding tissues will be harvested for tissue pathology studies to provide a final assessment of the performance of the new hyperthermia method. The performance of the optimized treatment method will be assessed using criteria analogous to the figure of merit, with the ideal of uniform heat-induced damage (as seen by breakdown of heat-shock proteins) inside the prostate and zero damage in the rectal wall and surrounding tissues. Distribution of thermal effects will be directly compared to thermal doses quantitatively estimated from the 3D time-dependent MRI measured temperature maps. These assessments will provide guidance for future development of the optimized hyperthermia method proposed here; for instance, insight will be gained into the feasibility of higher-temperature, short-time treatments. Successful completion of the research proposed here would be a major advance toward industrial and clinical development hyperthermia systems for safe, effective treatment of prostate cancer.

Acknowledgments

This work was supported by the Department of Defense Congressionally Directed Medical Prostate Cancer Research Program (DAMD17-0201-0124).

Reference List

Apfel R.E. (1986) Prediction of tissue composition from ultrasonic measurements and mixture rules. J Acoust Soc Am, 79:148-152.

Astrahan M.A., Ameye F., Oyen R., Willemen P., Baert L., and Petrovich Z. (1991) Interstitial temperature measurements during transurethal microwave hyperthermia. J Urol, 145:304-308.

Astrahan M.A., Sapozink M.D., Cohen D., Luxton G., Kamp T.D., Boyd S., and Petrovich Z. (1989) Microwave applicator for transurethal hyperthermia of benign prostatic hyperplasia. Int J Hyperthermia, 5:283-296.

Bardati F. and Gerosa G. (1990) On the solution of the non-linear bio-heat equation. Journal of Biomechanics, 23:791-798.

Berkhoff A.P., van den Berg P.M., and Thijssen J.M. (1994) Simulation of wave propagation through aberrating layers of biological media. 94 A.D.,1797-1800.

Bornstein B.A., Zouranjian P.S., Hansen J.L., Fraser S.M., Gelwan L.A., Teicher B.A., and Svensson G.K. (1993) Local hyperthermia, radiation therapy, and chemotherapy in patients with local-regional recurrence of breast carcinoma. Int J Radiat Oncol Biol Phys, 25:79-85.

Buchanan M.T. and Hynynen K. (1994) Design and experimental evaluation of intracavitary ultrasound phased array system for hyperthermia. IEEE Trans Biomed Eng, 41:1178-1187.

Cain C.A. and Umemura S.A. (1986) Conentric-ring and sector vortex phased array applicators for ultrasound hyperthermia therapy. IEEE Trans Microwave Theory Tech, MTT-34:542-551.

Caretr D.L., MacFall J.R., Clegg S.T., Wan X., Prescott D.M., Charles H.C., and Samulski T.V. (1999) Magnetic resonance thermometry during hyperthermia for human high-grade sarcoma. Int J Radiat Oncol Biol Phys, 40:815-822.

Chung A., Hynynen K., Cline H.E., Colucci V., Oshio K., and Jolesz F.A. (1996) Optimization of spoiled gradient-echo phase imaging for in vivo localization of a focused ultrasound beam. Magn Reson Med, 36:745-752.

Damianou C.A. and Hynynen K. (1993) Focal spacing and near-field heating during pulsed high temperature ultrasound therapy. Ultrasound Med Biol, 19:777-787.

Daum D. and Hynynen K. Optimization of thermal dose using switching mode patterns of a spherically shaped square element phased array. 2, 1309-1312. 1996. IEEE Ultrasonics Symposium Proceedings.
Ref Type: Conference Proceeding

DePoorter J. (1994) The proton resonance frequency method for noninvasive MRI thermometry: Study of susceptibility effects. In,426.

Diederich,C.J. and Hynynen,K. (1990) The development of intracavitary ultrasonic applicators for hyperthermia: a design and experimental study. Med Phys, 17:626-634.

Duck F.A. (1990) Physical properties of tissue: a comprehensive reference book. Academic Press, London.

Ebbini E.S. and Cain C.A. (1991) Experimental evaluation of a prototype cylindrical section ultrasound hyperthermia phased-array applicator. IEEE Trans Ultrason Ferroelectr Freq Contr, 38:510-520.

Fosmire,H., Hynynen,K., Drach,G.W., Stea,B., Swift,P., and Cassady,J.R. (1993) Feasibility and toxicity of transrectal ultrasound hyperthermia in the treatment of locally advanced adenocarcinoma of the prostate. Int J Radiat Oncol Biol Phys, 26:253-259.

Goss,S.A., Johnston,R.L., and Dunn,F. (1978) Comprehensive compilation of empirical ultrasonic properties of mammalian tissues. J Acoust Soc Am, 64:423-457.

Goss,S.A., Johnston,R.L., and Dunn,F. (1980) Compilation of empirical ultrasonic properties of mammalian tissues. II. J Acoust Soc Am, 68:93-108.

Gray H. (2000) Gray's Anatomy. Churchill Livingstone, London.

Hall,A.S., Prior,M.V., Hand,J.W., Young,I.R., and Dickinson,R.J. (1990) Observation by MR imaging of in vivo temperature changes induced by radio frequency hyperthermia. J Comput.Assist.Tomogr., 14:430-436.

Hallaj,I.M. and Cleveland,R.O. (1999) FDTD simulation of finite-amplitude pressure and temperature fields for biomedical ultrasound. J Acoust Soc Am, 105:L7-12.

Hinkelman,L.M., Liu,D.L., Waag,R.C., Zhu,Q., and Steinberg,B.D. (1995) Measurement and correction of ultrasonic pulse distortion produced by the human breast. J Acoust Soc Am, 97:1958-1969.

Hinkelman,L.M., Mast,T.D., Metlay,L.A., and Waag,R.C. (1998) The effect of abdominal wall morphology on ultrasonic pulse distortion. Part I. Measurements. J Acoust Soc Am, 104:3635-3649.

Hirama M., Ikeda O., and Sato T. (1982) Adaptive ultrasonic array imaging through an inhomogeneous layer. J Acoust Soc Am, 71:100-109.

Hurwitz,M.D., Kaplan,I.D., Svensson,G.K., Hynynen,K., and Hansen,M.S. (2001) Feasibility and patient tolerance of a novel transrectal ultrasound hyperthermia system for treatment of prostate cancer. Int J Hyperthermia, 17:31-37.

Hutchinson E.B. and Hynynen K. (1996) Intracavitary phased arrays for non-invasive prostate surgery. IEEE Trans Ultrason Ferroelectr Freq Contr, 43:1032-1042.

ICRU,I.C.o.R.U.a.M. (1998) Tissue Substitutes, Phantoms, and Computational Modelling in Medical Ultrasound. Maryland Report 61, Bethesda.

ICRU,I.C.o.R.U.a.M. (1999) Tissues Sustitutes, Pahntoms and Computation Modelling in Medical Ultrasound. ICRU, Bethesda.

Ishihara,Y., Calderon,A., Watanabe,H., Okamoto,K., Suzuki,Y., Kuroda,K., and Suzuki,Y. (1995) A precise and fast temperature mapping using water proton chemical shift. Magn Reson Med, 34:814-823.

Kaplan,I., Kapp,D.S., and Bagshaw,M.A. (1991) Secondary external-beam radiotherapy and hyperthermia for local recurrence after 125-iodine implantation in adenocarcinoma of the prostate. Int J Radiat Oncol Biol Phys, 20:551-554.

Kuroda,K., Chung,A.H., Hynynen,K., and Jolesz,F.A. (1998) Calibration of water proton chemical shift with temperature for noninvasive temperature imaging during focused ultrasound surgery. J Magn Reson Imaging, 8:175-181.

Lee R.J., Buchanan M.T., Kleine L.J., and Hynynen K. (1999) Arrays of multielement ultrasound applicators for interstitial hyperthermia. IEEE Trans Biomed Eng, 46:880-890.

Leyons B.E., Britt R.H., and Strohbehn J.W. (1984) Localized hyperthermia in the treatment of malignant brain tumors using an interstitial microwave antenna array. IEEE Trans Biomed Eng, 31:53-62.

Lizzi F.L., Rorke M.C., King D.L., Feleppa E.J., Kalisz A., Sokil-Melgar J.B., and Nowakowski J. (1992) Simulation studies of ultrasonic backscattering and B-mode images of liver using acoustic microscopy data. IEEE Trans Ultrason Ferroelectr Freq Contr, 2:212-226.

Manry,C.W., Jr. and Broschat,S.L. (1996) FDTD simulations for ultrasound propagation in a 2-D breast model. Ultrason Imaging, 18:25-34.

Mast T.D. (2000) Empirical relationships between acoustic parameters in human soft tissues. Acoustics Research Letters Online, 1:37-42.

Mast T.D., Hinkleman L.M., Orr M.J., Sparrow V.W., and Waag R.C. (1997) Simulation of ultrasonic pulse propagation through the abdominal wall [published erratum appears in J Acoust Soc Am 1998 Aug;104(2):1124]. J Acoust Soc Am, 102:1177-1190.

Mast T.D., Souriau L.P., Liu D., Tabei M., Nachman A.I., and Waag R.C. (2001) A k-space method for large-scale models of wave propagation in tissue. IEEE Trans Ultrason Ferroelectr Freq Contr, 48:341-354.

Mast,T.D., Hinkelman,L.M., Metlay,L.A., Orr,M.J., and Waag,R.C. (1999) Simulation of ultrasonic pulse propagation, distortion, and attenuation in the human chest wall. J Acoust Soc Am, 106:3665-3677.

Mast,T.D., Hinkelman,L.M., Orr,M.J., and Waag,R.C. (1998) The effect of abdominal wall morphology on ultrasonic pulse distortion. Part II. Simulations. J Acoust Soc Am, 104:3651-3664.

Maurieb E.N. (1999) Human anatomy & physiology. Addison Wesley Longman, New York.

Montorsi,F., Guazzoni,G., Colombo,R., Galli,L., Bergamaschi,F., and Rigatti,P. (1992) Transrectal microwave hyperthermia for advanced prostate cancer: long- term clinical results. J Urol, 148:342-345.

Mulkern,R.V., Panych,L.P., McDannold,N.J., Jolesz,F.A., and Hynynen,K. (1998) Tissue temperature monitoring with multiple gradient-echo imaging sequences. J Magn Reson Imaging, 8:493-502.

Nachman A.I., Smith J., and Waag R.C. (1990) An equation for acoustic propagation in inhomogeneous media with relaxation losses. J Acoust Soc Am, 88:1584-1595.

Nock L., Trahey G.E., and Smith S.W. (1989) Phase aberration correction in medical ultrasound using speckle brightness as a quality factor. J Acoust Soc Am, 85:1819-1833.

Nyborg W.L. (1981) Heat generation by ultrasound in a relaxing medium. J Acoust Soc Am, 70:310-312.

O'Donnell M. and Fleming R.Y. (1988) Phase-aberration correction using signals from point reflectors and diffuse scatters: Measurements. IEEE Trans Ultrason Ferroelectr Freq Contr, 35:768-774.

Overgaard J. (1989) The current and potential role of hyperthermia in radiotherapy. Int J Radiat Oncol Biol Phys, 16:535-549.

Overgaard,J., Gonzalez,G.D., Hulshof,M.C., Arcangeli,G., Dahl,O., Mella,O., and Bentzen,S.M. (1996) Hyperthermia as an adjuvant to radiation therapy of recurrent or metastatic malignant melanoma. A multicentre randomized trial by the European Society for Hyperthermic Oncology. Int J Hyperthermia, 12:3-20.

Payne,A., Mattingly,M., Shelkey,J., Scott,E., and Roemer,R. (2001) A dynamic two-dimensional phantom for ultrasound hyperthermia controller testing. Int J Hyperthermia, 17:143-159.

Pennes H.H. (1948) Analysis of tissue and arterial blood temperatures in the resting human forearm. Journal of applied physiology, 1:93-122.

Pierce A.D. (1989) Acoustics: An Introduction to Its Physical Principles and Applications. Acoustical Society of America, Melville, NY.

Prionas,S.D., Kapp,D.S., Goffinet,D.R., Ben Yosef,R., Fessenden,P., and Bagshaw,M.A. (1994) Thermometry of interstitial hyperthermia given as an adjuvant to brachytherapy for the treatment of carcinoma of the prostate. Int J Radiat Oncol Biol Phys, 28:151-162.

Robinson D.E., Wilson L.S., and Kossoff G. (1981) Shadowing and enhancement in ultrasonic echograms by reflection and refraction. J Clin Ultrasound, 9:181-188.

Sanghvi N.T., Fry F.J., Bihrle R., Foster R.S., Phillips M.H., Syrus J., Zaitsev A.V., and Hennige C.W. (1996) Noninvasive surgery of prostate tissue by high-intensity focused ultrasound. IEEE Trans Ultrason Ferroelectr Freq Contr, 43:1099-1110.

Sapareto S.A. and Dewey W.C. (1984) Thermal dose determination in cancer therapy. Int J Radiat Oncol Biol Phys, 10:787-800.

Servadio,C. and Leib,Z. (1991) Local hyperthermia for prostate cancer. Urology, 38:307-309.

Silverthorn D.U. (2001) Human Physiology an integrated approach. Printice Hall, New Jersey.

Smith N.B. and Hynynen K. (1998) The feasibility of using focused ultrasound for transmyocardial revascularization. Ultrasound Med Biol, 24:1045-1054.

Smith,N.B., Buchanan,M.T., and Hynynen,K. (1999) Transrectal ultrasound applicator for prostate heating monitored using MRI thermometry. Int J Radiat Oncol Biol Phys, 43:217-225.

Sneed,P.K. and Phillips,T.L. (1991) Combining hyperthermia and radiation: how beneficial? Oncology (Huntingt), 5:99-108.

Sparrow V.W. and Raspet R. (1991) A numerical method for general finite amplitude wave propagation and its application to spark pulses. J Acoust Soc Am, 5:2683-2691.

Tabei,M., Mast,T.D., and Waag,R.C. (2002) A k-space method for coupled first-order acoustic propagation equations. J Acoust Soc Am, 111:53-63.

ter Haar,G. (2001) High intensity ultrasound. Semin.Laparosc.Surg., 8:77-89.

Tu,S.J., Hynynen,K., and Roemer,R.B. (1994) Simulation of bidirectional ultrasound hyperthermia treatments of neck tumours. Int J Hyperthermia, 10:707-722.

Waag R.C., Nilsson J.O., and Astheimer J.P. (1983) Characterization of volume scattering power spectra in isotropic media from power spectra of scattering by planes. J Acoust Soc Am,1555-1571.

Young I.R., Hajnal J.V., Oatridge A., Roberts Y., Ling J., and Hill-Cottingham R. (1995) In vivo studies of the chemical shift method of temperature measurement in human calf muscle with verification using implanted temperature probes. Proc Int MRM,1175.

Yuan X., Borup J., Wiskin J., Berggren M., and Johnson S. (1999) Simulation of acoustic wave propagation in dispersive media with relaxation losses by using FDTD method with PML absorbing boundary condition. IEEE Trans Ultrason Ferroelectr Freq Contr, 46:14-23.

Zemanek J. (1971) Beam behavior within the nearfield of a vibrating piston. J Acoust Soc Am, 49:181-191.

Smith, N.B. "Therapeutic Applications of Ultrasound: Treatment of Prostate Disease and Noninvasive Drug Delivery", Invited talk to Case Western Reserve University-Department of Biomedical Engineering, 14 March 2002.

PENNSTATE
Department of Bioengineering

Therapeutic Applications of Ultrasound: Treatment of Prostate Disease and Noninvasive Drug Delivery

Nadine Barrie Smith

The Pennsylvania State University
College of Engineering
Department of Bioengineering
University Park, PA 16802

Therapeutic Ultrasound Arrays

Prostate Cancer

- Hyperthermia: unfocused US heating 42-45°C for 30-60 min (1.5 MHz)
- Controlled heating using MRI

Benign Prostatic Hyperplasia

Focused heating to ablate tissue: 60-100°C for 1-10 seconds (1.5 MHz)

Noninvasive Drug Delivery

Develop a practicable device to transdermally deliver insulin across skin without bioeffects (20 kHz)

Prostate Cancer

- In the US alone: 179,300 new cases of prostate cancer 2000.
- With a estimated 37,000 deaths per year, this is the second leading cause of cancer death in men (American Cancer Society).
- Current treatment : Surgery
  Hormone therapy
  Chemotherapy
  Radiotherapy
  Wait-and-see
- One clinically used treatment is to use transrectal ultrasound hyperthermia in conjunction with external beam irradiation.

Transrectal Array

- Ultrasound offers an attractive means of noninvasive localized hyperthermia treatment of tumors in the prostate due to the proximity of the prostate to the rectum.
- IDE approved device, current in use in Phase II patient trials at Dana-Farber Cancer Institute, Boston, MA.

MRI Thermometry

- Traditionally, invasive thermometry has been used to measure temperatures in the target region. Thermocouples may bypass the regions of greatest temperature elevation.
- Explores the potential of MR guidance and thermometry for clinical therapy. This method relies on frequency changes resulting from temperature-dependent variations in the molecular shielding constant of the water molecule

Materials and Methods

Power Field Simulations
(Rayleigh-Sommerfeld Integral)
O'Neil 1949

⇩

Temperature Simulations
(Bio-heat transfer equation)
Pennes 1948

⇩

Thermal Dose
(estimate of time required for a hyperthermia treatment, 30 minutes at 43°C)
Sapareto and Dewey, 1984

MATERIALS AND METHODS :

Power field simulations (Rayleigh-Sommerfeld Integral)

Acoustic pressure $p_i(x,y,z)$ at any point i in the field

$$p_i(x,y,z) \approx \sqrt{\frac{2W\rho}{cA}}\left(\frac{fS}{d}\right)e^{i(\phi-\frac{2\pi d}{\lambda})}i-d\alpha)$$

net power deposition at (x,y,z)

$$q(x,y,z) = \frac{\alpha P_{ac}'(x,y,z)}{\rho c}$$

O'Neil 1949

⇩

Temperature simulations (Bio-heat transfer equation)

Pennes 1948

⇩

Thermal Dose Sapareto and Dewey, 1984

- estimate of time required for a hyperthermia treatment
- 30 minutes at 43°C

T_{ref} = reference temperature
$T(t)$ = temperature function
t_{heat} = time of elevated temperature
Δt = time interval
TA = average temperature during Δt

Computer Tomography (CT)

12 patients w/ Prostate
AutoCAD

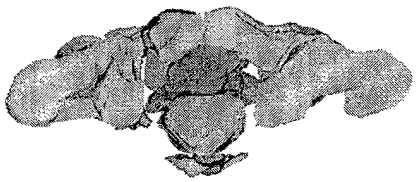

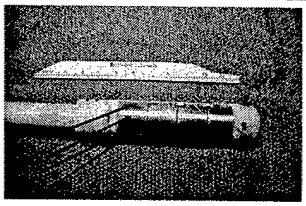

- 16 channels, 4 x 4 pattern. Applicator machined from Delrin®.
- Cut from 25 mm O.D., 15 mm long cylinders of PZT-8 material (EDO, Salt Lake City). Scored on inner surface.
- 120° angular beam field and length 6 cm would heat the entire gland. Diameter limited to 23 mm.

Array Exposimetry

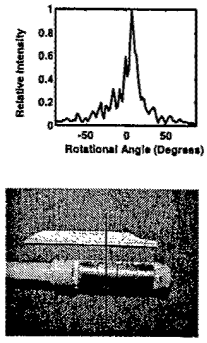

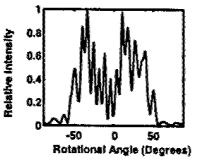

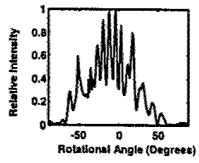

Non-Invasive MRI Thermometry

Applications
- (a) hyperthermia
- (b) focused ultrasound surgery
- (c) laser induced ablation
- (d) cryosurgery
- (e) RF microwave

Invasive techniques using; thermocouples interfere with the temperature distribution and give information at a few pre-determined sites.

Proton Resonance Frequency Shift :
- ± 0.5-1.0 °C temperature resolution
- 1 mm spatial resolution

MRI Temperature Proton Chemical Shift

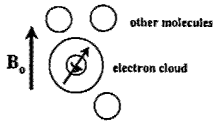

ω, resonant frequency
γ, gyromagnetic ratio
B_o, static field
σ, shielding constant

shielding constant (σ) ⇦ hydrogen bonding strength ⇦ intensity of molecular motion ⇦ Temperature (T)

In MRI, the spatial position and the chemical shift are encoded by phase and frequency of the precession of the protons, respectively.

Temperature Measurements: (Ishihara *et al.*, 1995)

Temperature sensitive proton resonant frequency shift

where ΔT = temperature change (°C)

$\Delta\phi$ = phase change (rads)
TE = Echo Time (sec)

$\gamma = 2\pi * 42.58$ MHz/T

$B_o = 1.5$ T

$\alpha(T)_{muscle} = -0.00909$ ppm/°C

$\alpha(T)_{oils} = -4.59 \times 10^{-5}$ ppm/°C

Temperature vs. Time

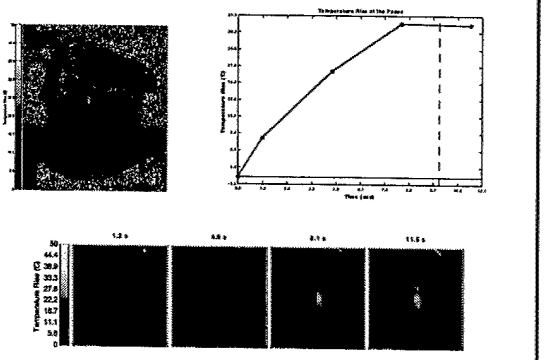

Materials and Methods :

- Experiments
  - *Ex vivo* bovine muscle
  - *In vivo* rabbit muscle (IACUC approval: ketamine-xylazine)
  - *In vivo* canine prostate
  - *Ex vivo, in vivo* MRI feedback
- Temperature probes
  - Thermocouple (copper and constantan, 50μm dia)
  - Luxtron fiber optic with a brass catheter surrounding.
- MRI: 1.5 Tesla Clinical Scanner (GE Medical Systems, Milwaukee, WI)

Experimental Set-up : MRI-Ultrasound System

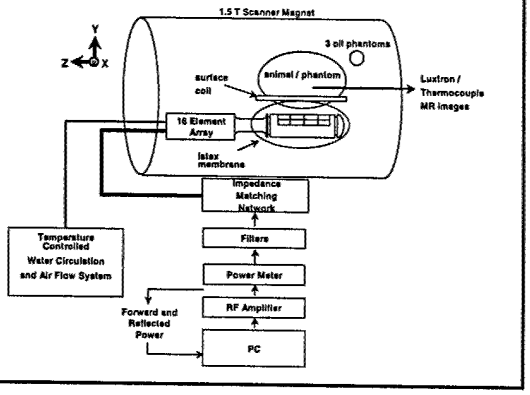

Ex vivo MR Temperature results

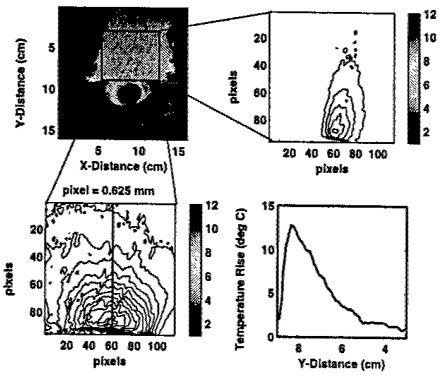

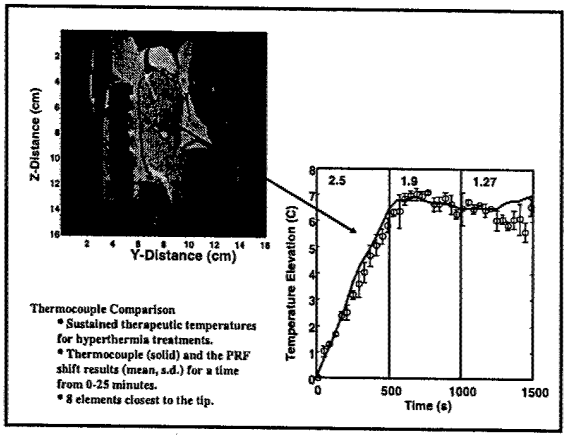

Thermocouple Comparison
- Sustained therapeutic temperatures for hyperthermia treatments.
- Thermocouple (solid) and the PRF shift results (mean, s.d.) for a time from 0-25 minutes.
- 8 elements closest to the tip.

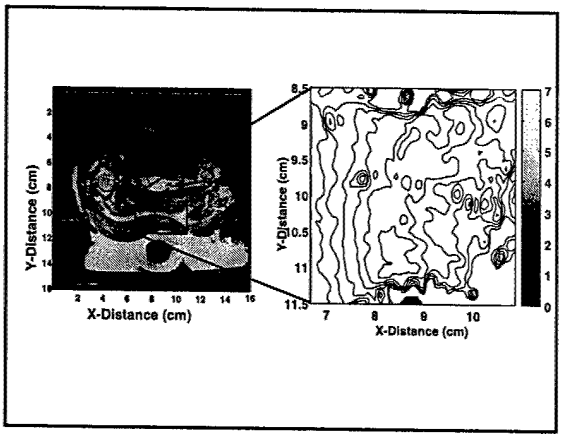

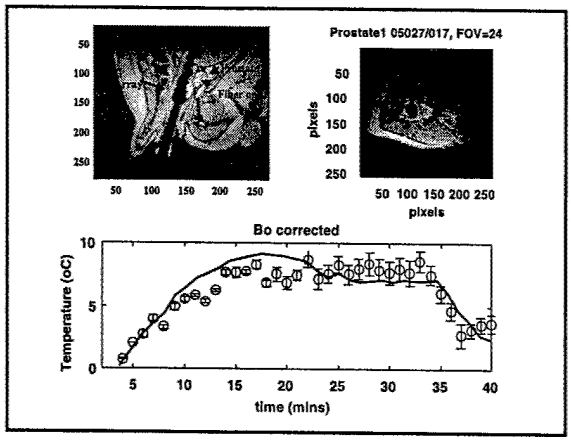

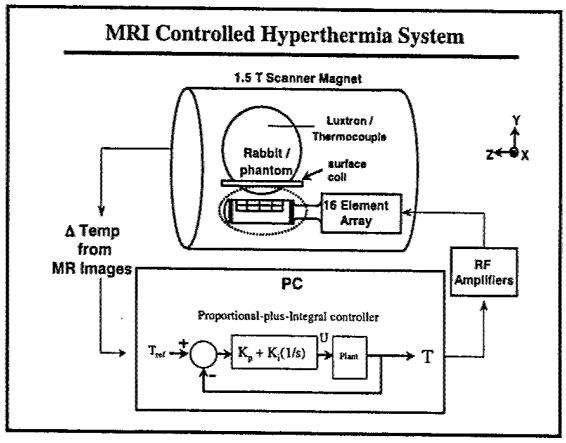

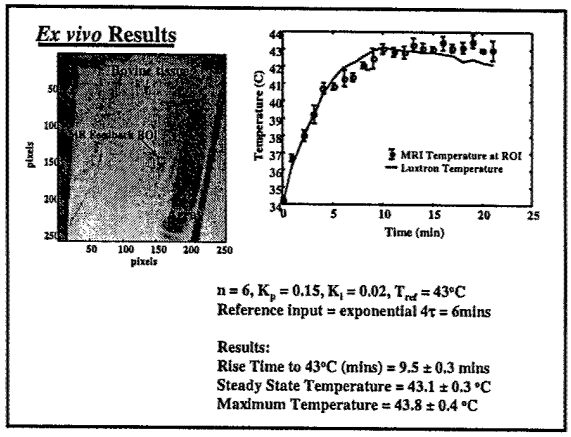

$n = 6$, $K_p = 0.15$, $K_i = 0.02$, $T_{ref} = 43°C$
Reference input = exponential $4\tau = 6$mins

Results:
Rise Time to 43°C (mins) = 9.5 ± 0.3 mins
Steady State Temperature = 43.1 ± 0.3 °C
Maximum Temperature = 43.8 ± 0.4 °C

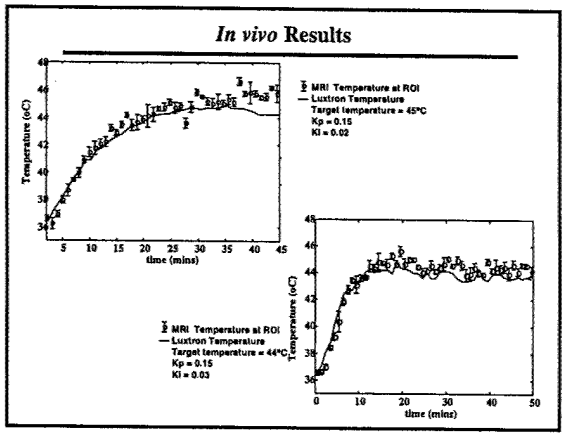

Therapeutic Ultrasound Arrays

Prostate Cancer

- •Hyperthermia: unfocused US heating 42-45°C for 30-60 min (1.5 MHz)
- •Controlled heating using MRI

Benign Prostatic Hyperplasia

Focused heating to ablate tissue: 60-100°C for 1-10 seconds (1.5 MHz)

Noninvasive Drug Delivery

Develop a practicable device to transdermally deliver insulin across skin without bioeffects (20 kHz)

Focused Ultrasound for Treatment of Benign Prostatic Hyperplasia

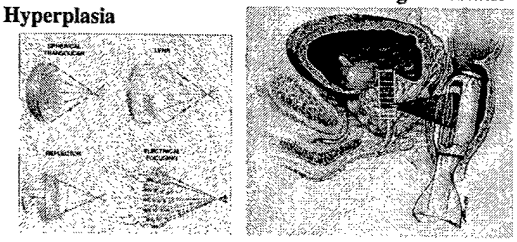

- can elevate tissue temperature in the focal zone up to 60-100 oC C in a very short duration (< 10 sec) to ablate selected cancer tissue while leaving the surrounding tissue safe
- •can be applied externally and contact free to targeted cancer tissue.
- •can produce sharp and predictable lesions

Specific Aims

- Design a focused 2-D, linear array for ablating abnormal prostate tissue.
- Use a 1.5 MHz, PZT transducer with a maximum of 20 elements (up to 64)
- Theoretically evaluate the pressure field using Rayleigh Integral.
- Can steer the US focus with a custom (computer) amplifier:
  amplitude: 0-60 electrical watts per channel
  phase: ±1°
- Experimentally evaluate the pressure field using hydrophone data and compare to theoretical results.

Two Dimensional Array Geometry

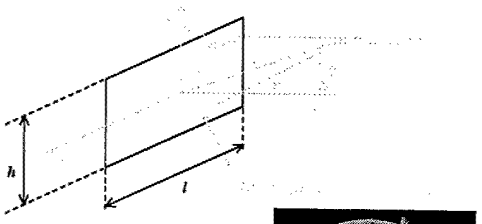

- Solid piece of PZT ceramic was cut through 70% of its thickness.
- Each element was individually wired, while the front face of the ceramic was grounded.

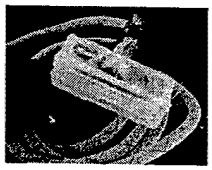

Grating Lobe Reduction Techniques

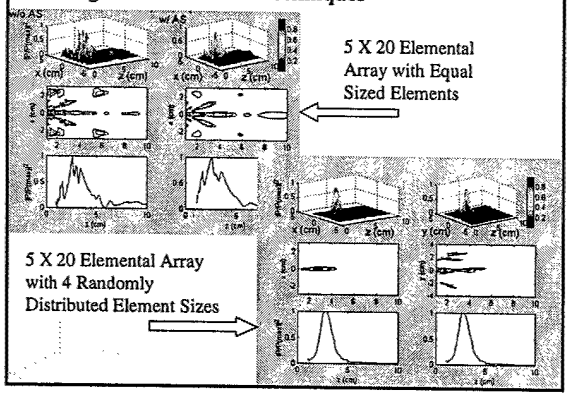

One-Dimensional Experimental Results

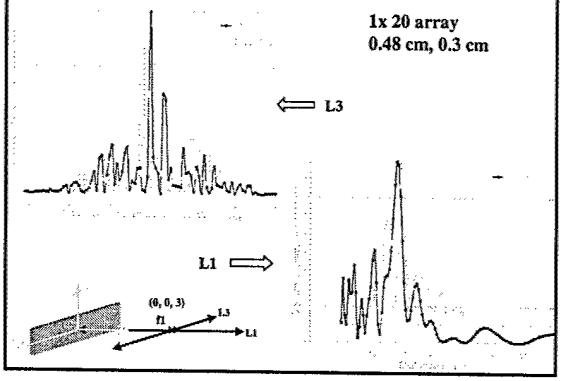

Two Dimensional Experimental Results 4 x 5 array

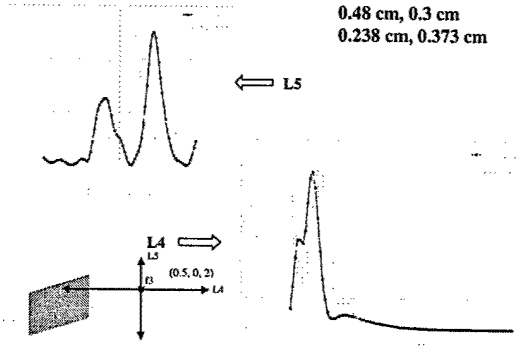

Therapeutic Ultrasound Arrays

Prostate Cancer

- Hyperthermia: unfocused US heating 42-45°C for 30-60 min (1.5 MHz)
- Controlled heating using MRI

Benign Prostatic Hyperplasia

Focused heating to ablate tissue: 60-100°C for 1-10 seconds (1.5 MHz)

Noninvasive Drug Delivery

Develop a practicable device to transdermally deliver insulin across skin without bioeffects (20 kHz)

Noninvasive Drug Delivery

- Approximately 15.7 million people in the United States suffer from diabetes. From a human and economic perspective, it is one of the most costly diseases (Congressionally Established Diabetes Research Working Group 1999).
- Diabetes is a disease in which the body does not properly produce or utilize insulin.
- Until a cure can be found, management of diabetes sometimes requires painful repetitive injections of insulin up to three times each day depending on the person.
- Studies have shown that ultrasound mediated transdermal drug delivery offers promising potential for noninvasive drug administration (Mitragotri et al. 1995a; Mitragotri et al. 1996; Mitragotri and Kost 2000).

Compound	Preparation	Frequency	Intensity	Device	Investigator
Aldosterone	in vitro human	20 kHz	125 mW/cm²	Sonicator¹	(Johnson et al. 1996)
Benzene	in vitro human	1 – 3 MHz	0 – 2 W/cm²	Sonicator⁴	(Mitragotri et al. 1995b)
Bicarbonate	in vivo rat	20 kHz	1 W/cm²	Sonicator¹	(Mitragotri et al. 2000a)
Butanol	in vitro human	20 k, 3 M	0 – 2 W/cm²	Sonicator⁴	(Mitragotri et al. 1995b)
Caffeine	in vitro human	1 – 3 MHz	0 – 2 W/cm²	Sonicator⁴	(Mitragotri et al. 1995b)
Calcium	in vivo rat	20 kHz	1 W/cm²	Sonicator¹	(Mitragotri et al. 2000a)
Corticosterone	in vitro human	20 kHz	125 mW/cm²	Sonicator¹	(Johnson et al. 1996)
Dexamethasone	in vitro human	1 MHz	1.4 W/cm²	Sonicator²	(Johnson et al. 1996)
Dextran**	in vivo rat	20 kHz	1 W/cm²	Sonicator¹	(Mitragotri et al. 2000a)
Estradiol	in vitro human	1 MHz	1.4 W/cm²	Sonicator²	(Johnson et al. 1996)
Glucose**	in vitro human	20 kHz	1 W/cm²	Sonicator¹	(Kost et al. 1996)
Inulin	in vivo rat	20 kHz	1 W/cm²	Sonicator¹	(Mitragotri et al. 2000c)
Lidocaine	in vitro human	1 MHz	1.4 W/cm²	Sonicator²	(Johnson et al. 1996)
Linoleic acid	in vitro human	1 MHz	1.4 W/cm²	Sonicator²	(Johnson et al. 1996)
Mannitol	in vivo rat	20 kHz	7 W/cm²	Sonicator¹	(Mitragotri Kost 2000)
Progesterone	in vitro human	1 – 3 MHz	0 – 2 W/cm²	Sonicator⁴	(Mitragotri et al. 1995b)
Salicylic acid	invivo guinea pigs	2 - 16 MHz	0.2 W/cm²	Panametrics³	(Bommannan ea 1992)
Sucrose	in vitro human	20 kHz	125 mW/cm²	Sonicator¹	(Johnson et al. 1996)
Testosterone	in vitro human	1 MHz	1.4 W/cm²	Sonicator²	(Johnson et al. 1996)
Urea	in vivo rat	20 kHz	1 W/cm²	Sonicator¹	(Mitragotri et al. 2000a)
Water	in vitro human	20 kHz	125 mW/cm²	Sonicator¹	(Johnson et al. 1996)

1. VCX 400, Sonics and Materials
2. Sonopuls 463, Henley International
3. Precision Acoustic Devices and Panametrics
4. Leader Electronics Corp., Japan
5. Sonopuls 474, Henley International

Summary of papers using ultrasound for enhanced insulin delivery

Preparation	Frequency	Intensity	Device	Reference
in vitro human *in vivo* rat	20 kHz	I_{ssa} = 12.5 - 225 mW/cm²	sonicator¹	Mitragotri et al., 1995
in vitro human	20 kHz	0.1 - 1* W/cm²	sonicator²	Zhang et al., 1996
in vivo rat	20 kHz	2.5, 10* W/cm²	sonicator³	Boucaud et al., 2000
in vivo rat	48 kHz	0.6 - 4.3* mW/cm²	ultrasonic bath⁴	Tachibana 1991
in vivo rabbit	105 kHz	1.7* mW/cm²	piezoelectric transducer⁵	Tachibana 1992

Legend: ¹ Brand not indicated; ² W-385 Heat Systems Ultrasonics, Inc., Farmingdale, NY; ³ VCX 400, Sonics and Materials, Newtown, CT; ⁴ Cole Parmer Instrument Co, Chicago, IL; ⁵ Transducer company not indicated.

NIH Transducer Resource Center

Insulin Delivery Transducers

- Miniature in size
- Frequency range will be between 20 – 100 kHz.
- Capability of generating sufficient high pressure and intensity
- High efficiency

Cymbal single element transducer and arrays

- Compact, light structure
- Resonance frequency adjustable between 20-50 kHz
- Low cost ($1)
- Accurate and precise exposimetry

Cymbal single element transducer

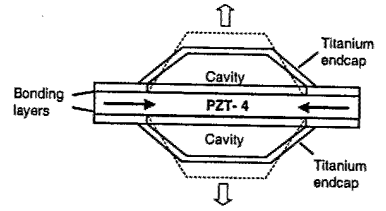

- Lead zirconate-titanate (PZT) ceramic
- Radial motion (i.e. the vibration moves from the center of the disc to the edges with radial symmetry)
- Cavities amplify the radial displacement into large axial displacement normal to the caps

Cymbal single element transducer

- Water-proof, electrical matching.
- Encased in a URALITE® polymer (acoustic impedance = water).

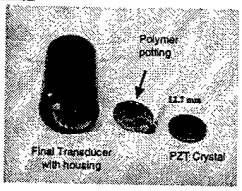

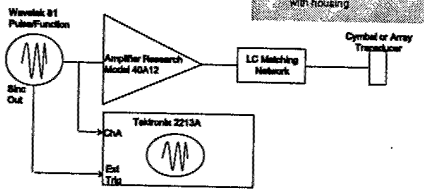

Standard Array

- Increase the spatial ultrasound field.
- Four cymbal transducers arranged in a 2 x 2 pattern.
- Connected in parallel. Electrical matching.
- 22 grams

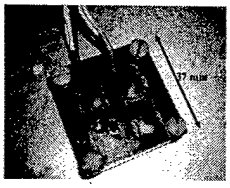

Stack Array

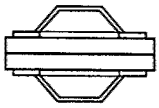

x 4

- Stack two piezoelectric discs.
- Polar directions of the two ceramic discs were opposite.
- Increase the efficiency. Electrical matching.

Theoretical and experimental evaluation: cymbal single element

Transducer Computer Model (PSpice)

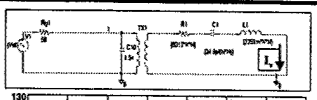

In Water Response

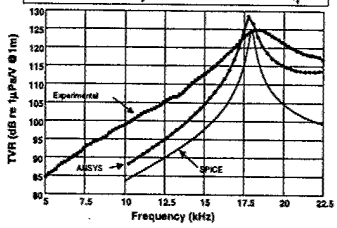

The single element cymbal transducer was modeled using two different simulation programs, ANSYS® and PSpice®. The experimental result was compared against the simulations and plotted as a function of the transmitted voltage response (TVR).

Ultrasound Exposimetry

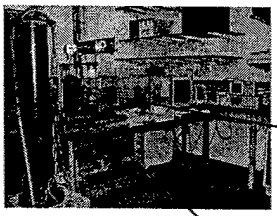

- Acoustic Output Labeling Standard for Diagnostic Ultrasound Equipment
- Standard for how manufactures should specify acoustic output data. (American Institute of Ultrasound in Medicine)

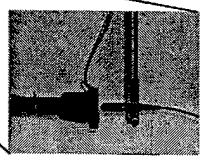

- Degassed, distilled water.
- Anechoic using sound absorbing material.
- Automated using computer control.

Exposimetry: Cymbal single element

P_c = Maximum, peak compressional pressure
P_r = Minimum, peak rarefactional pressure
I_{sptp} = Spatial peak, temporal peak intensity
I_{spta} = Spatial peak, temporal average intensity (RMS value)
I_{sppa} = Spatial peak, pulse average intensity (I_{spta} / duty factor)

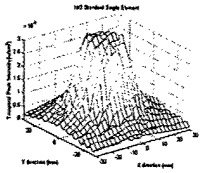

- Electrically driven under similar conditions
- AWG = 1Vpp w/ pulse duration of 200 ms and pulse repetition period of 1 second (i.e. 20% duty cycle).
- Amplifier gain was 50 dB. Multiple scannings, 3-5 each.
- Determined over a plane 1 mm from the transducer face.

Intensity (mW/cm²)	Single element cymbal	2 x 2 Stack Array	2 x 2 Standard Array
I_{sptp}	16.6 ± 4.3	51.1 ± 5.0	204.9 ± 20.1
I_{spta}	2.2 ± 3.1	10.4 ± 2.3	67.8 ± 0.4

Exposimetry: Standard Array

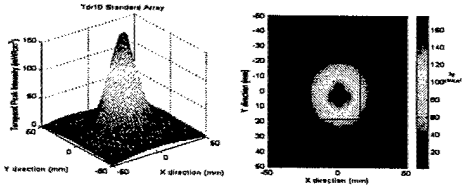

Plane	P_c	P_r	I_{sptp}	I_{spta}	I_{sppa}	I_{sata}
0 mm	54738.8	-55375.7	207.2	31.1	1.6	25.8
1 mm	51633.6	-51633.6	180.1	28.0	1.4	24.0
2 mm	49125.5	-49762.5	167.3	25.6	1.3	22.1
5 mm	43552.1	-44149.3	131.7	20.3	1.0	17.4

Pressure in Pa; intensity in mW/cm².

In vivo experiments

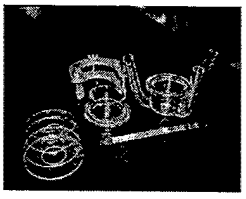

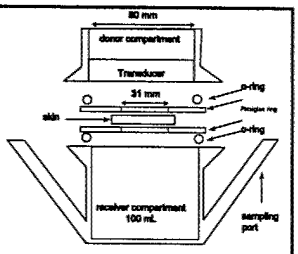

- For determining transport of insulin across in vitro human skin, a Franz diffusion cell was specially fabricated.
- Skin was placed between the upper and lower compartment with insulin in the donor compartment.
- Insulin concentrations in the receiver compartment measured over one hour was determined using a spectrophotometer.

In vivo experiments

- A total of 25 abdominal *in vitro* skin samples (skin bank) were used for 12 Humalin® and 13 Humalog® insulin transmission experiments.

- Visual and microscopic examination of the post ultrasound exposed skin did not produce any noticeable damage or significant change to the skin.

(U/hr)	Humulin®	Humalog®
Control (U/hr)	6.3 ± 14.0 (n=2)	17.2 ± 3.7 (n=5)
Single element cymbal	11.1 ± 4.9 (n=2)	
Stack Array	29.7 ± 0.2 (n=1)	27.8 ± 0.2 (n=2)
Standard Array	39.6 ± 11.7 (n=7)	36.6 ± 1.6 (n=6)

Preliminary *In vivo* experiments

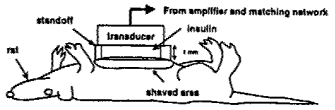

- Using three rats, the transmission of insulin across the skin was determined by monitoring the glucose level in rats under control and ultrasound exposure conditions.

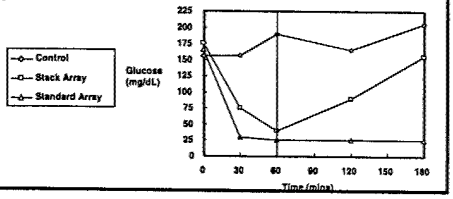

Therapeutic Ultrasound Arrays Conclusions

Prostate Cancer

- The spatial temperature maps indicate that the cylindrical transducers can easily provide the necessary temperature increase over the desired region while allowing control over the desired temperature elevation.

Benign Prostatic Hyperplasia

- Theoretical calculations showed that it is possible to have a two-dimensional linear transducer array focus anywhere in a specified prostate volume.
- Aperiodic element sizing and amplitude shading techniques were used to reduce side-lobe levels successfully.

Noninvasive Drug Delivery

- Promising but there are more "unknowns" than "knowns."
- Unknowns: optimal frequency, minimal intensity, effect of a change in TDR spatial area, mechanism.

Acknowledgments

- Whitaker Foundation
- Department of Defense Congressionally Directed Medical - Prostate Cancer Research Program - Idea Development Award
- Encapsulation Systems, Inc. Broomall, PA www.encsys.com
- Intersclence Research Inc. of Focus Surgery, Inc., Indianapolis, IN (SBIR Phase 2) www.focus-surgery.com
- NIH Transducer Resource Center (Dr. K. Kirk Shung - Director)

NIH Transducer Resource Center

Janelle Haser
Emiliano Malone
Osama M. Al-Bataineh
Khaldon Y. Saleh
Lei Sun
Seungjun Lee